

# Modular Design in Natural and Biomimetic Soft Materials

Aaron M. Kushner and Zhibin Guan\*

**Keywords:**

biomimetic materials ·  
dynamic materials ·  
hierarchical assembly ·  
peptide materials ·  
self-assembly



**U**nder eons of evolutionary and environmental pressure, biological systems have developed strong and lightweight peptide-based polymeric materials by using the 20 naturally occurring amino acids as principal monomeric units. These materials outperform their man-made counterparts in the following ways: 1) multifunctionality/tunability, 2) adaptability/stimuli-responsiveness, 3) synthesis and processing under ambient and aqueous conditions, and 4) recyclability and biodegradability. The universal design strategy that affords these advanced properties involves “bottom-up” synthesis and modular, hierarchical organization both within and across multiple length-scales. The field of “biomimicry”—elucidating and co-opting nature’s basic material design principles and molecular building blocks—is rapidly evolving. This Review describes what has been discovered about the structure and molecular mechanisms of natural polymeric materials, as well as the progress towards synthetic “mimics” of these remarkable systems.

## 1. Introduction to Biomimicry

Biomimicry or biomimetics is “the study of the formation, structure, or function of biologically produced substances and materials (such as enzymes or silk) and biological mechanisms and processes (such as protein synthesis or photosynthesis) especially for the purpose of synthesizing similar products by artificial mechanisms which mimic natural ones.”<sup>[1]</sup> Beginning with early examples, such as Da Vinci’s bird-inspired aircraft illustrations, biomimetic design has evolved into an important concept for basic scientific research as well as for many engineering applications.<sup>[2–7]</sup>

Biomimicry at the molecular level is particularly exciting, as it allows scientists to study, manipulate, augment, and imitate biological systems with powerful and precise synthetic methods. Some modern molecular biomimetic research targets include synthetic enzymes,<sup>[8,9]</sup> membranes<sup>[10]</sup> and ion channels,<sup>[11]</sup> artificial photosynthesis,<sup>[12]</sup> and, recently, synthetic cellular living systems.<sup>[13]</sup> The sub-areas of materials research that fit under the umbrella of molecular biomimicry have expanded dramatically over the last few decades to include bioengineered<sup>[14]</sup> and hybrid-polymer materials,<sup>[15–17]</sup> biomineralization,<sup>[18–24]</sup> and adhesives,<sup>[25,26]</sup> as well as morphological,<sup>[27]</sup> surface,<sup>[28]</sup> and functional extracellular matrix mimics.<sup>[29,30]</sup>

One of the early examples of the application of the biomimetic concept to organic materials science was the artificial liposomes designed by Ringsdorf in the 1980s.<sup>[31,32]</sup> Although several books have been devoted to the progress made in the field, biomimetic materials science possesses tremendous potential and opportunity for further development. Indeed, the research area is currently generating an enormous amount of interest, driven by the intersection of three powerful forces in physical/biological science research: 1) the broad realization that an interdisciplinary, collaborative approach to research can deliver rapid advances, 2) the exponential growth in the capabilities of analytical technol-

## From the Contents

<b>1. Introduction to Biomimicry</b>	9027
<b>2. <math>\beta</math> Turns/Spirals</b>	9028
<b>3. <math>\beta</math>-Sheet Fibrils</b>	9033
<b>4. <math>\beta</math>-Sheet Nanocomposites</b>	9038
<b>5. <math>\alpha</math>-Helix-Based Fibers</b>	9041
<b>6. PPII Helix-Based Fibers</b>	9044
<b>7. Tertiary Folded Domain</b>	9046
<b>8. Summary and Outlook</b>	9049

ogies and computational power, which allow elucidation of the structural and molecular organization of natural materials down to the smallest length-scales, and 3) the maturation of synthetic techniques, both chemical and biological, thereby allowing the facile construction of high-fidelity model systems as well as high-performance bio-inspired polymers. The rise in prevalence of the interdisciplinary mindset, as well as the recent development of analytical and synthetic methods, offer materials scientists an unprecedented opportunity to understand the molecular and structural mechanisms behind the multifunctionality,<sup>[33]</sup> adaptability, robustness, strength, toughness,<sup>[34]</sup> and elasticity<sup>[35]</sup> found in biological materials, and to translate these concepts into improvements in synthetic materials.

Biomimetic materials science involves three main components: 1) the elucidation of structure–function relationships from the study of biomimetic model systems, 2) the extraction, application, and adaptation of the underlying physical/chemical design principles, and 3) the discovery of new approaches to materials science challenges and new pathways to synthesis and manufacture, which extend the scope of the natural system to produce new materials.<sup>[36,37]</sup> This Review is primarily focused on biomaterials based on peptide/protein structures, the understanding of the molecular mechanisms which contribute to their excellent mechanical properties, and the application of that understanding towards the development of biomimetic synthetic materials. For each protein-based material subclass, we will first summarize what is known about nature’s molecular design, and then describe the design and synthesis of new materials inspired by the natural model systems.

[\*] Dr. A. M. Kushner, Prof. Dr. Z. Guan  
Department of Chemistry, University of California  
Irvine, CA 92697-2025 (USA)  
Fax: (+1) 949-824-2210  
E-mail: zguan@uci.edu  
Homepage: <http://chem.ps.uci.edu/~zgguan>

**Table 1:** Examples of advanced biological polypeptide materials.

Secondary & tertiary structure	Natural system	Natural function	Mechanical characteristics
$\beta$ turn/spiral	elastin	ideal connective elastomer, mechanical-energy storage material	resilience, deformation-tolerance, durability
$\beta$ sheet	amyloid-type fibrils	adhesion, encapsulation	stiffness, environmental stability
$\beta$ sheet nanocomposite	spider dragline silk	macroscopic structural engineering	stiffness, extensibility, toughness
$\alpha$ -helical coiled coil	vimentin	cellular structural integrity	toughness, enthalpic elasticity
polyproline type II triple helix	collagen	microscopic structural scaffolding extracellular matrix	elasticity, toughness, strength
tandem tertiary folded domains	titin	dissipative connective interface, damage protection, skeletal muscle suspension	recoverable toughness, passive elasticity

The scope of this Review is outlined in Table 1. Nature uses the 20 natural amino acids to engineer polypeptide materials with a wide range of high-performance mechanical properties. One widespread structural feature in natural structure-building biomaterials is the repetitive modular design that exists in many structural proteins,<sup>[38]</sup> including elastins, collagens, fibronectins, cadherins, and the skeletal muscle protein titin.

Modularity—starting from the amino acid monomers—is ubiquitous in natural protein-based structural materials;<sup>[39]</sup> this modularity aids the “controlled complexity”<sup>[40]</sup> of the bottom-up construction<sup>[41]</sup> and hierarchical self-organization<sup>[42]</sup> across multiple length-scales ultimately yielding the required advanced mechanical properties—so-called “collective emergent properties”<sup>[43]</sup>—that dramatically exceed the sum of the mechanical properties of their individual constituents. These structural proteins are important components in many soft tissues, and play essential roles in life processes. They possess excellent elasticity, and thus are capable of undergoing high deformation without rupture, storing or dissipating the energy involved in the deformation, and then returning to their original state when the stress is removed. When constantly subjected to myriad stresses, many structural proteins also demonstrate remarkable adaptive and dynamic mechanical behavior.

In this Review, we categorize the natural protein materials on the basis of the types of their modular repeat units, secondary folding structures such as  $\beta$  turn/spiral,  $\beta$  sheet,

$\alpha$  helix, polyproline II (PP-II) helix, as well as tertiary folded domains (Table 1). By mimicking these design principles, we have a tremendous opportunity to address some of the most fundamental challenges of materials science, such as material failure, benign synthesis and recyclability, confinement effects, as well as multiscale synthesis and fabrication.<sup>[44]</sup>

## 2. $\beta$ Turns/Spirals

### 2.1. Elastin

Mammalian elastin is a cross-linked rubber used by nature to provide a “lossless” connection between the softer, more viscous anatomical elements and the stiffer, higher-modulus ones. Elastin is an ideal mechanical energy storage material with a long lifetime that is employed, for example, in oscillating motor systems such as the heart, arteries, and lungs. The highly resilient elasticity of elastin, which is nearly devoid of hysteresis in cyclic stress/strain measurements, means that very little energy is dissipated thermally, with the majority of the mechanical energy stored during deformation. Thus, elastin-based biological elastomer components are characterized by extreme durability.<sup>[45]</sup> In addition, mammalian elastin sustains a large elongation at break, similar to man-made rubber systems.

The precursor of elastin is the soluble protein polymer tropoelastin, which consists of large (ca. 72 kDa), highly



Aaron M. Kushner received his BS from the University of California at Berkeley in 1999. While there, he also carried out research with Professor Carolyn Bertozzi at the Lawrence Berkeley National Laboratory. After graduation, he joined the medicinal chemistry department at Theravance, Inc., where he worked with Dr. John Griffin and Dr. Mathai Mammen. In 2004, he joined the Guan group at University of California, Irvine, where he was a recipient of the Eli Lilly fellowship. He has also received the Mike Zack and Hal Moore awards for graduate student research, and received his PhD in 2010.



Zhibin Guan is professor of Chemistry at the University of California, Irvine. He obtained his BS and MS from Peking University (China) and PhD from the University of North Carolina, Chapel Hill. Following post-doctoral research at Caltech, he spent five years at DuPont CR&D before moving to academia in 2000. He has received numerous awards, including the Beckman Young Investigator award, the Camille Dreyfus Teacher-Scholar Award, and the Humboldt Bessel Award. He was elected a Fellow of the American Association for Advancement of Science in 2008. His research interests span organic, biological, and macromolecular materials chemistry.



conserved modular repeat domains of  $(VPGXG)_n$ , where X represents a variable position, which in the case of elastin can be occupied by any amino acid other than proline. (The single-letter codes for amino acids are used in this Review.) These elongated repeat domains are connected by short, less-repetitive, alanine- and lysine-rich regions, with the lysine residues spatially grouped into tetrads.<sup>[46]</sup> The lysine-alanine sections provide amine functionality for the formation of oxidative cross-links, permanently fixing the structure. The lysine-alanine repeats are thought to adopt an  $\alpha$ -helical conformation, thereby resulting in the cofacial presentation of amines required for covalent cross-linking.<sup>[47–49]</sup> In addition to ordered self-assembly of cross-linking domains, the complete immersion of the protein polymer rubber in water and resultant equilibrium swelling is essential to its high-performance, mechanical energy storage properties.

As a permanently set elastomer, native elastin is highly insoluble and thus difficult to characterize. Additionally, recent experiments point to the secondary structure of the constituent polypeptide chains being highly dynamic. As a result, a single consensus structure/property relation has been elusive. In the following section, the representative structural models proposed for elastin are briefly summarized.

Hoeve and Flory<sup>[50]</sup> used calorimetry and subsequent thermodynamic arguments to propose a model of elastin elasticity that is very similar to that of classical rubber networks: long polymer chains randomly connected in a network, which remain mobile and amorphous (i.e., non-glassy) either intrinsically or, as in the case of elastin, after equilibrium swelling and plasticization by water. This elasticity model of rubber, which attributes the restoring force to the reduction of conformational entropy upon chain elongation, agrees with the near-ideal mechanical energy storage observed in the natural system. This model also agrees with NMR experiments, which illustrate the highly dynamic, and by inference disordered and random, nature of the polymer backbone.<sup>[51]</sup>

Whereas the random-network model correlates well with the average mechanical and thermodynamic properties of elastin, microcalorimetry studies suggest that the conformational disorder of elastin actually increases up to 70% extension. This clearly shows that at the microscopic level, the random-network model does not provide a precise picture of the molecular conformations adopted by this high-performance functional bio-elastomer.<sup>[52,53]</sup>

The classical model also ignores the highly ordered, modular, amphipathic nature of the protein backbone sequence between covalent cross-links. It seems unlikely that nature would expend the energetic cost for this order without some folding-derived effect on performance. The “liquid-drop” model proposes that the designed sequence programs hydrophobic collapse of the polymer side chains, thereby resulting in a “two-phase” network of spherical globules connected by covalent bonds formed between the hydrophilic residues on the exterior of the spherical particles.<sup>[54]</sup> These globules would then deform under stress into prolate spheroids. This model of interlinked compacted protein particles, however, is inconsistent with the aforementioned highly dynamic nature of the polypeptide backbone.

To better account for the inherent complexity in a way that does not contradict the observed spectroscopic data, Gray et al. put forward the two-phase “oiled-coil” model. In this research, transgenic, copper-deficient pigs were used to generate non-cross-linked elastin for higher-resolution sequencing of the backbone.<sup>[46]</sup> In this model,  $\beta$  turns, which are formed as the more hydrophobic V and P residues are forced inward, present the hydrophilic polyamide backbone for “oiling” by surrounding water molecules. A series of these turns yields a “coil” which is free of exterior inter- or intramolecular hydrogen bonds, thereby leaving only the hydrogen bond within the turn. This structure is consistent with the observed lack of a viscous, enthalpic component to the strain behavior, as the internal hydrogen bonds are likely only cleaved at high strains. The primary mechanism of elasticity in the “oiled-coil” model is therefore entropic, as the exposure of hidden hydrophobic side chains imposes order on previously free solvent water molecules when the  $\beta$ -turn-rich folded state uncoils and extends under stress. The sequential-turn protein assembles into a fibrillar, hydrated structure in which the turns are covalently connected through a permanent set of lysine-tetrad  $\alpha$ -helical domains. This mechanism is in agreement with electron microscopy studies of native elastin.<sup>[55]</sup>

While the proposed degree of stable secondary structure in the “oiled-coil” model would seem to disagree with ultrafast chain dynamics, it is possible that high-frequency thermal oscillation and flexing of the springlike “oiled-coils” could also explain the observed dynamics of the backbone. The more recent “librational” entropy theory of elastin elasticity, put forward by the Urry research group,<sup>[56–58]</sup> follows similar logic. In this model, the tandem  $\beta$  turns of the pentapeptide type II adopt a long-range “ $\beta$ -spiral” conformation (Figure 1). Longer-range “swaying” or “rocking” oscillations of these springlike structures would, in theory, be dampened when the macromolecule is stretched, thereby shifting them to a higher frequency and thus resulting in a decrease in the librational entropy and subsequent increase in the restoring force.

Although the librational mechanism likely contributes to local elastic response, recent simulations of hydrated poly-(pentapeptide)s suggest that the idealized linear  $\beta$ -spiral

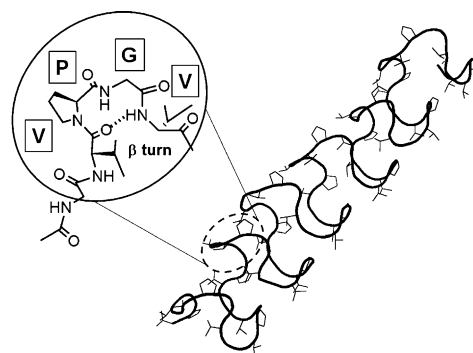


**Figure 1.** The proposed “ $\beta$ -spiral” conformation of VPGVG tandem repeats in elastin. Pymol representation from an entry in the Protein Data Bank courtesy of the Daggett research group.

model substantially overestimates the long-range order of the polymer network. Although some ordered secondary structure likely exists dynamically along the polypeptide backbone, it is suggested that water plays a key role in the elasticity of the elastin through hydrophobic hydration, thereby creating the entropic driving force behind the lower critical solution temperature (LCST) behavior observed in many amphipathic polymers.<sup>[59]</sup> This phenomenon may be the primary driving force behind the entropic restoring force of elastin. The well-characterized LCST behavior of elastin-like amphiphilic polymers<sup>[60]</sup> supports this hypothesis. The physiological temperature at which elastin operates is above the critical LCST value for hydrophobic collapse, but it is likely held in a frustrated intermediate state by the existence of permanent cross-links. This molecular mechanical frustration, which is known to contain substantially fewer hydrogen bonds between the main chains than is observed in typical globular proteins,<sup>[61]</sup> provides a plausible mechanism for both the ease of extension and the lossless resistance to further deformation, and therefore also for the resilient, durable macroscopic character of elastin.<sup>[40,62,63]</sup> The highly dynamic nature of elastin chains also supports a “frustrated collapse” mechanical model.

## 2.2. Elastin Mimics

The combined advanced elasticity, durability, and stimulus-responsive nature (e.g., LCST behavior) of elastin make it a promising biomimetic target. Numerous elastin-like polypeptides (ELPs) have been synthesized, by recombinant DNA expression<sup>[64]</sup> and chemical synthesis,<sup>[65]</sup> as both model systems for mechanistic study and as biomaterials for various biomedical applications (e.g., protein purification, drug delivery, tissue engineering).<sup>[66–72]</sup> These polymers are then assembled and/or cross-linked to varying degrees to obtain the final bulk biomimetic material.

### 2.2.1. Linear Elastin Mimicking Model Systems

Once the primary repetitive amino acid sequence for tropoelastin was obtained, simple polypeptide mimics could be synthesized. Urry et al. first synthesized short (VPGVG)<sub>1–3</sub> oligomers, which were investigated by <sup>1</sup>H NMR spectroscopy. This provided solid evidence for the existence of a preferred  $\beta$ -turn conformation adopted by the VP-GV tetrad, and the authors further hypothesized that a “stacking” of these turns in series would lead to a  $\beta$ -spiral type structure.<sup>[73]</sup> After confirming the energetic favorability of the proposed  $\beta$  turn with a crystal structure of *cyclo*(VPGVG)<sub>3</sub>,<sup>[74]</sup> the Urry research group again used NMR spectroscopy to characterize *cyclo*(VPGVG)<sub>6</sub>,<sup>[75]</sup> including the derivation of the pitch and helicity of the hypothesized extended spiral. Mathematical methods were then applied to the torsions, dihedral angles, and distances of these simple analogues to extrapolate the idealized  $\beta$ -spiral structure.<sup>[76]</sup> Yao and Hong used isotopically enriched (VPGVG)<sub>3</sub> to enhance the backbone signals in the solid-state NMR (ssNMR) spectrum, and found that the only hydrogen bonds in the main chain were present in the  $\beta$ -turn

units.<sup>[77]</sup> The authors point out that if such a polymer were stretched, and in agreement with microcalorimetry studies, these  $\beta$ -spiral structures would be distorted, thereby breaking the conformationally restrictive intraturn hydrogen bonds, and thus actually increasing the conformational entropy on deformation.<sup>[52,53]</sup>

The development of recombinant DNA technology led to various higher molecular weight poly(pentapeptide) polymers becoming available. These were used by Urry et al. to amplify the LCST transition during CD, NMR, and dielectric relaxation studies.<sup>[78]</sup> The dielectric relaxation studies showed increasing resonant behavior centered at approximately 25 MHz during the temperature-induced transition, which the authors attribute to the proposed librational mode of the  $\beta$ -spiral-type secondary structure.<sup>[79]</sup> Radiation was then applied to cross-link the intermediate-stage coacervates, and subsequent thermoelastic studies showed a dramatic increase in the elastomeric restoring force as the temperature was raised through the LCST transition.<sup>[58]</sup>

CD and <sup>1</sup>H NMR “exon-by-exon” studies performed on isolated chemically synthesized domains of tropoelastin confirm the highly dynamic, labile, and microenvironment-dependent conformation state of any local peptide region, with both polyproline II (PPII, a helical secondary structure found in proteins and protein materials that requires no stabilization through intrahelical hydrogen bonds) and  $\beta$ -turn structures represented in the conformational equilibrium. This led the authors to propose a “sliding  $\beta$  turn” (Figure 2) rather than an extended  $\beta$  spiral.<sup>[80]</sup> Arad and Goodman synthesized and studied decapeptide analogues that replaced the turn hydrogen bond of the amide at the variable position of the pentapeptide repeat unit with an ester.<sup>[81]</sup> They found in subsequent NMR and CD studies that much of the average secondary structure remained, as the highly flexible polypeptide was able to adopt alternate, low-energy  $\gamma$ - and  $\beta$ -turn conformations.<sup>[82]</sup> The authors point out that strong conformational preference and high flexibility are not mutually exclusive if a rapid equilibrium with a low energy barrier is maintained between multiple secondary structures of the backbone. However, 2D NMR studies on recombinant high-mass modular repeat ELPs, as well as shorter hexa(pentapeptide)s, showed that even this dynamic equilibrium model may overestimate the long-range order of the system, thus suggesting that conformational entropy must at some level play a role in elasticity.<sup>[83,84]</sup> Yamaoka and co-workers quantified the thermodynamic effects of various external conditions, such as salt concentration and surfactant addition, on the LCST, and came to the conclusion that the conforma-

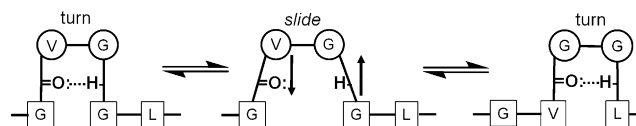


**Figure 2.** The “sliding  $\beta$ -turn” model of the conformational dynamics of the elastin backbone. The equilibrium intraturn hydrogen bond ruptures, thereby allowing the VG turn to “slide” to the right and become a GG turn. In this way, metastable turns propagate up and down the elastin chain.

tion space is undoubtedly complex, with multilevel interdependence of intramolecular backbone conformations and intermolecular association/aggregation states.<sup>[85]</sup>

Realizing that the identity of the time-resolved exact secondary structure of elastin is neither attainable nor the most relevant structure parameter, Meyer and Chilkoti focused instead on the average state, as reflected in the sequence- and environment-specific, and therefore tunable and stimuli-responsive, metric of LCST. To aid the further design of model and functional ELPs, the authors derived an empirical three-parameter equation based on concentration, sequence, and chain length that quantitatively predicts the LCST for an ELP of any given length, concentration, and composition.<sup>[86]</sup>

The arrival of high-resolution single-molecule force spectroscopy (SMFS) and atomic force microscopy (AFM) allowed further characterization of high-molecular-weight recombinant ELPs by microscopy. Urry et al. found that below the critical temperature, (GPGVP)<sub>251</sub> and (GVGIP)<sub>260</sub> terminated with two cysteine residues display near-perfect storage of the strain energy when stretched and relaxed by the probe tip of the microscope.<sup>[45]</sup> These curves could be fit well with the wormlike chain (WLC) model of molecular elasticity.<sup>[87]</sup> Above the LCST, the extension curve shows an abrupt change from an initial low-modulus region to an increased modulus zone that maintains a roughly constant value throughout the remainder of the pull. This behavior implies that, at least at the single-molecule level, the hydrophobically collapsed structure has a significant amount of order that unfolds under stress in much the same manner as one would expect from an extended  $\beta$  spiral or a  $\beta$ -turn-rich random coil. Further SMFS studies by Valiaev and co-workers show that a reduced entropic penalty is required for mechanical unfolding in an apolar solvent environment, which reflects the significance of the “hydrophobic hydration” model of lossless elastic resistance to deformation.<sup>[88]</sup>

### 2.2.2. Cross-Linked ELP Materials from Recombinant and Synthetic Polypeptides

As a consequence of its highly repetitive, modular sequence, the core elastic protein polymer of elastin is easily emulated; however, the complex processes of controlled deposition, assembly, and cross-linking are not. In an attempt to improve the mechanical properties of the earliest direct side-chain-coupled<sup>[65]</sup> and radiation-cross-linked<sup>[58]</sup> elastin-mimic model systems, several research groups have turned to traditional chemical cross-linking<sup>[89]</sup> and sequence-directed assembly.

McMillan and Conticello introduced regularly spaced lysine cross-linking functionalities every fifth repeat to obtain [(VPGVG)<sub>4</sub>(VPGKG)]<sub>n</sub>.<sup>[90]</sup> The lysine substitution at the flexible fourth residue of the repetitive elastic motif was treated with a bis-*N*-hydroxysuccinimide (NHS) ester to afford gels with up to 17% intermolecular cross-linking of the amine functionality. The introduction of cross-linking modules to the backbone did not compromise the LCST properties, which indicates that the elastic behavior of the natural system should be retained. However, cross-linking-triggered

coacervation occurred, unlike in the case of biological elastin synthesis, where the permanent network is set after, not before or during, coacervation and assembly. Martino et al. increased the extent of cross-linking by incorporating two reactive amines in each repeat unit.<sup>[91]</sup> Despite elastin-like “physicochemical” properties, such as characteristic CD spectra and connected-fibril morphology, the uncontrolled cross-linking of short (< 3 kDa), solution-synthesized, tandem repeats—this time with glutaraldehyde (GTA)—prevented the realization of high-performance elastin-like mechanical properties.

Welsh and Tirrell also used the (VPGIG)<sub>n</sub> tandem repeat, this time programming the lysine residues to be situated near the termini of the recombinant protein polymer, rather than evenly spaced throughout the backbone.<sup>[92]</sup> GTA was again employed, and, in the absence of an additional self-assembly director, no improvement in the control of the cross-linking was expected due to the complex profile of the amine-aldehyde reaction product. However, when the hydrogels were stretched under physiologically relevant conditions, by using a special testing chamber, the samples revealed a respectable elongation-to-break metric of about 250–400%, although the tensile strength and modulus were orders of magnitude lower than elastin. The first two parameters, however, are highly dependent on minor defects, thus illuminating one of the core challenges of biomimetic materials science: demonstrating a conclusive link between microscopic design and macroscopic properties. However, the strategic placement of amine groups at the polymer termini appeared to improve the tensile properties of the material compared to those with random or 100% incorporation.

A more radical assembly/processing alternative was employed by Huang et al. by forcing concentrated solutions of engineered polypentads through an electrospinning apparatus, which resulted in fine, fibrous networks with controllable dimensions.<sup>[93]</sup> Interestingly, 10 nm surface folds observed on these fibers are close in size to thin filaments observed after aggregation of native tropoelastin, which indicates that the stretching conditions of the spinning process induced by shear flow and an electric field may support the oriented self-assembly of polymers. In this case, the resulting nonwoven material demonstrates a respectable strength and modulus of 35 MPa and 1.8 GPa, respectively, but at the cost of the desired energy storage and shape-recovery mechanics found in high-performance elastin-based structures, such as arterial blood vessels. In further studies, the authors introduced a solid-state photo-mediated acrylate cross-linking step after spinning, which allowed the mechanical characterization of water-plasticized samples.<sup>[94]</sup> These materials behaved comparably to native elastin in terms of initial modulus (0.45 MPa) and elongation-to-break (105%). Importantly, the degree of cross-linking obtained by solid-state NMR spectroscopy agrees reasonably well with the degree of cross-linking predicted for a theoretical ideal rubber elastomer possessing a similar mechanical profile.

In further studies, the same research group engineered ABA triblock protein copolymers in an attempt to achieve ordered assembly in a process similar to the self-assembly of hard and soft domains in triblock thermoplastic elastomers

such as polystyrene-*b*-polybutadiene-*b*-polystyrene. In addition to improved control over the physical cross-linking process and ultimate network morphology, this approach enabled fine-tuning of the size and sequence of the middle block, and therefore the viscoelastic and mechanical properties. Indeed, the authors found that simply switching the Pro-Gly type II  $\beta$ -turn-forming motif to a Pro-Ala type I turn resulted in a transformation from an elastic to a plastic tensile character.<sup>[95]</sup> In a further refinement of this approach, the modular protein polymer LysB10 was engineered to have hydrophobic, plasticlike end blocks, with lysine pairs flanking each block (Figure 3a).<sup>[96]</sup> Glutamic acid was included in the soft elastic midblock to increase the hydrophilicity and

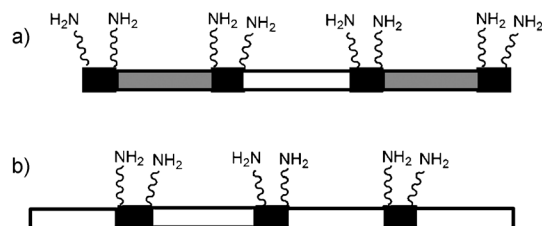


**Figure 3.** Design of bioengineered cross-linkable elastin-mimetic proteins. a) Thermoplastic elastomer of the A-B-A type (black: lysine cross-link domain, white: elastic (VPGXG)<sub>n</sub>, gray: plastic domain (IPAVG)<sub>n</sub>). b) Elastic domains separated by lysine cross-linking domains.

presumably water-induced plasticization. After casting below the LCST and GTA vapor-phase treatment to induce permanent set, any un-cross-linked material was dissolved away. This left 88 wt % of the original material, which suggests a high degree of permanent network formation after assembly. Lim et al. achieved similar results with A, ABA, and BABA recombinant block copolymer ELPs cross-linked with tris(hydroxymethyl)phosphines.<sup>[70]</sup> Lysine diisocyanate (LDI) has also been used to cross-link multiblock ELPs, thereby resulting in elastin-like mechanical characteristics (Figure 3b).<sup>[97]</sup>

In an attempt to more closely mimic nature's sequential approach to assembly and cross-linking, Keeley et al. engineered an elastin-mimic protein polymer with distinct alanine-rich, lysine-containing assembly/cross-linking domains separating the (VPGVG)<sub>n</sub> elastic recoil modules.<sup>[98,99]</sup> The authors hypothesized that temperature-triggered phase separation of the hydrophobic elastic sections at temperatures above the LCST might lead to advantageous orientation of the cross-linking domains. This ordering might allow oxidative formation of desmosines, which require the proximity of multiple lysine residues during the subsequent oxidation with pyrroloquinoline quinone (PQQ), unlike the above-mentioned synthetic cross-linking approaches. Indeed, lysine groups were permanently cross-linked under mildly oxidizing conditions after aggregation. The impressive resilient elasticity of these materials, as measured by bulk mechanical testing, and the elastin-like aggregates, as observed by electron microscopy, demonstrates the effectiveness of this approach.

### 2.2.3. Hybrid Elastin Mimics

Although high-molecular-weight, monodisperse, high-fidelity ELPs can be obtained by recombinant DNA techniques, the process is labor-intensive and typically low-yielding. To improve the efficiency and variability of ELP synthesis, several research groups have synthesized linear elastin-mimic hybrid polymers (EMHPs) by employing some nonpeptidic elements in the polymer construction.

#### 2.2.3.1. Hybrid Polymers with Elastin Motifs in the Main Chain

Grieshaber et al. used the versatile copper-catalyzed Huisgen “click” triazole cyclization<sup>[100]</sup> to obtain high-molecular-weight EMHPs.<sup>[101]</sup> In these model systems, the backbone was constructed by AA-BB polymerization by azide-alkyne cycloaddition of cross-linking alanine-lysine bis(alkyne) pentad modules and PEG-bis(azides) to simulate the entropic spring domains. The use of this polymerization approach enables systematic adjustment of the peptide sequence, water interactions, and covalent cross-linking to tune the mechanical properties of the resulting material. Although resilient materials were obtained, there was not a dramatic difference between the hydrated and dehydrated forms, thus indicating that a different mechanism of entropic elasticity than that of elastin may be at play, not surprisingly considering that monophilic PEG domains replaced the amphiphilic VPGXG entropic spring cassette domains of elastin in this model system.

Recently, Chen and Guan designed a new class of linear elastin “entropic spring domain” mimics, by also taking advantage of the known efficiency and functional-group tolerance of copper-catalyzed “click” chemistry to link together VPGXG pentads to form high-mass polymers (Figure 4).<sup>[102]</sup> Unlike the previous “click” EMHP example, an AB-type monomer was used, thereby simplifying the synthesis by rendering stoichiometry irrelevant. The authors synthesized three azide-alkyne pentad monomers: 1) VPGVG, which is expected to adopt a  $\beta$ -turn conformation, 2) GVGVP, with the proline residue placed next to the spacer to disrupt the  $\beta$  turn of the core VPG sequence and enforce a “random-coil” geometry, and 3) V<sup>D</sup>PGVG, which is based on the well-known propensity of the D-proline-glycine dyad to adopt a type II'  $\beta$  turn, as an alternate turn motif. After polymerization, the presence of these conformations was confirmed by CD spectroscopy. However, all three polymers displayed classic LCST behavior, and as the first

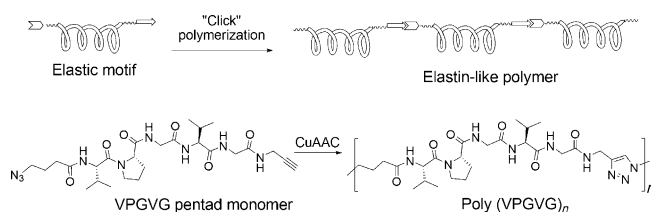


**Figure 4.** Bioinspired modular synthesis of elastin-mimic polymers through “click” chemistry. Reprinted from Ref. [102] with permission. Copyright 2010 American Chemical Society.

two polymers possessed very similar mechanical properties, this study further suggests that hydrophobic hydration, rather than well-defined secondary structure, plays the crucial role in the elasticity of elastin. The simple modular “click chemistry” provides an efficient approach to access a broad range of elastin-mimic polymers for many potential biomaterials applications.

### 2.2.3.2. Hybrid Materials having Elastin Motifs in the Side Chains

A more radical biomimetic approach is to use pentad side chains, thereby decoupling any observed LCST behavior from the direct hydrophobic collapse of the backbone itself. Thus, the dynamics of the chain conformation are fundamentally different from those of elastin. Van Hest and co-workers synthesized EMHPs with VPGVG side chains by using atom-transfer radical polymerization (ATRP). Although the degree of polymerization was low ( $DP < 10$ ), the heavy monomer afforded reasonable molecular weights for this initial system.<sup>[103]</sup> By growing the chain from both ends of a PEG block, ABA polymers were obtained that showed the characteristic concentration-dependent LCST behavior associated with elastin-like and amphiphilic polymers composed of unnatural monomers.<sup>[104]</sup> A linear dependence of the LCST on the molecular weight, analogous to peptide ELPs, was found for the side-chain elastin mimics. Noting that classical polymer thermodynamics predict that the LCST is not dependent on polydispersity,<sup>[105]</sup> Fernandez-Trillo et al. were able to tune the transition smoothly over a 10°C range by simply mixing various polymers in specific ratios.<sup>[106]</sup>

Roberts et al. synthesized norbornene with a VPGVG side chain for ring-opening metathesis polymerization with the Grubbs catalyst.<sup>[107]</sup> Despite the known sensitivity of the catalyst to polar functionality,<sup>[108]</sup> the authors were able to obtain side-chain EMHPs (albeit with  $DP < 10$ ) by performing the polymerization at low temperature (0°C). Studies on the resulting polymers showed that the LCST behavior and the size of the collapsed globules were similar to those of high-mass ELPs obtained by genetic engineering. By adjusting the solvent mixture to avoid aggregation, Conrad and Grubbs were able to obtain high-molecular-weight VPGVG/PEG<sub>4</sub> side-chain copolymers.<sup>[109]</sup> The authors were able to linearly adjust the solvent/self-interaction parameters, and hence the LCST, by random incorporation of the two side-chain monomers in various ratios.

In summary, at the macroscopic level, mammalian elastin is a fairly simple system, in that its mechanical properties can be accurately modeled by the classical theory of the elasticity of ideal rubber. At the microscopic level, on the other hand, the picture becomes increasingly dynamic and complex. However, the apparent key driving force of the function and performance of elastin—hydrophobic hydration-driven protein folding, which is manifested in the observed LCST—is in fact one of the most fundamental tools of life itself, being involved in every aspect of biological conversion and transduction of mechanical energy.<sup>[110]</sup> Thus, mimicking this behavior is not only useful for structural materials, but can also provide valuable lessons for energy efficiency and sustainable consumption.<sup>[111]</sup>

## 3. $\beta$ -Sheet Fibrils

The assembly of  $\beta$ -sheet peptides/proteins in natural, synthetic, and hybrid systems was recently reviewed.<sup>[112,113]</sup> In this section, we will focus on the structures and materials-related properties of natural  $\beta$ -sheet fibrillar assemblies, followed by a survey of the most recent advances in the design and fabrication of their biomimetic analogues. The term “amyloid” will be used to describe multiscale aggregates of  $\beta$ -sheet fibrils of either natural fiber-forming proteins or synthetic sequence analogues thereof.

### 3.1. Amyloid Fibrils

“Amyloid” is the name most commonly associated with the plaques of long, stiff fibers found in Alzheimers and other disease pathologies, although evidence suggests that the elongated fibers represent the end-state of the disease, and that most physiological damage is done by the shorter oligomers that are precursors to fibril formation.<sup>[114,115]</sup> Recently, the adventitious use of long-range functional amyloid fibers in biology was reported. Amyloid-based biological materials include super-adhesives,<sup>[116,117]</sup> tough encapsulants,<sup>[118]</sup> pigment stabilizers,<sup>[119]</sup> and stiff neuronal interconnects;<sup>[119]</sup> these and other functions were recently reviewed by Smith and Scheibel.<sup>[120]</sup> Thus, nature is able to take advantage of the superior mechanical strength, high aspect ratio, and resistance to chemical degradation of the spontaneously assembled  $\beta$ -sheet fibrils. Of further advantage to synthetic nanotechnology is that, unlike stiff biological fibers such as actin filaments<sup>[121]</sup> or microtubules,<sup>[122]</sup> amyloid fibers do not require complex signaling or constant energy input to maintain their mechanical function.<sup>[123]</sup>

The high-resolution microstructure of amyloid protofibrils has recently been further investigated by X-ray diffraction,<sup>[124,125]</sup> electron microscopy,<sup>[126]</sup> atomic force microscopy,<sup>[127]</sup> and 2D NMR spectroscopy,<sup>[128]</sup> as well as by comparison with known structures<sup>[129]</sup> and molecular dynamics simulations.<sup>[130]</sup> However, a sequence-to-microstructure correlation remains unclear, because of the large number of observed crossed- $\beta$  isoforms of amyloids. This complex mixture of kinetically trapped equilibrium morphologies suggests a large and nonlinear dependence of the final structure on the specific sequence and environment of the assembly. A wide variety of helical twists, pitches, and cross-over distances can even be observed among protofibrils with identical amino acid sequences.<sup>[131]</sup>

In 1935 the biophysicist William Astbury was the first to propose that proteins might exist in a “fibrous” state as well as the accepted “globular” form.<sup>[132]</sup> Eanes and Glenner went on to identify the “cross- $\beta$ ” X-ray signature<sup>[133]</sup> that is now considered to be the definitive marker of the “amyloid” protein state: extended fibers consisting of repeating  $\beta$ -sheets oriented perpendicular to the fiber axis.

One compelling molecular mechanism for fibril assembly was recently revealed by the Eisenberg research group.<sup>[134–136]</sup> The authors identified the smallest “active” segments of known amyloidogenic proteins. These peptides were synthe-



sized and found to both nucleate and inhibit fibril growth from whole proteins in a concentration-dependent manner. The research group then obtained microcrystals of these peptides; determination of their structures yielded an atomically resolved model cross-section of the cross- $\beta$  fibril spine. The resulting structures suggest that long-range fibril assembly occurs through axial intersheet hydrogen bonds (main-chain and side-chain) between “steric-zipper” laterally stapled sheets. The authors went further, computationally identifying the “amyloyme”, all the segments within three major genomes that possess a sequence for acting as a “steric zipper” and therefore intrinsically possess the ability to nucleate fibrils.<sup>[137]</sup> The number of proteins with suitable sequences is, from the perspective of a protein-based life form, disturbingly high. However, the authors note that, with the limited conformational flexibility of a short sequence buried in a stable, folded globular protein, fibril nucleation is thankfully difficult, and most proteins containing a zipper-capable sequence seem to have evolved with conformational restrictions strategically located to prevent undesired amyloid nucleation. From a nanotechnology standpoint, of course, the observed sequence promiscuity of amyloidogenic proteins suggests that the fine-tuning of fibril-based materials for specific mechanical properties and biological interactions should be attainable.

Smith et al. studied the mechanical properties of insulin-derived  $\beta$ -sheet fibrous aggregates by AFM, where they observed surprisingly high strength and stiffness values comparable to other excellent structural materials such as silk and steel.<sup>[138]</sup> Further studies suggested that the measured values are close to the maximum predicted for defect-free structures.<sup>[139]</sup> This is difficult to imagine for a structure that, while fundamentally dynamic, assembles irreversibly with a high kinetic bias. The authors point out, however, that any structural defects would present preferential fracture sites, thereby enabling ordered growth to resume at the fracture faces. This self-correcting behavior, along with a unique and relatively linear relation between rigidity and cross-section shape, supports the idea that these structures comprise a generic class of materials.<sup>[140]</sup>

Despite the difficulty in obtaining large-scale structure/property correlation for a system with a high degree of structural variability and notorious insolubility, further insight into the microscopic mechanism behind the superior mechanical properties of amyloids and amyloid-like fibers has been obtained by molecular modeling and AFM techniques. One key observation relates to the critical length of hydrogen-bond arrangements necessary for cooperative rupture and high strength. Atomistic computational studies of mechanical protein modules by Keten and Buehler have shown that under a uniform shear load, simultaneous rupture of the hydrogen bonds occurs only up to a maximum cluster size of four bonds.<sup>[141]</sup> This size limit for maximum strength enhancement is likely a result of the “energy balance” concept of fracture mechanics. This model describes the maximum mechanical strength as a function of the competition between the core dissociative effect of the entropic constraints placed on the protein backbone by the ordered structure and the associative energy of cooperative hydrogen-bond forma-

tion.<sup>[142]</sup> The cross- $\beta$  structure is composed of short, stacked  $\beta$ -sheet repeats that form a dense array of small hydrogen-bonded clusters, thus maximizing microscopic cooperative behavior and large-scale mechanical strength at longer length-scales without sacrificing too much entropy in any one structural element.<sup>[130]</sup> Cooperative rupture of the short  $\beta$ -sheet repeats has also been observed at the single-molecule level in algal adhesive amyloids.<sup>[143–145]</sup>

Molecular dynamics studies of the compression behavior of single amyloid protofibrils reveal that the assembly of a protein polymer into an amyloid or amyloid-like form results in an increase in the persistence length by several fold.<sup>[146]</sup> While this stiffness metric is still an order of magnitude lower than the all-covalent carbon nanotubes (CNTs), the preparation of  $\beta$ -sheet fibrils is easier and more environmentally friendly, and their rich and tunable chemical functionality offers a promising approach to addressing a long-standing challenge in polymer chemistry: rational control over macromolecular architecture by variation of the length, sequence, stereochemistry, and charge balance.<sup>[147]</sup> With further study, biomimetic, multiscale cross- $\beta$  aggregates should ultimately be amenable to spatiotemporal and mechanical-property-specific “bottom-up” microfabrication.

### 3.2. $\beta$ -Sheet Fibril Mimics

#### 3.2.1. Functional Materials from Amyloidogenic Proteins/Peptides

One simple approach to achieving useful materials based on the hierarchical assembly of  $\beta$  sheets is to use external thermal and chemical stimuli to obtain the controlled assembly of a readily available wild-type protein that possesses an amyloidogenic sequence. Although such proteins have a tendency to rapidly form insoluble, unprocessable plaques and aggregates, Knowles et al. were able to achieve nanoscopic control over the fibrillization process to obtain high-performance films by careful temporal adjustment of the pH value and post-assembly plasticization (Figure 5a).<sup>[148]</sup> The authors first incubated unmodified hen lysozyme in dilute HCl solution (3 % w/w) at 65 °C. This combination of gentle denaturing and elevated temperature substantially blocked uncontrolled kinetic aggregation, thus favoring slow thermodynamic self-assembly over a period of two weeks. When cast from solution after the addition of PEG400 plasticizer (0.8 % v/v), the films displayed liquid-crystalline nematic order, as observed by polarization microscopy. Further X-ray diffraction experiments confirmed the sought-after ordering across a hierarchy of length scales: nanometer ordering of the cross- $\beta$  structure within the fibrils, and micrometer order in the stacking of the fibrils. The films displayed a Young's modulus on the order of 6 GPa, which is comparable to the strongest biological materials, such as keratin, collagen, and silk. In addition, the processing of individual cross- $\beta$  fibrils into films yielded bulk materials with only slightly reduced mechanical properties compared to the individual microscopic structures (Young's modulus 2–12 GPa). This is in direct contrast to films generated from high-performance carbon-based materials, such as “Bucky

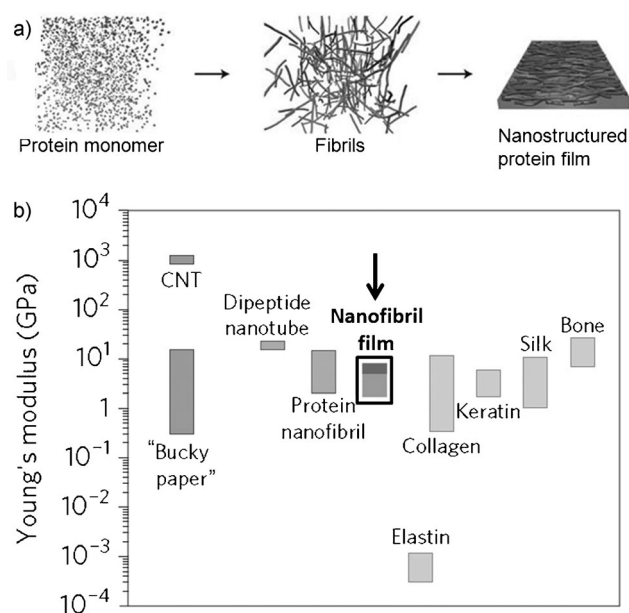


**Figure 5.** a) Protein monomers (hen lysozyme) are first assembled into amyloid-like fibrils, which are then stacked into films. b) Comparison of the Young's moduli of different materials shows that the artificial nanostructured protein films have high moduli. The modulus decay upon assembly into films is much less for protein nanofibrils than for other stiff nanofibrils such as carbon nanotubes. Reprinted from Ref. [148] with permission. Copyright 2010 Nature Publishing Group.

paper", which suffer dramatic loss of modulus and strength compared to the individual molecular components (Figure 5b). The authors attribute this advantageous behavior to the rich functional surface of the proteinaceous fibrils, which favor the establishment of robust and efficient inter-fibril contacts.

Another approach is to utilize a smaller, fibril-forming segment of the larger native protein. Scheibel et al. chose the N-terminal and middle region of yeast Sup35p, which they had previously identified as forming cross- $\beta$  fibrils with diameters of 9–11 nm, a suitable size and shape for nanocircuitry.<sup>[149]</sup> The bidirectional growth of fibrils could be controlled by mechanical agitation during assembly. The fibers were metalized with gold in a three-step process starting with conjugation of cysteine to gold nanoparticles (Au-NPs) followed by two enhancement steps, which resulted in continuous metallic connections between the electrodes, as indicated by the observed ohmic  $I$ - $V$  characteristics. The authors note that the high stability of the fibers to environmental stresses such as temperature, salt, denaturants, acids, and bases is promising for future industrial-scale processes. In addition, the proteinaceous nature of the fibril scaffold enables a broad platform of chemical diversity for future bionic and sensing applications.<sup>[150]</sup>

The Gazit research group was able to simplify the fibril sequence even further. Proposing that  $\pi$ - $\pi$  stacking may play a key role in fibril assembly, they compiled the sequences of known disease-causing amyloids, and noted that most contained at least two phenylalanine or tyrosine residues within the shortest active segment of 5–10 amino acids. However,

these aromatic residues are among the rarest—occurring in only 3.9 and 3.3% of available positions, respectively, in natural proteins.<sup>[151]</sup> In addition, these residues are among the most highly conserved, which implies specific and selective function. With this in mind, the research group simply dispersed concentrated solutions of diphenylalanine in aqueous solvent, and observed the spontaneous assembly of hollow, high-aspect ratio, high-persistence-length nanotubes (Figure 6). The tubes were then used to cast silver nanowires,

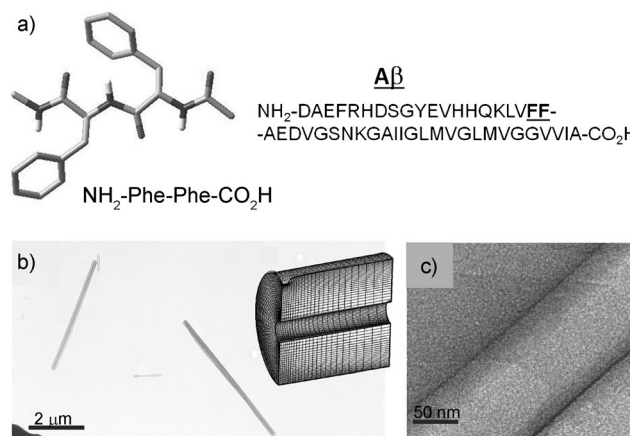


**Figure 6.** Self-assembly of peptide nanotubes by a molecular recognition motif derived from the  $\beta$ -amyloid polypeptide. a) The central aromatic core of the  $\beta$ -amyloid polypeptide is involved in the molecular recognition process that leads to the formation of amyloid fibrils. b) TEM images of the nanotubes formed by the diphenylalanine peptide. c) HRTEM images of the peptide nanotubes. Adapted from Ref. [152] with permission. Copyright 2003 American Association for the Advancement of Science.

which could be obtained with high uniformity after enzymatic degradation of the diphenylalanine nanotube mold.<sup>[152]</sup> The tubes were further characterized by nanoindentation by using AFM, which afforded an estimated Young's modulus of 19 GPa, compared to 1 GPa for microtubules.<sup>[153]</sup>

The Artzner research group discovered a unique  $\beta$ -sheet-based nanotube system that forms spontaneously from a solution of the Lanreotide octapeptide (Figure 7a).<sup>[154]</sup> The peptide is a short  $\beta$ -turn unit with three hydrogen bonds which is covalently stabilized by an intramolecular disulfide bond and presents a cooperative D-A-D and complementary A-D-A H-bond recognition motif on the upper and lower edge of the turn unit. Systematic segregation of the aromatic and aliphatic units drives unidirectional, face-to-face dimerization of the turn unit, thus presenting three cooperative hydrogen bonds on each edge and resulting in spontaneous cross- $\beta$  assembly into hollow nanotubes of micrometer length and a rigidly monodisperse radius. These tubes further assemble into a hexagonally packed lattice. The key to the remarkable order of the assembly system is the presence of an overall +2 charge per peptide, which balances the attractive forces and prevents uncontrolled aggregation.

The authors propose that the resulting nanotube structures, similar to natural amyloids, are the result of a kineti-

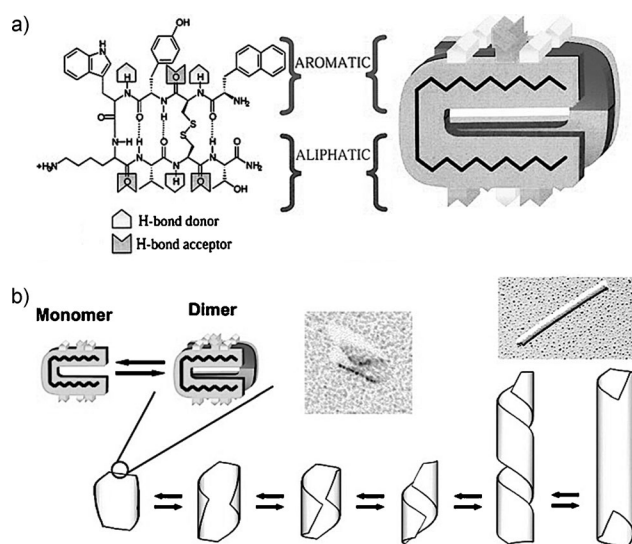


**Figure 7.** a) The Lanreotide molecule in the planar  $\beta$ -hairpin conformation, which is stabilized by the disulfide bridge, the  $\beta$  turn, and intramolecular hydrogen bonds. b) Intermediates and sequence of the nanotube self-assembly process. The formation of Lanreotide nanotubes is described by a sequence of equilibria between the different intermediate oligomeric species (monomer, dimer, open ribbons, helical ribbons, and short nanotubes). Adapted from Ref. [154] with permission, copyright 2003 National Academy of Sciences, and Ref. [155], copyright 2010 American Chemical Society.

cally biased equilibrium process, which could eventually lead to defect-free or even self-healing/self-correcting nanomaterials.<sup>[155]</sup> The Lanreotide cross- $\beta$  nanotube assembly serves as a model biomimetic hierarchical assembly system. As a consequence of the high solubility, highly ordered and uniform structure, and fast nucleation and elongation steps of this model system, in contrast to natural amyloid assemblies, the clear observation of intermediate ordered states and transformations is facile (Figure 7b). Concentration- and temperature-dependent X-ray and microscopy studies reveal a three-step pathway marked by successive energy road-blocks: monomer/dimer, dimer/open ribbon, and open ribbon/nanotube equilibria are clearly observed. The authors observe that the “spontaneous emergence of such well-defined complex and multiscale supramolecular architectures is strongly enhanced when the formation route is punctuated with stable” well-defined, long-lifetime intermediate states, “each of them preparing the next assembly step. Furthermore, the precise and unequivocal self-assembly process is driven by the subtle balance of van der Waals attractive and repulsive electrostatic forces.”<sup>[155]</sup>

While the nanotube-like aspects of cross- $\beta$  amyloid mimics make them promising candidates for high-performance structural and nanoelectronic materials, as well as useful model systems of self-assembly, the propensity for the assembly of  $\beta$  sheets into long-range, highly interacting, hydrophilic structures is also a useful property for achieving novel soft materials, such as hydrogels. This is a promising avenue of study, as the resulting materials incorporate

protein-like tunability into the material nanostructure for control over the functionality and mechanical properties, and the materials themselves are completely derived from abundant natural resources.<sup>[156]</sup>

Aggeli et al. noticed that the peptides K24 and K27, each with two diphenylalanine core motifs, readily form  $\beta$ -sheet structures in lipid bilayers. X-ray and FTIR analysis showed that the peptides assembled into  $\beta$ -sheet tapes when extracted into amphiphilic solvents, with a rheologically derived upper limit for the film thickness of 0.7 nm, thus implying single-molecule thickness.<sup>[157]</sup> The tapes quickly formed a stable gel, which could be denatured to a simple Newtonian fluid by the addition of sodium dodecylsulfate (SDS), which screens peptide amphiphilicity and induces the formation of  $\alpha$  helices. From these experiments and previous literature reports, the research group suggested a set of criteria for the rational design of gel-forming peptides: 1) cross-strand attractive forces between side chains, 2) constrained assembly limited to one dimension by recognition of the lateral  $\beta$  strand, and 3) surface functionality of the tape such that solubility is maintained during and after assembly.

Zhang and co-workers also observed the assembly of helical tapelike intermediates into ribbons, fibrils, and fibers in a concentration-dependent manner with their KFE-8 amphiphilic octapeptide.<sup>[158]</sup> This system, which yields fibers of identical chirality and similar dimensions to natural amyloids, provides a simplified version of the dynamics of amyloid assembly. In further studies, Vauthey et al. switched from the KFE-8 alternating-philicity peptide to a head-to-tail hydrophilic/hydrophobic arrangement such as  $V_6D_2$  and found that these relatively inexpensive and functionalizable peptides assembled into large, hollow,  $\beta$ -sheet bilayer nanotubes and vesicles.<sup>[159]</sup> The Deming research group also successfully employed the head/tail peptide amphiphile strategy to obtain tunable, rapidly recovering hydrogels for potential biotechnology applications.<sup>[160]</sup>

Aulisa et al. took the rational design of  $\beta$ -sheet-forming peptide amphiphiles a step further. The peptide  $K_2(QL)_6K_2$ , for example, possesses a bifacial alternating hydrophilic (glutamine) and hydrophobic (leucine) core, a standard common cross- $\beta$ -fibril motif.<sup>[161]</sup> To limit assembly to one dimension, the core sequence was flanked by self-repelling charged lysine (positive) or glutamic acid (negative) residues. By adjusting the subtle balance between repulsion and attraction, the authors were able to control gelation through the pH value and ionic strength modulation, thereby leading to the formation of highly uniform double-sided cross- $\beta$  tapes with lengths on the order of several micrometers, and thus elegantly demonstrating the biomimetic strategy of molecular frustration to achieve the controlled assembly of functional materials with higher order.<sup>[161]</sup> Further lengthening and interlocking of the fibers could be achieved by adding divalent cations to cross-link the flanking acid residues, as well as by covalent capture of the gel network through oxidation of the cysteine residues on the exposed hydrophilic face of the fibers. As with the amphiphilic peptide system developed by Aggeli et al., the gels displayed thixotropic behavior, that is, thinning under shear, but rapidly recovering stiffness after the removal of shear force. Thus, the gels can be

injected easily and recover their mechanical properties spontaneously in situ. Further covalent assembly and enhancement of the stiffness of the  $\beta$ -sheet gels was also achieved in a biocompatible manner by Jung et al. by using native chemical ligation.<sup>[162]</sup>

Although the ordered charge in amphiphilic peptides is promising as a design strategy for biomimetic amyloid-type materials, there are undoubtedly some applications where the dimensional restrictions on assembly that are necessary for solubility are undesired. Various chemically triggered assembly strategies were developed to increase the dimensionality of the assembly process while maintaining the solubility necessary for process control. For example, Collier et al. demonstrated the externally triggered assembly of amyloid-mimic peptides by the light/temperature-induced rupture of salt-containing liposomes, which led to the screening of the repulsive forces in charged peptides and temporal/spatial control of the aggregation.<sup>[163]</sup> Cao and Raleigh utilized a “switch” peptide approach to achieve triggered assembly (Figure 8).<sup>[164]</sup> Ser20 of the IAPP (amylin) amyloid forming

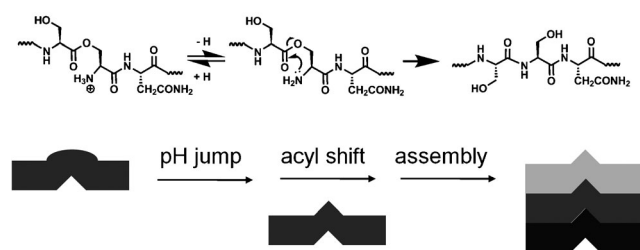


**Figure 8.** The “switch-peptide”-triggered assembly approach. Adapted from Ref. [164] with permission. Copyright 2010 American Chemical Society.

peptide was incorporated into the sequence through an ester bond between the adjacent residue and the serine hydroxy group, thereby disrupting the hydrogen-bonding system of the  $\beta$ -sheet core. When the dangling ammonium group of the amino acid was deprotonated by raising the pH value, rapid transamidation occurred, which restored the hydrogen-bonding scheme and led to spontaneous fiber formation.<sup>[164]</sup> Recently, Bowerman and Nilsson developed a terminal-cysteine-cyclized KFE derivative.<sup>[165]</sup> Reduction of the disulfide opened the macrocycle, thereby triggering amphipathy-mediated assembly of filaments.

By incorporating an artificial  $\beta$ -turn unit between two amyloid-mimic peptides, one may stabilize the resulting extended cross- $\beta$  structures. To this end, Kelly and co-workers used their previously developed cationic peptidomimetic receptor, which contains a 2,8-dibenzofuryl  $\beta$ -turn mimic.<sup>[166]</sup> The authors introduced anionic peptide guests to catalyze long-range assembly, although under certain conditions the receptor itself assembled through intercalating  $\beta$  sheets and stabilizing interactions between cationic and aromatic functions. Numerous highly amyloid-like fibril morphologies were observed, the structures of which could be easily controlled by altering the pH value or ionic strength of the premix solutions. By employing a similar strategy, Schneider

et al. used a D-Pro-D-Pro artificial turn for the pH-triggered assembly of  $\beta$ -sheet hydrogels from the MAX1 polypeptide.<sup>[167]</sup>

Since the biomimetic strategies discussed so far for the assembly of  $\beta$ -sheet fibrils consist of short single- or double-strand  $\beta$ -sheet-forming sequences, as well as whole protein polymers, the resulting assemblies are usually either extremely hard and brittle, as in the case of di(phenylalanine), or extremely soft, such as MAX1-derived hydrogels. It would be advantageous to develop an amyloid-mimic system that incorporates the toughness inherent in the hierarchical amyloid nanostructure while maintaining the beneficial tunability and chemical functionality of short peptide biomimetic systems. To this end, Yu et al. devised a convergent synthetic method to obtain high-molecular-weight peptide polymers that form  $\beta$ -sheet fibrils, while avoiding the inherent complexity of bio-engineering. Reasoning that the covalent linkage of multiple short strand-forming sequences would entropically favor strong, multiscale hierarchical assemblies, the authors employed their previously developed 1,3-triazole turn-forming unit<sup>[168]</sup> to connect many short, synthetically accessible alanine repeat blocks through copper-catalyzed “click” azide–alkyne [2+3] cycloaddition polymerization (Figure 9).<sup>[169]</sup> To prevent premature assembly, an acid-labile

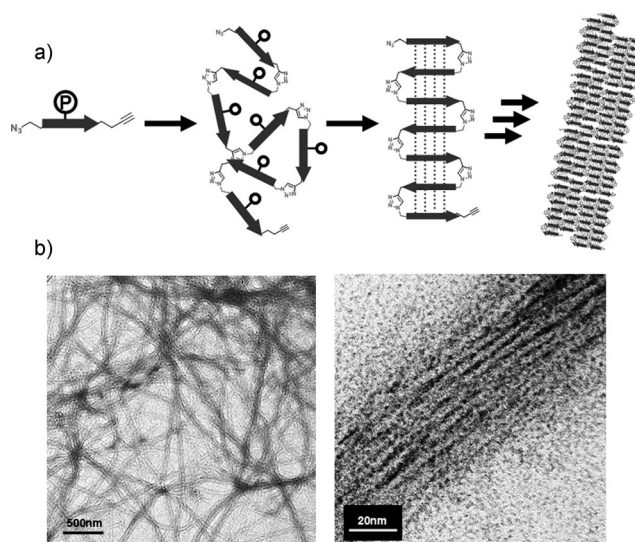


**Figure 9.** a) Cycloaddition-induced folding and self-assembly: [2+3] cycloaddition leads to the polymerization of a protected peptide monomer. Upon deprotection, the polypeptides fold into well-defined antiparallel  $\beta$  strands, and the self-assembly of multiple  $\beta$  sheets forms hierarchical nanofibrils. b) A representative TEM image of nanofibrils of the  $\beta$ -sheet polymer and a high-magnification view of one nanofibril. Reprinted from Ref. [169]

dimethoxybenzyl (DMB) amide-protecting group was required during synthesis. After a pH-triggered cleavage, the peptide polymers assembled into long, hierarchically organized fibrils. With further sequence variation and more controlled processing, the authors expect the modular  $\beta$ -sheet polymer to yield a tunable range of advanced functional properties.



### 3.2.2. Functional Materials from Oligomer/Polymer–Peptide Hybrids

Another pathway to amphiphilic, self-assembling  $\beta$ -sheet systems is to incorporate a non-peptide tail, which adds another dimension of assembly control. This approach was elegantly demonstrated by Hartgerink et al.<sup>[170,171]</sup> By modulating the repulsive charge balance through the pH value, the peptide–alkyl conjugates assembled reversibly into uniform and high aspect ratio fibers, with the  $\beta$  sheets oriented perpendicular to the fiber axis and the greasy dodecyl tails packed into the interior. The inclusion of cysteine in the sequence enabled permanent covalent capture of these structures through the formation of intermolecular disulfide bonds. Paramonov et al. further illustrated the importance of the assembly of cross- $\beta$  hydrogen bonds close to the fiber core, as opposed to simple hydrophobic packing, by observing that selective methylation of amides adjacent to the alkyl tail prevented assembly of the fibrils. IR spectroscopic studies, both parallel and perpendicular to the fiber axis, confirmed a layer structure intermediate between the twisted helix and the cross- $\beta$  fiber, thus revealing the molecular basis for both the axial stability of the nanofibers and elongation along the  $z$ -axis.<sup>[172]</sup> Recently, Pashuck et al. showed that it is possible to fine-tune this axial stability (stiffness) by varying the V/A sequence and thus the degree of hierarchical cooperative connectivity of the  $\beta$  sheets within the fibril.<sup>[173]</sup> For further control of the assembly properties, a photolabile *o*-nitrobenzyl protecting group was installed nearest to the alkyl tail.<sup>[174]</sup>

Smeenk et al. also used the chimeric approach, this time with the opposite polarity. The research group expressed a polyalanine  $\beta$ -sheet core with glutamic acid groups strategically placed to block post-assembly aggregation along the wider fibril axis by charge repulsion. PEG blocks were then conjugated to terminal cysteine residues, thus restricting assembly to one dimension and resulting in uniform fibrils several micrometers in length.<sup>[175]</sup>

By capitalizing on modern controlled polymerization techniques, several research groups have taken the chimeric fibrillar assembly strategy a step further. Hentschel et al. used assembly design triggered by a switch peptide with both hydrophobic poly(*n*-butyl acrylate)<sup>[176]</sup> and hydrophilic PEG<sup>[177]</sup> chimeric peptide polymer conjugates to obtain ordered tape structures in organic and aqueous media, respectively. Enzymatically triggered assembly was also demonstrated,<sup>[178]</sup> as well as nondestructive post-assembly chemical modification.<sup>[179]</sup> The same research group then incorporated oligothiophenes into the assembly system,<sup>[180]</sup> with the ultimate goal of generating conducting molecular wires with controlled nanostructure. The Frauenrath<sup>[181,182]</sup> and van Hest<sup>[183]</sup> research groups employed a similar strategy to provide a template for polyacetylene synthesis through the assembly of  $\beta$ -sheet-forming oligopeptides, thereby resulting in highly uniform molecular wires formed from amyloid-like helical tapes.

Despite serious research challenges inherent to such insoluble systems, substantial progress has been made toward both the understanding and the mimicking of  $\beta$ -

sheet fibril materials. With further effort it is likely that both the tunable assembly and high-performance mechanical properties of this relatively simple nanoarchitecture will lead to profound technological advances.

## 4. $\beta$ -Sheet Nanocomposites

Silk is a remarkable proteinaceous structural material that has been used in nature for 400 million years, was adapted for the mass production of silk fiber a few millennia ago, and was only recently reverse engineered and synthesized *in vivo*. The limited availability of this useful class of material during World War II inspired the design and synthesis of the “artificial silk” nylon, thus launching the modern revolution in the development of materials from petrochemical feedstock.<sup>[184]</sup> The fundamental protein building blocks of these fibrous materials are designed for specific mechanical characteristics, rather than for the catalytic and recognition functions of most globular proteins, thus making them intriguing scaffolds for advanced biomaterials.<sup>[185]</sup> The variable modular design strategy and environmentally friendly synthesis make silk an almost universal basis for a wide range of synthetic materials.<sup>[186]</sup> The highly repetitive primary sequence structure and bulk properties of various silk proteins were recently reviewed.<sup>[187]</sup>

### 4.1. Spider Dragline Silk

Many naturally produced structural protein polymer fibers are classified as silks. The moth *Bombyx Mori*, for example, produces a stiff but brittle silk thread for protective larval cocoons.<sup>[188]</sup> Spiders are another well-known silk producer. The silk manufacturing apparatus in spiders has evolved over hundreds of millions of years, and often the same organism is capable of “spinning” exceptional fibers with widely varying mechanical properties, each adapted to a specific application.<sup>[189]</sup> In addition to the “dragline” silk that provides the mechanical support for insect-trapping structures and a superb lifeline for spider mobility, many spiders, for example, synthesize an elastin-like silk, which after spinning, coating with a specific molecular cocktail, and wetting with water becomes an ideal ballistic trap.<sup>[190–192]</sup> In each case the mechanical properties of the silk are a direct result of the specific polypeptide sequence and extrusion conditions (Figure 10).

The dragline silk of spiders is one of nature’s true multifunctional supermaterials (Table 2).<sup>[193]</sup> Under tension or compression, it out-performs most man-made materials (Young’s modulus: 10–50 GPa; elongation to break: 10–30%; tensile strength: 1.1–1.4 GPa),<sup>[193–195]</sup> and it possesses other advanced properties such as shape memory.<sup>[196]</sup> The dragline silk biopolymer has long been studied, since it was identified early on as an ideal model for biomimetic advanced materials. As with the other materials described, recent advances in high-resolution microscopy and spectroscopy, computational modeling, and processing power have yielded significant

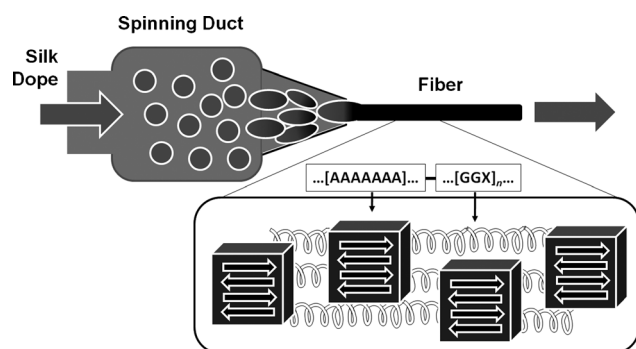


**Figure 10.** The synthesis of a  $\beta$ -sheet nanocomposite superfiber: the spinning process and self-assembled morphology of spider dragline silk.

**Table 2:** A comparison of the mechanical properties of common high-strength fibers.<sup>[a]</sup>

Material	Tensile strength [MPa]	Elongation at break [%]	Toughness [MJ m <sup>-3</sup> ]
<i>Bombyx mori</i> cocoon silk	600	18	70
<i>Araneus diadematus</i> dragline silk <sup>[b]</sup>	1100	27	160
nylon	900	18	80
kevlar 49	3600	2.7	50
high-tensile steel	1500	0.8	6

[a]. Adapted from Ref. [193] with permission, copyright Portland Press Limited. [b] Spider dragline silk is the toughest known fiber material, natural or synthetic.

insight into the molecular mechanism behind the remarkable properties of silk, much of which was reviewed recently.<sup>[197–199]</sup>

Although the high  $\beta$ -sheet content of dragline silk was established early on by X-ray diffraction studies on silk fibroin,<sup>[200]</sup> the amino acid sequence of the protein precursor leading to the strongest and toughest silk fiber, that of major ampullate silk, was not definitively established until 1990.<sup>[201]</sup> Xu and Lewis successfully sequenced a partial cDNA fragment reverse-transcribed from mRNA generated by forced silking of the common dragline silk model organism *nephila clavipes*.<sup>[202]</sup> The researchers found that the protein sequence was in general not rigidly conserved, but two clear repetitive segments were identified: a series of repeating modules of 4–6 alanine residues flanked by 3–4 GGX-type repeats. Thus, the protein structure resembles a segmented multiblock copolymer.

In a simplistic model, the structure of bulk dragline silk can be viewed as a semicrystalline material made of entangled, interacting amorphous protein polymer chains physically cross-linked and reinforced by strong and stiff antiparallel  $\beta$ -sheet nanocrystals.<sup>[203,204]</sup> These crystallites comprise 20–35 % of the material volume.<sup>[205]</sup> The presence of both highly oriented crystallites and weakly oriented “protocrystals”<sup>[206]</sup> is essential for the unusually high compressive strength of the silk fiber, possibly to reap the benefits of a “graded” modulus that reduces the probability of premature catastrophic failure as a consequence of interfacial

stress. Equally as important is the size of the crystallites, which are limited to < 10 nm by strategically placed glutamine and other polar, bulky residues that disrupt long-range crystal packing. Atomistic simulations by Keten et al. have shown that this restriction of crystallite size limits the number of simultaneously loaded hydrogen bonds to approximately four per sheet, which is the most stable number for interstrand interactions. By capping the growth at this value, the sequence design effectively limits the incorporation of defects during crystallite assembly. Subsequent deformation is thus distributed evenly, allowing concerted, cooperative failure at the maximum possible stress.<sup>[207]</sup>

Although the self-assembled nanoparticle component is crucial to the ultimate mechanical characteristics of the composite, it comprises only a minor fraction of the material volume. In addition to the elastin-like GPGXX motif, the “soft” GGX repeat segment is a major component of the hierarchical composite material, and therefore its secondary structure is highly relevant to the mechanical performance of dragline silk. The polymer chains of this matrix can be effectively modeled as amorphous, although local variability in the modulus of the matrix is essential to model fidelity. Recent X-ray studies indicate a relatively high degree of alignment and secondary order within the “amorphous” silk component, thus leading to the “two-phase” matrix model proposed by Jelinski et al.<sup>[208]</sup> From the data, the authors proposed an extended  $3_1$ -helix conformation for the GGX repeat segments, which is consistent with the elongational flow of the silk gel solution during spinning. This arrangement allows for efficient but noncrystalline packing through interstrand hydrogen bonding, which could lead to a significant enhancement of the mechanical properties compared to a purely amorphous matrix, while still maintaining the conformational flexibility required for elasticity. To further assess the level of order of this matrix component, van Beek et al. fed spiders <sup>13</sup>C-enriched amino acids and studied the resulting silks by solid-state NMR spectroscopy with 2D correlation techniques.<sup>[209]</sup> After analyzing the torsions of the  $\alpha$ -carbon atoms, the authors found an “order correlation function” of 0.742, which is in agreement with the “two-phase” matrix concept. The mechanical properties of the silk can, therefore, be modeled as a function of the volume fraction of highly ordered ( $\beta$ -crystallite) relative to less-ordered (matrix) components.<sup>[210]</sup>

As a modular self-assembled nanocomposite,<sup>[211]</sup> the design of dragline silk enables fine control over the crystallite size, aspect ratio, and interfacial energy, while avoiding the conventional roadblocks to ideal mechanical enhancement of nanocomposites, such as high mixing viscosity and exfoliation of the particle aggregates. Thus, the spider is able to achieve the desired balance of initial modulus, tensile strength, extensibility, and resilience for each specific application.

Unlike man-made high-performance polymers such as kevlar, which require harsh and environmentally unfriendly processing conditions,<sup>[212]</sup> the silk protein polymer hierarchically assembles into a functional fiber from aqueous solution at ambient temperatures by using mild chemical and thermal cues. The literature covering the silk spinning process was recently reviewed.<sup>[198]</sup> Unlike the other natural materials

described in this Review, spider silk is extruded *in vivo* by a complex spinning process. Thus, the chemical, mechanical, and thermal conditions under which the stable pre-spun solution of the polymer is dehydrated to form a dry fiber (i.e., the “processing conditions”) are at least as important to the final mechanical properties of the silk as the specific primary sequence of the protein polymer feedstock itself.<sup>[213,214]</sup> There are two primary models for dragline silk spinning: 1) The protein precursors exist in an ordered, liquid-crystalline pre-spun state that optimizes dope viscosity and suppresses the formation of defects during crystallization,<sup>[199]</sup> and 2) lyotropic partitioning yields intermediate colloidal states, thereby preventing premature aggregation during assembly of the crystallites.<sup>[215]</sup> Both rely on careful spatial control of an ordered cascade of chaotropic/kosmotropic chemical cues (such as specific ion concentration and pH) mediated by special cells lining the spinning duct.

Two recent studies provide key insights to aid our understanding of the molecular mechanism that directs the assembly of silk fiber.<sup>[216]</sup> Their research focused on the role of the nonrepetitive (NR) N and C termini of the silk-dope precursor protein, which were found to adopt a rare  $\alpha$ -helical-barrel tertiary structure. Askarieh et al. constructed “mini-spidroins”, with only four repetitive cosegments between the termini, to test the hypothesis that the N-terminal NR region is responsible for triggering the pH-dependent aggregation of the spidroin.<sup>[217]</sup> By observing the thermodynamic and chemical stability of the folded protein, as well as the LCST behavior, Hagn et al. showed that the C-terminal region serves as the primary spatial director of ordered fiber formation (Figure 11).<sup>[218]</sup> Remarkably, both research groups found that the terminal region of the spidroin is not only responsible for the ordered assembly of the fiber, but also acts to delay undesired aggregation and catastrophic precipitation in the concentrated storage state of the silk dope.

## 4.2. Spider Dragline Silk Mimics

### 4.2.1. Recombinant Silk Mimics

Expression of recombinant DNA protein of silk-mimic protein polymers and its subsequent processing has been

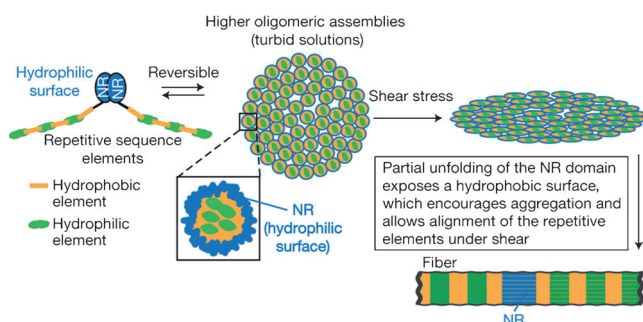


**Figure 11.** The key organizing role played by the nonrepetitive (NR) domain of silk fibroin during the intricate process of silk-fiber assembly. Reprinted from Ref. [218] with permission. Copyright 2010 Nature Publishing Group.

nicely reviewed.<sup>[219]</sup> The bioengineering approach has allowed researchers to systematically vary the 1) chain conformation, 2) lamellar thickness, 3) unit-cell structure, and 4) lamellar surface structure of nanocrystals in a monodisperse manner.<sup>[220]</sup> Krejchi et al. used this biosynthetic approach to perform targeted structure/property studies on isolated  $\beta$ -sheet nanocrystallite segments, with the aim of mimicking the high degree of control over the chain architecture and supramolecular organization exemplified by spider dragline silk.<sup>[221]</sup>

Qu et al. subsequently bioengineered a modular protein polymer incorporating both  $\beta$ -sheet-forming and elastin-like repeats.<sup>[222]</sup> For the hard blocks, the soluble amphiphilic oligopeptide (AEAKEAKAK)<sub>2</sub> designed by Zhang et al.<sup>[223]</sup> was used to undergo a pH-triggered switching from an  $\alpha$ -helix to a  $\beta$ -sheet conformation. The GPGQQ elastin mimic was chosen as the soft-block repeat unit. As predicted, the polymer displayed irreversible hydrogelation through assembly of a  $\beta$  sheet as conditions were adjusted to disfavor the soluble  $\alpha$ -helix structure of the hard-block repeat.<sup>[222]</sup>

One major challenge of working with larger bioengineered silk mimics is the premature and irreversible aggregation of the alanine-rich segments. To avoid this complication, Valluzzi et al. engineered a silk protein with strategically placed methionine residues.<sup>[224]</sup> These could be oxidized to increase the polarity of the protein, thereby reversibly adding a polar sulfoxide in place of an otherwise hydrophobic residue. The authors found that the methionine trigger, once reduced to induce assembly of the aggregate, did not interfere with the silk assembly process, thus allowing facile manipulation of the otherwise intractable silk protein. In addition, unlike native silk and most mimics, the assembly could be reversed by reoxidation of methionine.<sup>[225]</sup> As these triggering conditions are relatively harsh, Winkler et al. installed serine phosphorylation/dephosphorylation sites to yield a milder enzymatic assembly signal.<sup>[226]</sup>

Nagapudi et al. took an alternative approach, deviating substantially from the natural design by engineering an ABA (hard-soft-hard) polypeptide silk mimic with three large blocks rather than multiple short segments, analogous to polystyrene-*b*-polybutadiene-*b*-polystyrene systems. This “protein thermoplastic elastomer” could be cast into mechanically robust films, whose properties such as strength, toughness, and extensibility could be easily controlled by varying the process parameters of solvent, temperature, and pH value.<sup>[227]</sup>

Researchers attempting to produce engineered high-fidelity dragline silk mimics on an industrial scale face additional challenges. For example, the repetitive nature of the sequence prevents the use of PCR, and the codon arrangement makes prokaryotic expression difficult.<sup>[228]</sup> In the 1990s, researchers at DuPont successfully cloned and expressed complete dragline silk genes in a bacterial vector,<sup>[229]</sup> which—by using modern microfabrication techniques—enabled spinning processes that incorporated varying degrees of mechanical and chemical control.<sup>[230]</sup> Lazaris et al. achieved a significant breakthrough by using mammalian cells to produce high-mass, soluble silk protein polymer mimics in the milk of transgenic goats.<sup>[231]</sup> However, the low

yield and aggregation during storage prevented the realization of commercially viable silk-mimic materials using this approach. Recently, Huemmerich et al. employed a combination of solid-phase DNA synthesis and PCR to obtain genes suitable for high-yield expression in *E. coli*, thereby circumventing the inherent synthetic challenges discussed above.<sup>[232]</sup> In addition to performing structure/property studies on the nonrepetitive domains, as discussed above, the authors developed a biomimetic spinning process which could potentially lead to the best mechanical properties of synthetic silk fibers.<sup>[233]</sup>

#### 4.2.2. Hybrid Silk Mimics

Despite long-standing interest in the development of spider dragline silk mimics, the inherent challenges associated with controlling the crystallization of  $\beta$ -sheet peptides and the importance of the complex spinning process make this an extremely challenging prospect. Noting the conceptual similarity between synthetic thermoplastic elastomers and the dragline silk design, Rathore and Sogah took advantage of AA + BB diamine/diisocyanate type polymerization to combine short  $\beta$ -sheet-forming AGAG repeats with different soft PEG regions.<sup>[234]</sup> In situ formation of isocyanates from PEG diacids followed by condensation afforded high-molecular-weight polyureas (8–16 kDa) in good yield. Simple casting of concentrated trifluoroethanol solutions resulted in microphase-separated films with a high  $\beta$ -sheet content as determined by AFM, FTIR and <sup>13</sup>C NMR spectroscopy, as well as X-ray diffraction. In subsequent tensile tests, the research group observed promising mechanical properties—about an order of magnitude weaker than spider silk (in the absence of any processing optimization). Shao and co-workers used a similar approach, with both a short aliphatic spacer<sup>[235]</sup> and a longer polyisoprene soft block, which also yielded polymers with a high  $\beta$ -sheet content.<sup>[236]</sup>

Despite these elegant studies, the design of a synthetic polymer that can imitate both the structure and mechanical properties of spider dragline silk remains a major challenge. It will require a careful consideration and subtle balancing of the various molecular parameters that control polymer secondary structures to achieve optimal mechanical properties.<sup>[237]</sup> In addition, the fiber spinning process is extremely important for obtaining the desired mechanical characteristics.<sup>[238,239]</sup> Further progress in this area will likely come from close collaborations between chemists, biologists, materials scientists, and engineers.

## 5. $\alpha$ -Helix-Based Fibers

### 5.1. Natural $\alpha$ -Helix-Based Hierarchical Fibers

The  $\alpha$  helix is one of the most important secondary conformations of peptide/protein polymers. Pauling et al. opened the door to the modern elucidation of protein structure with their presentation of the proposed  $\alpha$ -helix structure in 1951.<sup>[240]</sup> From a materials science perspective, the springlike molecular structure is simple and compelling.  $\alpha$ -

Helical hierarchically assembled fibrous proteins, such as vimentin and keratin, play a key structural role as the “truss” design elements of the eukaryotic cell—maintaining the mechanical integrity of the cell under stress<sup>[241]</sup>—and forming the structural basis of strong, robust bulk materials such as hair, horn, and hoof.<sup>[242]</sup>

At its core level of hierarchical structure, the  $\alpha$  helix is based, like many of the protein material systems described in this Review, on the O···H–N hydrogen bond. The next level, the 3.6 residues per complete helical turn, contains three of these hydrogen bonds, and many turns arranged in tandem form the  $\alpha$ -helical filament.<sup>[243]</sup> Filaments of this type can further assemble into dimers or “coiled coils.” For example, the cytoskeletal intermediate filament (IF) vimentin is a homodimeric “coiled coil” of two  $\alpha$ -helical proteins. The dimer is polarized, with a “head” and “tail”, and this orientation, combined with short exohelical protein folds, encodes the ultimate assembly of long-range, mechanically robust fibrils.<sup>[244,245]</sup>

Unlike synthetic materials, where even small defects or cracks typically lead to orders of magnitude reductions in mechanical strength, natural materials such as hair possess a remarkable tolerance to defects. Recently, molecular dynamics simulations on idealized  $\alpha$ -helix networks demonstrated a similar behavior, as a result of the concerted reversible rupture of the three hydrogen bonds of the helical turn. This unfolding event travels along the filament in an “elongation wave”, dissipating energy and revealing hidden length, until the helix is completely uncoiled, and the stress is passed along the network to the next  $\alpha$ -helix module. The organization of these helical modules into hierarchical nanostructures results in materials with both high strength and excellent tolerance of defects.<sup>[34]</sup>

When two of these helices are assembled into a coiled coil, the resulting materials display “superelasticity”, that is, they are capable of sustaining large deformations at high strengths. This behavior is analogous to the increase in rope strength with an increasing number of constituent braids. Additionally, coiled-coil  $\alpha$ -helix dimers possess a nonlinear stress/strain response, known as strain hardening, above the behavior expected from a random coil entropic spring or single helix. This phenomenon has been attributed to an  $\alpha$ – $\beta$  transition,<sup>[246]</sup> which was observed in X-ray studies on strained keratin fibers.<sup>[247,248]</sup> Essentially, as the proximal  $\alpha$  helices unfold, a solvophobic driving force induces the two strands to redimerize, this time in a stiff  $\beta$ -sheet conformation.

Recently, Waite and co-workers identified a new superelastic coiled-coil material in the egg sac of the channeled whelk *Busycon Canaliculum*. Remarkably, unlike keratin, which shows only slow recovery, the bio-encapsulant spontaneously recovered its original  $\alpha$ -helical dimer structure after release of the stress, spontaneously reversing the  $\alpha$ – $\beta$  transition (Figure 12).<sup>[249]</sup> By using this mechanism, the material combines high modulus, reversible extensibility, and impact/energy dissipation properties, which are ideal for insulating damage-prone tissues. The authors were further able to show that the material conforms to the Clausius–Clapeyron free energy relation for polymer fibers under



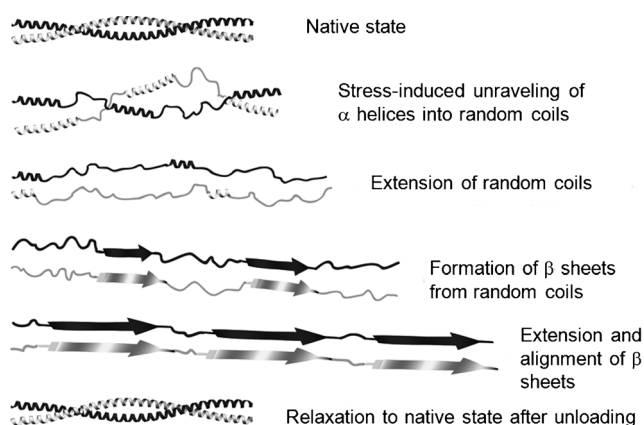


**Figure 12.** Schematic diagram of the  $\alpha$ -helix to  $\beta$ -sheet transition during straining. This enthalpic, rather than entropic, mechanism leads to high energy dissipation and rapid recovery, an indispensable combination of mechanical properties for life in the tidal zone. Adapted from Ref. [249] with permission. Copyright 2009 Nature Publishing Group.

stress, thus proving the previously hypothesized existence of a truly enthalpic, rather than entropic, form of elasticity.

## 5.2. $\alpha$ -Helix-Based Mimics

### 5.2.1. $\alpha$ -Helix Model Systems

The coiled-coil  $\alpha$ -helix motif represents a powerful design strategy for biomimetic hierarchical materials. The dimerization of short  $\alpha$ -helical peptide segments is among the most prevalent driving forces for protein folding, and is thus crucial to many important biological processes. As a result, the fundamental structure/property relationships governing the kinetics and thermodynamics of the assembly of coiled coils have been extensively studied,<sup>[250–254]</sup> which has led to a rare and well-defined set of methods for the design of hierarchical materials.

The research elucidating the core parameters of coiled-coil assembly is well-reviewed.<sup>[255–258]</sup> Briefly, the structure was proposed by Crick<sup>[259]</sup> to consist of two right-handed  $\alpha$  helices wrapped around each other with a slight left-handed superhelical twist. The sequence, elucidated by Hodges et al.<sup>[260]</sup> as well as McLachlan and Stewart,<sup>[261]</sup> consists of periodic repeating amphipathic heptad modules, defined as positions (abcdefg)<sub>n</sub>. As revealed by O'Shea et al.,<sup>[262]</sup> the “inside-group” positions **a** and **d** face into the supercoil, and provide the primary driving force for dimerization (Figure 13).<sup>[263]</sup> These positions typically encode the hydrophobic “leucine-zipper” core of the coiled-coil “peptide velcro”,<sup>[264]</sup> although buried polar residues such as arginine and asparagine are often included to control the specificity and orientation.<sup>[265]</sup> Positions **e** and **g** are typically charged amino acids that mediate intra- and interhelical electrostatic interactions, and thus the equilibrium between dimers, trimers, and higher oligomers,<sup>[266,267]</sup> and are often arranged to destabilize undesired pairings. The pH-dependent nature of these charged positions enables a convenient trigger for external control of peptide dimerization. Positions **b**, **c**, and **f** make up the

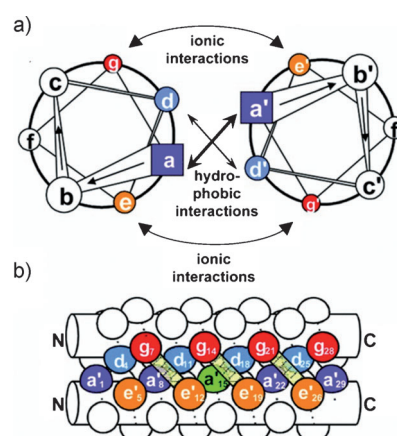


**Figure 13.** Schematic representation of a parallel dimeric coiled coil. a) Top view: arrangement of the heptad positions. b) Side view: the helical backbones are represented by cylinders, the side chains by knobs. Whereas residues at positions **a** and **d** make up the hydrophobic interface, residues at positions **e** and **g** pack against the hydrophobic core. They can participate in interhelical electrostatic interactions between residue *i* (position **g**) of one helix and residue (*i*' + 5) of the other helix (position **e**'), as indicated by the hatched bars. Adapted from Ref. [263] with permission. Copyright 2000 Elsevier.

“outside group”, and facilitate the nondestructive placement of solubilizing functionality for model dimers and offer a convenient handle for the programming of further hierarchical assembly. Extensive computational<sup>[268–271]</sup> and biological<sup>[272,273]</sup> studies have been carried out to elucidate the “interactome”,<sup>[274]</sup> a comprehensive set of molecular  $\alpha$ -helix “tectons”<sup>[275]</sup> that self-assemble from complex mixtures with limited cross-talk, and thus hold promise for the design of complex, hierarchical structural networks.

### 5.2.2. Hierarchical $\alpha$ -Helix-Based Materials

Petka et al. were among the earliest to take advantage of the leucine-zipper coiled-coil motif in the controlled synthesis of functional biomimetic materials.<sup>[276]</sup> By using recombinant protein engineering, they synthesized a triblock protein polymer consisting of a coiled-coil hydrophobic zipper assembly module flanked by hydrophilic random-coil polyelectrolyte domains, thereby allowing independent engineering of interchain and solvent interaction parameters. The triblocks were then further polymerized by oxidation of terminal cysteine residues. Most of the **e** and **g** positions of the helical heptad modules were populated with glutamic acid, which destabilized the coiled-coil structure in basic solution, thus facilitating pH control of gelation.

Formation of higher-order fibrils from designed coiled-coil peptides was observed by Kojima et al.<sup>[277]</sup> Initially intended to form simple coiled-coil bundles, the  $\alpha$ 3 peptide was found to assemble into fibers made up of smaller fibrils oriented along the long axis of the fibers when the salt concentration was elevated. While hydrophobic effects were assumed to provide the major driving force for the higher assembly, the authors suggest that charge-screening-mediated reduction of electrostatic repulsion between filaments must also play a role.

Following this early study, several research groups became engaged in the de novo design of higher-ordered fibrils from short  $\alpha$ -helical coiled-coil peptides. Potekhin et al. developed the  $\alpha$ FFP ( $\alpha$ -fibril-forming) peptide,<sup>[278]</sup> reasoning that multiple identical heptad repeats could facilitate the fibril-like assembly of elongated bundles through axially staggered association because of the possible offset of one or more heptads. To increase the thickness of the fibrils, alanine was placed at position **e**, where hydrophobic residues are known to encourage four- and five-stranded coiled coils. Glutamic acid and arginine were placed in positions **f** and **g** to encourage the formation of interhelical salt bridges between **f** and **g'**, again biasing the assembly in favor of thicker, five-stranded coiled coils. Finally, glutamine residues were placed in positions **b** and **c** to form an interhelical hydrogen-bonding network. X-ray diffraction studies showed that this novel peptide yielded uniform soluble fibrils with a diameter of 2.5–3 nm, consistent with the five-stranded coiled-coil design made up of axially oriented  $\alpha$  helices. Further studies using STEM to determine the mass-per-unit-length of the fibrils found that the cross-sections contained ten  $\alpha$  helices, thus suggesting that the final fibrils are in fact dimers of five-stranded protofilaments, a structure that would enable the formation of an extensive interbundle hydrogen-bond network between the glutamines in the **b** and **c** positions.<sup>[279]</sup> The authors note that although the design was intended to yield fibrillogenesis at neutral pH, it in fact only occurred below pH 6, thus suggesting an overestimation of the importance of the **f**–**g'** salt bridge. By simple substitution of glutamic acid with serine, extended, ordered fibrillogenesis was observed at neutral pH.<sup>[280]</sup> Conticello and co-workers further elaborated this model<sup>[281]</sup> by incorporating a reversible pH-sensitive trigger for assembly inside the hydrophobic core by substitution of three isoleucine residues with histidine.<sup>[282]</sup> This configuration also enabled the selective ion-induced assembly of fibrils.<sup>[283,284]</sup>

Rather than rely on adventitious staggering of homooligomers, the Woolfson research group designed a staggered heterodimer that forms a coiled-coil structure with dangling, “sticky” ends to overcome the “blunt-ended” barrier to further coiled-coil assembly (Figure 14).<sup>[285]</sup> These self-assembling fiber peptides, SAF-p1 and SAF-p2, are based on a natural hexa-heptad 42-mer coiled-coil sequence. SAF-p1 was truncated by two heptads at one end, and SAF-p2 by two heptads at the other, with the core hydrophobic coiled-coil functionality retained in the center of both peptides. The authors found that mixtures of the two resulted not only in the desired longitudinally assembled fibrils of axially oriented  $\alpha$  helices, but also in substantial lateral assembly into larger fibers that could be covalently trapped by thioester-based ligation.<sup>[286]</sup> One possible explanation for higher assembly is that, as the fibrils elongate, cooperatively strong interfibril interactions can arise from individually weak associative functionality (avidity effect). Indeed, computational models suggest that the designed staggering of parallel, “sticky-ended” coiled-coil dimers would result in alternating patches of charge that could lead to further assembly.<sup>[285]</sup> The second generation SAF peptides was thus designed to increase the stability and thickness of the fibril through strategic place-

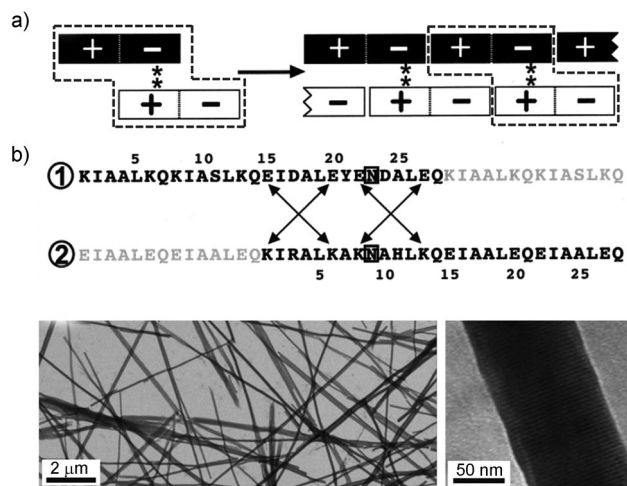


**Figure 14.** Design and sequences of the self-assembling fiber (SAF) peptides. a) Concept of a sticky-end assembly process together with the designed amino acid sequences. Complementary charges in companion peptides direct the formation of staggered, parallel heterodimers; the resulting “sticky ends” are also complementary and promote longitudinal association into extended fibers. b) The resulting periodically banded fibrils. Adapted from Ref. [285] with permission, copyright 2000 American Chemical Society, and Ref. [287].

ment of complementary charged residues winding around the exterior of the two coiled-coil peptides, thereby resulting in striated, uniform fibrillogenesis reminiscent of that found in intermediate filaments.<sup>[287,288]</sup> The research group also employed bent,<sup>[289]</sup> branched,<sup>[290]</sup> and hyperbranched<sup>[291]</sup> sticky-ended monomers to yield controlled two- and three-dimensional fiber morphology, in contrast to previous systems which formed linear, nonbranched fibers exclusively.

One difficulty in achieving higher-ordered aggregates from de novo synthesized coiled-coil structures is that these synthetic sequences are often significantly shorter than those found in natural  $\alpha$ -helical fibril/fiber-forming peptides, and thus form inherently weaker interactions. One strategy to overcome this challenge involves covalently connecting two coiled-coil-forming motifs. Wagner et al. followed this approach by connecting two GCN4 di-heptads with a di-alanine spacer to afford high-mass, oriented  $\alpha$ -helix fibers.<sup>[292]</sup> Lazar et al. incorporated naturally occurring  $\beta$ -turn units between the di-heptads, thereby leading to the intramolecular formation of coiled coils and further assembly to form “cross- $\alpha$ ”-type fibrils, with the helices aligned perpendicular, rather than parallel, to the fibril axis.<sup>[293]</sup> The authors found that only proline-containing turn sequences resulted in the fibril inducing formation of a coiled coil, whereas more flexible natural turn units and a PEG spacer did not.

Dong and Hartgerink attempted to find the minimum-length sequence required to form fibrillar coiled-coil assemblies by stabilizing the short di-heptad coiled coils by the placement of double hydrogen-bond-forming glutamic acids at **e**–**g'**.<sup>[294]</sup> While fibrils formed initially, they were unstable, converting into amyloid-like cross- $\beta$  structures over time. Thus, the introduction of an additional heptad repeat was required to form stable fibers. The same research group

showed that a long, sticky-ended, or covalently linked coiled-coil design is not required for the formation of fibrils, as substitution of lysine or tyrosine residues at the exterior **b** and **f** positions were sufficient to yield stable fibers of homo-oligomeric tri-heptads.<sup>[295]</sup> However, no X-ray data was provided to rule out cross- $\beta$  formation. Pagel et al. developed a tetra-heptad capable of switching between the two fibril motifs ( $\beta$  sheet/ $\alpha$  helix) that enabled the systematic study of the factors governing the final form of secondary/tertiary structure.<sup>[296]</sup>

While substantial progress has been made toward both the understanding and application of  $\alpha$ -helical coiled-coil hierarchical biomimetic materials, many hurdles still exist to realizing high-performance structural materials based on these building blocks. Interesting avenues of development include non-heptad repeats (e.g., hendecad, 11 amino acids)<sup>[297,298]</sup> photocontrol of coiled-coil dimerization,<sup>[299]</sup> and a stress-induced  $\alpha$ - $\beta$  transition.<sup>[300]</sup> One major challenge facing non-bio-engineered synthetic systems is the poor coiled-coil stability of short oligomerized heptad repeat units. A possible, as yet unexplored, approach might be to take advantage of either covalent<sup>[301,302]</sup> or chelated<sup>[303]</sup> “helix-stapling” strategies, with the goal of improving the initial folding stability of shorter peptides and increasing the number of designer interaction handles on the exterior of the coiled-coil structures.

## 6. PPII Helix-Based Fibers

### 6.1. PPII Helix-Based Hierarchical Fibers

Collagen is the essential mechanical building block of the musculoskeletal system.<sup>[304]</sup> It is the fundamental unit of tendon, provides the mineralization scaffold for bone, and is the key mechanical component of the extracellular matrix.<sup>[241]</sup> The mechanical properties of collagen are characterized by excellent resilience at small strains and exceptional toughness at larger deformations.

The core molecular structure (Figure 15) of collagen is the X-Y-G repeat unit (typically proline-(hydroxy)proline-glycine), which adopts a left-handed polyproline type II (PPII) helix conformation, three of which assemble to form the tropocollagen (TC) right-handed helical AAB or ABC heterotrimer.<sup>[305–310]</sup> Although the mechanism is not completely understood, the unexpectedly high stability of this AAB triple helix relative to other combinations is thought to be due to extensive intermolecular water-mediated hydrogen bonding<sup>[311–314]</sup> enabled by the *trans/exo* OH groups of the hydroxyproline residues. However, the electron-withdrawing and steric effects of these hydroxy groups have also been implicated,<sup>[315–317]</sup> and a model suggesting the importance of kinetic effects has been proposed.<sup>[318]</sup>

Compared to the coiled-coil  $\alpha$ -helix protofibrils of keratin and vimentin, assembly of the PPII triple helix yields a more elongated, compacted rodlike unit with a denser network of interhelical hydrogen bonds (the so-called Rich-Crick hydrogen bond connecting the glycine NH group of one PPII helix with the C=O group of a proline (X) on an adjacent chain).

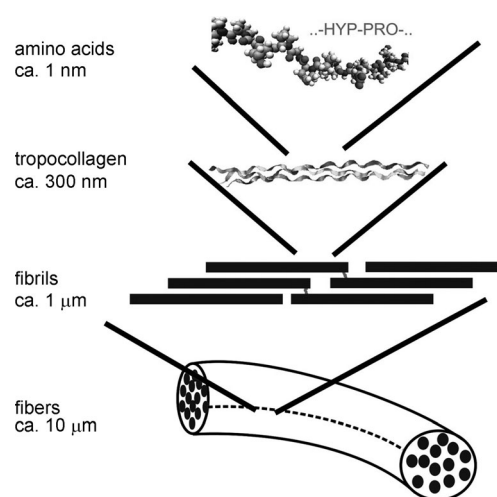


**Figure 15.** Schematic view of the modular, hierarchical design of collagen, ranging from the PPII structure at the nanoscale up to collagen fibers at the micrometer scale. Reprinted from Ref. [333] with permission. Copyright 2008 National Academy of Sciences.

The resulting protofibril assembly precursor is, therefore, designed for short-range elasticity, strength, and toughness rather than recoverable extension. The lack of side-chain bulk on the glycine residues provides space to allow the formation of the tightly packed triple helix, and the substitution of a single alanine for glycine in the central region of the peptide dramatically reduces the stability of the triple helix.<sup>[319]</sup> The TC modules then self-assemble through structural electrostatic<sup>[320]</sup> and entropic signals,<sup>[321–323]</sup> starting with a parallel, aligned, staggered spiral of five TC units per complete helical turn, extending with a distinct “pointed-end” morphology, and ultimately yielding a micrometer-scale elongated fibril<sup>[324–326]</sup> with a characteristic banded microstructure. During this process, permanent ionic<sup>[25,327,328]</sup> and/or covalent<sup>[329]</sup> bonds are formed between the TC subunits. Finally, several of these fibrils are encapsulated in a glycol–protein matrix to yield the load-bearing fibers.

The combination of extreme tensile strength and substantial extensibility which characterizes collagen-based materials can be traced to the semicrystalline, but still somewhat liquid,<sup>[330]</sup> nature of the collagen fibril.<sup>[331]</sup> The three deformation mechanisms afforded by the hierarchical nanostructure of collagen fibers—1) intermolecular shear, as a uniform viscous shifting of the relative fibril positions leads to a deviation from the linear elastic response, 2) permanent plastic deformation through slip-pulse propagation, and finally 3) fracture of individual TC molecules—yield extreme toughness and defect tolerance, as exemplified by leather and mussel byssal thread.<sup>[332,333]</sup>

### 6.2. PPII Helix-Based Mimics

#### 6.2.1. PPII-Helix Model Systems

The simple repeating sequence of tropocollagen proto-helices is well known, and thus simple mimics such as (Pro-Pro-Gly)<sub>n</sub> and (Pro-Hyp-Gly)<sub>n</sub> are readily accessible. Much of

the research on these collagen mimic peptides has focused on the determination of the structure of AAA homotrimers, with the goal of understanding the mechanism of stabilizing the triple helix and thus the structural basis of collagen-related disease states.<sup>[334–349]</sup>

One well-explored approach to stabilizing the triple helix is to attach the peptide precursors to a covalent scaffold that limits chain dynamics.<sup>[350]</sup> This drives the monomer/oligomer equilibrium in the desired direction by removing the principle entropic barrier to trimerization. Thus, shorter, more synthetically accessible peptides can be employed in these model systems. Early examples of scaffolds include lysine dimers derived from aminohexanoic acid<sup>[351–354]</sup> and 1,2,3-propanetricarboxylic acid.<sup>[355]</sup> Goodman and co-workers further expanded the template-assisted triple-helix-inducing toolkit with a set of more versatile scaffolds, such as *cis*-1,3,5-trimethylcyclohexane-1,3,5-tricarboxylic acid-Gly-OH (KTA),<sup>[356–358]</sup> tris(2-aminoethyl)amine)-(suc-OH)<sub>3</sub> (TREN),<sup>[359]</sup> and  $\beta$ -Ala-TRIS,<sup>[360,361]</sup> the latter derived from the tris(carboxyethylhydroxymethyl)aminomethane monomer of Newkome and Lin (Figure 16).<sup>[362]</sup> They used these

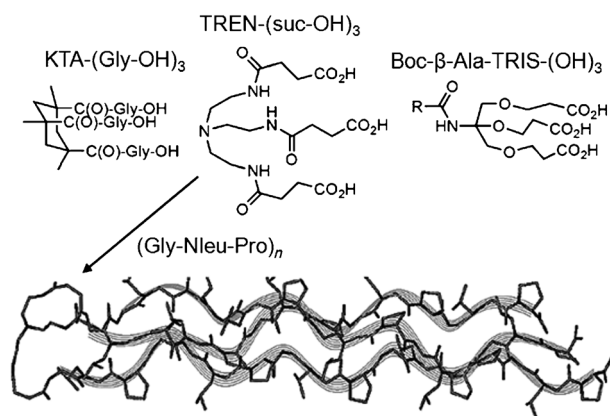


**Figure 16.** Template designs for triple-helix-inducing scaffolds. Reprinted from Ref. [362] with permission. Copyright 2002 American Chemical Society.

templates to explore the incorporation of peptoids into collagen mimics, and observed that *N*-isobutyllysine (NLeu) projected its steric bulk outward and did not disrupt assembly of the triple helix when substituted for proline in the triad repeats; such an exchange should provide a measure of protection from protease-induced degradation in eventual biomaterial applications.<sup>[363–366]</sup> The same research group demonstrated the feasibility of triple-helix templating triggered by metal complexation by using catechol-terminated peptides,<sup>[367]</sup> by following similar studies to those of Koide et al., who employed a bipyridine (bpy) motif.<sup>[368]</sup>

In pursuit of greater fidelity with the natural system, as well as more versatile scaffolds for potential further assembly, Guaba and Hartgerink developed a series of decatriad tropocollagen mimics that spontaneously assemble into AAB and ABC triple helices through ionic interactions between the amino acids.<sup>[369]</sup> Notably, peptides (EOG)<sub>10</sub> and (PRG)<sub>10</sub> exclusively formed highly stable ( $T_m > 54^\circ\text{C}$ ) heter-

otrimers from 1:1 mixtures, despite the fact that the individual peptides are not capable of forming stable triple helices because of the lack of proline-derived conformational restriction. Additionally, stable ABC triple helices self-assembled from 1:1:1 mixtures of the two oppositely charged peptides and the standard neutral repeat peptide (POG)<sub>10</sub>, likely because of overall charge neutralization. The authors also found that, unlike most TC mimics, the non-proline substitutions were tolerated at both the X and Y positions of the X-Y-G triad.<sup>[370]</sup> The stability of this type of ABC heterotrimer is comparable to that of the classic homotrimeric neutral (POG)<sub>10</sub> tropocollagen mimic, thereby allowing comprehensive, high-resolution NMR conformational analysis.<sup>[371]</sup> In previous systems, the partial unfolding<sup>[372]</sup> and/or lack of specificity with respect to composition<sup>[313]</sup> or register<sup>[373]</sup> complicated such studies. The power of this system was demonstrated when charged flanking regions were also employed to study the effect of glycine mutations on a central type I collagen sequence with a well-defined heterotrimeric composition.<sup>[374]</sup> Recently, the research group reported a similarly selective, highly stable assembly of an AAB heterotrimer by mixing one +10 (PRG)<sub>10</sub> and two -5 (EOGPOG)<sub>5</sub> peptides (Figure 17).<sup>[375]</sup>

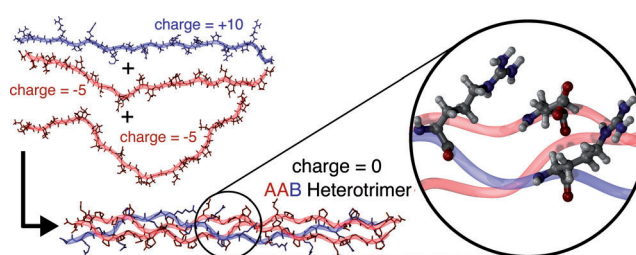


**Figure 17.** A combination of peptides that follow the canonical (X-Y-Gly)<sub>n</sub> amino acid repeat in a 2:1 ratio, in which the more abundant peptide has a charge -1/2 of the other, results in the formation of an AAB heterotrimeric collagen helix. Reprinted from Ref. [375] with permission. Copyright 2010 American Chemical Society.

### 6.2.2. Hierarchical PPII-Helix-Based Materials

The biocompatibility and excellent mechanical properties of collagen has resulted in great interest in expanding from simple models to viable biomimetic materials based on the assembly of higher-order fibers of TC protofilament mimics. One simple approach is to polymerize preformed deca-(X-Y-G)-tripeptides. Paramonov et al. accomplished this by native chemical ligation,<sup>[376]</sup> while Kishimoto et al. employed optimized EDC coupling conditions,<sup>[377]</sup> with both methods resulting in relatively monodisperse fibrous morphologies.

Kotch and Raines used strategically placed cysteine residues which spontaneously templated the formation of out-of-register triple helices from short X-Y-G repeating peptides, thereby leading to further “sticky-end”-mediated thermodynamic self-assembly.<sup>[378]</sup> Cejas et al. drove the assembly of TC mimics by incorporating phenylalanine and pentafluorophenylalanine residues at the termini, which led to the spontaneous supramolecular formation of fibrils



through the hydrophobic effect.<sup>[379]</sup> Przybyla and Chmielewski realized lateral assembly of TC-mimic homodimers by incorporating an ion-chelating bipyridyl group in the center of the peptide.<sup>[380]</sup> Longitudinal assembly was accomplished by the inclusion of triacid and diimidazole chelators at either end of the modules of the TC mimics.<sup>[381]</sup> Controlled assembly with reproducible particle size could be accomplished by varying the concentration of the metal ion, and disassembly was conveniently accomplished by the addition of EDTA. A combination of lateral and longitudinal assembly inducers was used to generate fibrous films with controlled morphology.<sup>[382]</sup>

Finally, Rele et al. achieved the first and only case of collagen-like D-periodic spacing after assembly of fibrils of a charged homotrimeric TC mimic. This remarkable success was accomplished simply by incorporating a positively charged arginine residue in the Y position of the first four triad repeats of a synthetic 24-mer, and a glutamic acid in the X position of the last four, which flanks a simple POG tetratriad, thereby leading to electrostatic collagen-like assembly.<sup>[383]</sup>

While significant advances have been made towards collagen-like biomimetic materials, substantial challenges remain, mostly in the area of controlled assembly, as there is limited flexibility in the sequence design and chemical functionality of the primary and secondary building blocks. One avenue that may bear fruit is the potential use of polyureas and other well-studied, synthetically accessible helical foldamers,<sup>[384]</sup> as well as glycosylated hydroxyproline derivatives.<sup>[385]</sup>

## 7. Tertiary Folded Domain

### 7.1. Titin Model of Modular Polymer Domains

The repeating modules of the biopolymers examined in the previous sections are all based on the secondary structures of folded peptides, including  $\beta$  turns/spirals (elastin),  $\beta$  sheets (amyloid, silk),  $\alpha$  helices (vimentin), and PP-II helices (collagen). In this section, we will examine modular biopolymers in which the repeating modules are folded tertiary protein domains.

Mechanochemical transduction plays an essential role in living systems. Many mechanosensitive proteins have modular domain structures with tandem arrays of tertiary folded protein domains. At the microscopic level, cells can sense and transduce a wide range of mechanical forces into distinct sets of biochemical signals that ultimately regulate cellular processes, including adhesion, proliferation, differentiation, and apoptosis.<sup>[241,386,387]</sup> At the macroscopic level, mechanochemical transduction enables a wide variety of physiological processes, including the senses of touch and hearing as well as balance and muscle contraction.<sup>[388–390]</sup>

To cope with constantly changing external mechanical stimuli, nature has evolved a broad range of polymeric materials with embedded mechanosensitive motifs that show stress-responsive adaptive and dynamic properties. For example, fibronectin, an important extracellular matrix (ECM)

protein for cell mechanotransduction, mechanically couples the ECM of cells to the cytoskeleton through integrins. Studies have shown that mechanical force can partially unfold the fibronectin modules to induce conformational changes in the cell-recognition sites, expose cryptic binding sites, and change the distance between synergistic binding sites.<sup>[386,391]</sup> Therefore, mechanical stress on ECM can regulate the binding of different integrins, which further initiates downstream intracellular signaling cascades.

A marvelous example of the design of modular domains is demonstrated in the skeletal muscle protein titin, a giant protein (3000 kDa, 1 mm long) of the muscle sarcomere (Figure 18). Titin is composed of 300 modules in two motif types, immunoglobulin (Ig) and fibronectin type III domains.<sup>[392,393]</sup> Whereas actin and myosin are motor proteins responsible for muscle contraction, titin contributes to the mechanical strength, toughness, and elasticity of the muscle.<sup>[394–396]</sup> Single-molecule studies have shown that titin exhibits a remarkable combination of high mechanical strength, fracture toughness, and elasticity.<sup>[119, 397–401]</sup> Further studies have revealed that the combination of these properties in titin arises from its unique modular domain structures.<sup>[402–407]</sup> Sequential unfolding of the domains results in the saw-tooth pattern in the force/extension curve, which provides the molecular basis for the combined high strength, high fracture toughness, and elasticity of these materials. Many cell-adhesion proteins,<sup>[408]</sup> such as fibronectins and cadherins, share the same tandem domain structure as titin.

The mechanistic explanation for the exceptional combination of mechanical properties in modular biopolymers can be visualized in terms of the different tensile properties of 1) a short chain or a rigid rod, 2) a long chain with multiple domains, and 3) a regular random-coil polymer.<sup>[406]</sup> For a short chain or a rigid rod, the force rises rapidly with relatively small extension, and the energy required to break the chain is small, thereby making it brittle. In contrast, a regular random-coil long-chain polymer can undergo much larger extension; however the material is relatively soft near maximum extension. Unlike either of these two, with a long polymer composed of a tandem array of modules folded by accumulative weak forces, such as the structure of titin,<sup>[377–382]</sup> the force rises quickly with extension, as with the short chain. However, when the force reaches a significant level, the tandem folded modules will sequentially unfold, thereby revealing hidden length, dissipating energy, and preserving the integrity of the covalent chain. The result is a large force sustained over the whole extension, which makes the polymer strong, along with a large area under the force/extension curve, thus making it tough as well.<sup>[406]</sup>

As a representative example of tandem modular mechanosensitive proteins, titin demonstrates a fascinating strategy to combine high tensile strength, toughness, and elasticity by using a modular domain design. By repetitive breaking of the reversible secondary interactions buried in each domain, the polymers can absorb a very large amount of energy without breaking the covalent bonds. This tandem domain design appears to be a general mechanism used in nature to achieve a combination of mechanical properties, and has been observed in many other biological macromolecules that play mechan-

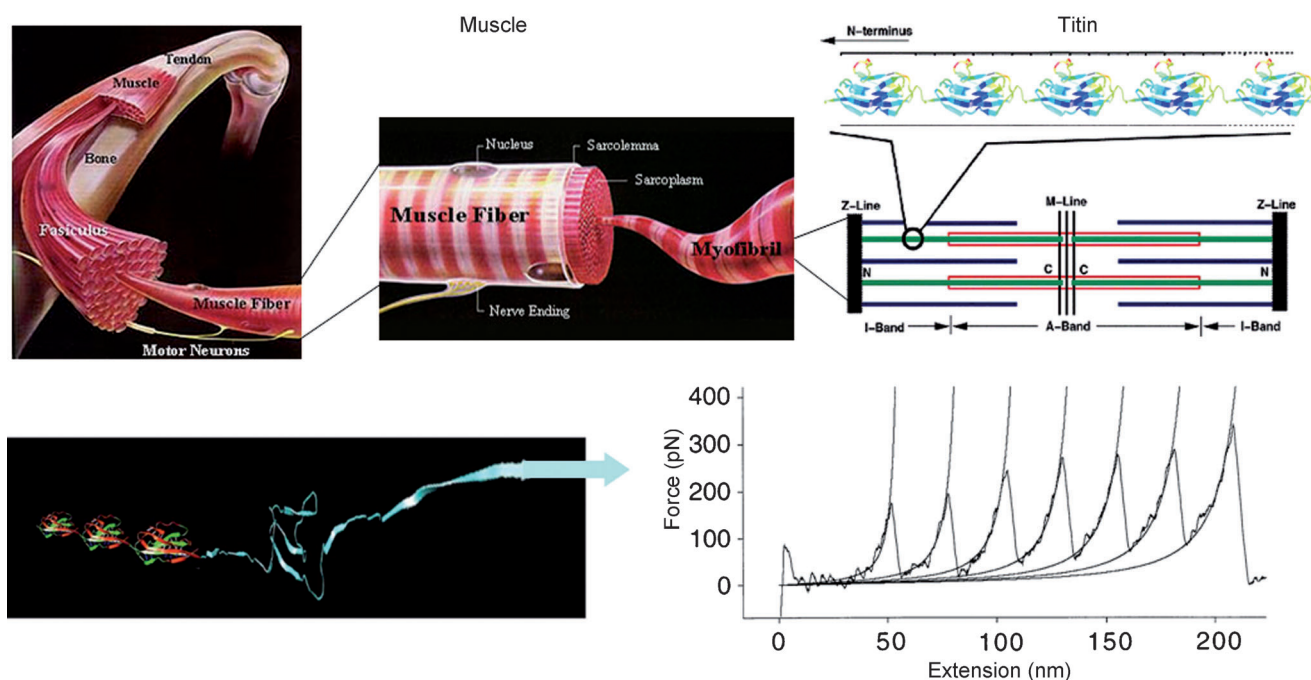


**Figure 18.** Titin is a 3000 kDa repeating modular tertiary-folded-domain protein that provides the core “suspension system” functionality for the bulk hierarchically assembled muscle machinery. The characteristic “saw-tooth” pulling profile of single titin molecules is directly responsible for the excellent strength, toughness, and elasticity found in mammalian muscle. Adapted from Ref. [400] with permission. Copyright 1997 American Academy for the Advancement of Science.

ical roles.<sup>[409]</sup> Besides titin, a number of other proteins with tandem domain structures have been investigated by SMFS.<sup>[394, 410–420]</sup>

## 7.2. Titin Mimics

### 7.2.1. Biosynthetic Titin Mimics

Li designed tandem-repeating titin mimics, replacing the I27 domains of titin with protein modules that have no known *mechanical* roles in biological systems.<sup>[421]</sup> The authors found that polypeptides of the GB1  $\beta$ - $\alpha$ - $\beta$  motif (GB1 is the streptococcal B1 immunoglobulin-binding domain of protein G) displayed a nearly ideal combination of mechanical properties at the single-molecule level, such as rapid, high-fidelity folding kinetics, low mechanical fatigue, and the ability to refold under residual stress.<sup>[422]</sup> They further probed the tunability of the system, successfully engineering increased mechanical stability into the GB1 domain by careful incorporation of ion-binding sites, as opposed to simple thermodynamic stabilization of the protein.<sup>[423]</sup> After a leucine-zipper-type construct had been added to each side of the synthetic modular domain protein, the polymer spontaneously formed hydrogels.<sup>[424]</sup> Recently, this research group successfully designed an artificial elastomeric protein that mimics the molecular architecture of titin through the combination of GB1 and resilin.<sup>[425]</sup>

Guzman et al. recently reported a titin-mimicking multi-domain poly(protein) with high mechanical strength.<sup>[426]</sup> Through a combination of bioinformatics screening, steered

molecular dynamics (SMD) simulations, protein engineering, and SMFS, a macrodomain protein with mixed  $\alpha + \beta$  topology was discovered to have exceptional mechanical stability. The unique architecture of the macrodomain protein is defined by a single seven-stranded  $\beta$  sheet, in the core of the protein, flanked by five  $\alpha$  helices. Unlike other mechanically stable proteins studied thus far, the macrodomain provides the distinct advantage of having the key load-bearing hydrogen bonds buried in the hydrophobic core, thus protected from water. This feature allows direct measurement of the force required to break apart the load-bearing hydrogen bonds under locally hydrophobic conditions. SMD simulations using constant velocity and constant force methods predicted an extremely high mechanical stability of the macrodomain. SMFS experiments confirm the remarkable mechanical strength of the macrodomain, with a rupture force as high as 570 pN measured (Figure 19), which is twice as high as the rupture force for the titin I27 domain under a comparable pulling rate. Furthermore, selective deletion of shielding peptide segments allowed the authors to examine the same key hydrogen bonds under hydrophilic environments in which the  $\beta$  strands are exposed to solvent, and thus verify that the high mechanical stability of the macrodomain results from shielding of the load-bearing hydrogen bonds from competing water. This study reveals that shielding water accessibility to the load-bearing strands is a critical molecular determinant for enhancing the mechanical stability of proteins. It also demonstrates that it is feasible to identify and engineer proteins that serve no mechanical functions in nature to have mechanical stability superior to natural mechanical proteins.

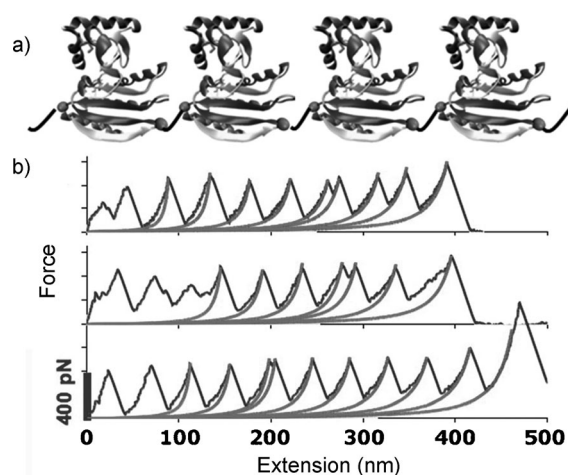


**Figure 19.** a) Schematic representation of the Afl521<sub>11-177</sub> polyprotein. b) Representative force curves at 1000 nm s<sup>-1</sup> with the WLC form showing multiple unfolding pathways. Adapted from Ref. [426] with permission. Copyright 2010 National Academy of Sciences.

### 7.2.2. Chemically Synthesized Titin Mimics

Guan and co-workers used titin as a model system to develop a series of biomimetic polymers containing reversibly unfoldable modules with the aim of addressing a fundamental challenge in material design: to combine the three most fundamental mechanical properties—tensile strength, fracture toughness, and elasticity—into one structure.<sup>[427]</sup> In addition, the research group is interested in introducing dynamic and adaptive properties into synthetic polymeric materials to mimic natural systems.<sup>[168, 428, 429]</sup>

The designs of synthetic modules are based on the careful examination and mechanistic understanding of the mechanical stability of titin. The Ig domain of titin exhibits a double  $\beta$ -sheet architecture. Molecular modeling and single-molecule studies indicate that the load-bearing region has six hydrogen bonds between  $\beta$  strands A' and G, which play a critical role in the mechanical stability of the protein.<sup>[399, 408]</sup> The mechanical unfolding is a two-stage on/off process: once the load-bearing hydrogen bonds are ruptured, the remaining part of the protein unfolds rapidly. From a simplistic viewpoint, the protein can be imagined to have a “zipper” to hold the load and a “loop” that rapidly unfolds once the zipper is ruptured.

Based on this analysis, Guan et al. first designed a modular polymer having loops folded by strong hydrogen bonds. In this design, a strong quadruple hydrogen-bonding motif, 2-ureido-4-pyrimidone (UPy), was employed to direct the formation of loops along a polymer chain. Developed initially by Meijer and co-workers,<sup>[430]</sup> UPy has been employed as a popular supramolecular motif for various materials applications because of its strong self-dimerization constant.<sup>[431–434]</sup> Based on the magnitude of the dimerization constant, the free energy required to break the UPy dimer is more than 11 kcal mol<sup>-1</sup>, which is comparable to protein-unfolding energy and lower than typical covalent-bond energies, therefore suiting the biomimetic purpose. A UPy-

containing diol monomer was incorporated into a linear polyurethane. Homodimerization between the UPy units on the polymer chain led to the formation of many folded loops (Figure 20).<sup>[428]</sup> At the molecular level, SMFS shows the characteristic saw-tooth pattern similar to those of polydo-

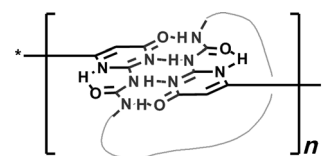


**Figure 20.** Modular polymer with UPy domains in the main chain. Adapted from Ref. [428] with permission. Copyright 2004 American Chemical Society.

main proteins. At the macroscopic level, the modular UPy polymer demonstrates a combination of high strength, toughness, and elasticity. The bulk mechanical data correlate well with the single-chain force/extension observation, thus proving the biomimetic concept: the introduction of modular structures held by sacrificial weak bonds into a polymer chain can successfully combine the three most fundamental mechanical properties (high tensile strength, toughness, and elasticity) into one polymer.

In the second-generation biomimetic modular design, a peptidomimetic  $\beta$ -sheet-based double-closed-loop (DCL) module was synthesized to overcome issues such as structural heterogeneity and interchain cross-linking.<sup>[435]</sup> The module in this system is composed of a  $\beta$ -sheet-like duplex that is connected at both ends with hydrocarbon loops. As a module is stretched, the force shears the hydrogen bonds in the duplex and the loops are extended. After releasing the force, the double-closed-loop topology should ensure that the strands rebound to their original pairs (Figure 21 a). The DCL module was synthesized by a multistep organic synthesis and its modular polymer was made by polymerizing the DCL monomer with 4,4'-methylenebis(phenylisocyanate) (Figure 21 d).

The modular polymers were subjected to SMFS studies with AFM by following the literature protocols.<sup>[439, 440]</sup> The saw-tooth patterns were observed in the force/extension curves, which are similar to those seen in both natural and synthetic modular polymers (Figure 21 c). The patterns in the force/extension curves were more uniform for the modular DCL polymer than for the first-generation modular design, which was attributed to its more uniform structure. The chain detaches from the surface typically after 60–120 nm stretching. The most probable peak force for unfolding each module is about 50 pN. This force is lower than that of our modular UPy polymers, which had an unfolding force of approximately 100–200 pN. This finding is consistent with the binding strengths of the two modules: the dimerization constant ( $K_{\text{dim}}$ ) measured in chloroform for the UPy and the current peptidomimetic  $\beta$ -sheet units are about  $10^7$  and  $10^4$ , respectively.<sup>[432, 438]</sup> The stretching curves can be fitted by the classical wormlike chain model for a single-polymer chain (Figure 21 c).

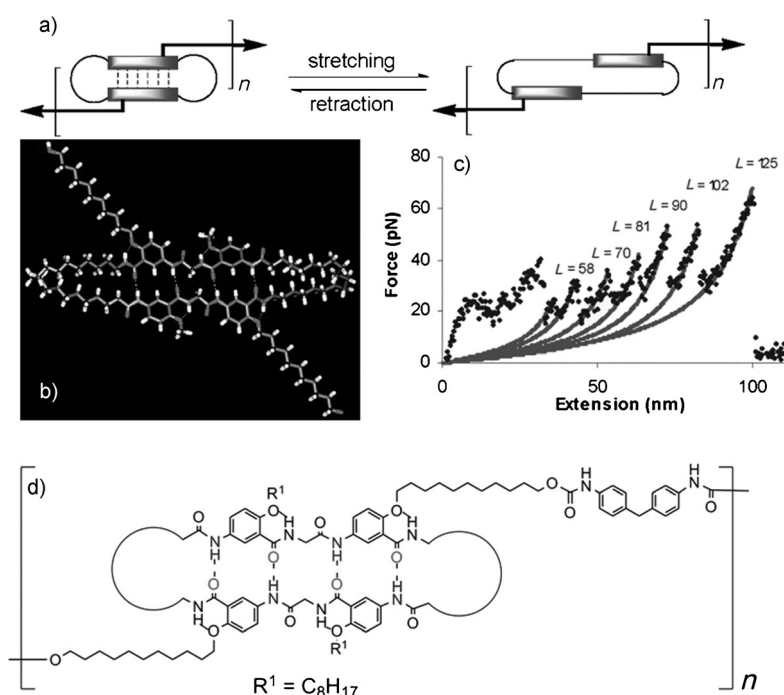


**Figure 21.** a) Schematic representation of the double closed loop (DCL) in a polymer. b) Molecular model of one DCL module used in the study. c) AFM force/extension curve for a single molecule of the DCL module. The solid line describes the WLC model, which fits at a 0.55 nm persistence length,  $L$  is the contour length during stretching. d) The chemical structure of the DCL polymer. Adapted from Ref. [435] with permission. Copyright 2004 American Chemical Society.

To gain further insight into the influence of modular structure on the mechanical properties of polymers, Guzman et al. carried out nanomechanical investigations on a homologous series of  $\beta$ -sheet mimics. Three  $\beta$ -sheet-mimicking modules containing 4, 6, or 8 complementary hydrogen bonds were used for both SMFS studies and SMD simulations to understand the relationship between the molecular unfolding force and chemical structure.<sup>[439]</sup> The SMFS studies showed a nonlinear relationship between the rupture force and the number of hydrogen bonds. The SMD simulations revealed that, as the strands get too long, the conformational flexibility will cause a mismatch in the dimerization, thereby lowering the apparent unfolding forces observed by SMFS.

A cyclic UPy module was further applied by Kushner et al. to simplify the synthesis and improve the mechanical strength for the third generation of modular design (Figure 22).<sup>[440]</sup> In this study, the modular polymer based on DCL of the UPy dimer module shows not only a com-

bination of elasticity, high modulus, and toughness, but also self-healing and adaptive properties. The modular polymer was synthesized by acyclic diene metathesis (ADMET) polymerization of a di-olefin UPy-DCL monomer. In tensile tests, after yielding at approximately 5 % strain, the modular polymer shows a strikingly large deformation with a relatively small increase in stress, a consequence of sequential unfolding of the folded modules, which results in the absorption of a large amount of energy and makes the polymer tough. In further studies, Kushner et al. observed interesting self-healing/shape-memory properties for this polymer.

For many practical applications, it might not be necessary to have the mechanosensitive modules (mechanophores)<sup>[441]</sup> in every repeat unit. Incorporation of a small amount of the hydrogen-bonding mechanosensitive module may be sufficient to dissipate energy and prevent fracture from occurring. With this in mind, Kushner et al. prepared a 3D poly(*n*-butyl acrylate) network containing a small amount (6 mol %) of a biomimetic modular cross-linker.<sup>[442]</sup> Comparison of the mechanical properties of the network with the modular cross-linker and a control network with a normal cross-linker demonstrates that the introduction of a small amount of a biomimetic module into the network dramatically enhances the mechanical properties of the polymer.

## 8. Summary and Outlook

In this Review we have outlined what is known about the molecular mechanism by which natural peptide-based materials achieve their remarkable mechanical properties and combinations thereof. In each section we presented a survey of the numerous attempts, by either biosynthesis or chemical

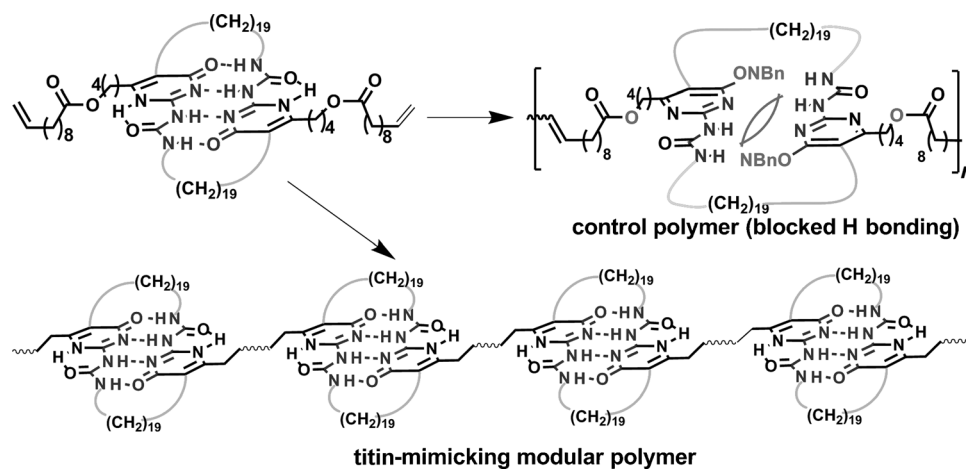


**Figure 22.** Design of strong, tough, elastic, and adaptive ADMET UPy-DCL polymers. Adapted from Ref. [440] with permission. Copyright 2009 American Chemical Society.



synthesis, to achieve novel functional materials by borrowing nature's design strategies. At the end of this Review, we try to summarize a few critical design principles universally employed by biological materials, as well as our perspective on the future direction of and key challenges facing the field of biomimetic materials.

Perhaps one of the most important design principles employed in the design of natural materials is programming weak molecular forces into macromolecular systems to guide both intramolecular folding and intermolecular hierarchical self-assembly into high-order structures. Modern synthetic methods make it easy to construct strong covalent bonds. However, we are still at an early stage in our attempts to introduce weak molecular forces into synthetic macromolecules in a well-defined and programmed manner. In a broader sense, a fundamental challenge remains in bridging the gap between synthetic and natural macromolecules: we need to learn more about how to program secondary molecular forces into macromolecules to translate local structures into high-order structures, and ultimately to control self-assembly across length scales ranging from nanometers and micrometers to the macroscopic level.

A second important principle used in the design of natural materials is the employment of both strong covalent bonds and weak noncovalent interactions to achieve a combination of seemingly orthogonal properties, such as high mechanical strength, while simultaneously remaining dynamic and adaptive. In natural polymeric materials, the polymer backbones are usually constructed through strong covalent bonds such as peptide (amide) linkages, which provide mechanical strength to the materials. However, in many cases, it is the accumulative weak forces programmed into the systems that generate exciting dynamic and adaptive properties (e.g., tough, stimuli responsive, shape memory, and/or self-healing). It remains a major challenge in the design of synthetic materials to strategically combine covalent and noncovalent forces for the design of advanced materials with strong and adaptive properties. Modern polymer chemistry provides efficient access to many synthetic polymers built of strong covalent bonds. On the other hand, supramolecular chemistry offers important lessons and motifs for programming weak molecular forces into various synthetic systems. One emerging research direction in modern materials chemistry is to seamlessly integrate supramolecular chemistry and polymer chemistry for the design of the next generation of advanced materials.<sup>[443,444]</sup>

A third important design principle ubiquitously employed in natural materials is repetitive modular design. As surveyed in Sections 2–7, natural polymeric materials often adopt a modular approach in which short peptides fold into well-defined secondary ( $\beta$  spiral,  $\beta$  sheet,  $\alpha$  helix, PPII helix) or even tertiary (titin) modules and then polymerize into linear polymers with a tandem array of modules. Presumably, natural evolution selects modular design both for the energy-efficient synthesis of materials and for advanced functional properties (see Section 7.1). Modular design also provides a practical solution to combining fine-structural control and efficient synthesis: since the secondary or tertiary structure within each module is precisely controlled, efficient

polymerization of many modules will link them into long polymers with the desired properties. The modular design offers exciting opportunities for many further biomimetic designs.

While presenting tremendous opportunities, the design of biomimetic materials also faces several challenges for further development. One major challenge is to design more atom-economic and environmentally friendly syntheses of biomimetic materials that can be sustainably produced on a large scale and at low cost. Current chemical and biochemical syntheses of biomimetic materials often involve multiple steps and create toxic waste, in sharp contrast to nature, where most materials are produced and processed under ambient conditions in aqueous solution. A second major challenge is to integrate optimal processing conditions and fine-chemical design and synthesis. For a material to perform at its highest potential, its degree of structural organization in the condensed phase is extremely important. In addition to well-defined chemical design and programming of various molecular forces and higher-order structures, the optimal processing conditions will help realize structural organization from the molecular level across the hierarchy of length scales. Nature provides many vivid examples of the combination of biochemical design and exquisite processing conditions to achieve marvelous materials, such as spider silks. Without optimal processing, the properties of many current biomimetic materials are far below the potential inherent in their designs.

Finally, despite major recent progress, it remains a core challenge to directly relate single-molecule properties to macroscopic properties in biomimetic material studies. Although the validity of molecular designs can now be analyzed with nanometer resolution, the dynamics and emergent properties are expected to change dramatically once multiple molecules are present in a condensed state, and methods to predict and identify these properties are currently limited and indirect.

Despite these major challenges, the design of biomimetic materials has an extremely bright future. Thanks to the major developments and breakthroughs in synthetic chemistry affording more efficient synthetic methods and an improved biological understanding of the deep molecular mechanisms of natural materials, together with advances in computational chemistry for modeling complex biomimetic systems and improvements in nanotechnology for nanoprocessing, we have never been better positioned to implement nature's design strategies in synthetic materials. A truly interdisciplinary approach involving chemists, biologists, biophysicists, materials scientists, and engineers means that many critical material design issues can now be addressed from the molecular level all the way through to advanced macroscopic applications. By mimicking nature's approach, we can design a new generation of advanced materials with useful properties that far exceed those available by current methods.

*We thank the US Department of Energy-Basic Energy Science (DE-FG02-04ER46162), National Institute of Health (R01EB004936), National Science Foundation (DMR-0135233), and Arnold and Mabel Beckman Foundation for*

financial support of our biomimetic material research program. Many colleagues and co-workers, whose names appear in the references cited, are gratefully acknowledged for their important contributions to this research field. As a consequence of space limitations, we apologize to authors whose important contributions have not been included here.

Received: October 16, 2010

Published online: September 5, 2011

- [1] <http://www.merriam-webster.com/dictionary/biomimetics>, **2011**.
- [2] C. G. Gebelein, *Biomimetic Polymers*, Plenum Press, New York, **1990**.
- [3] P. C. Rieke, P. D. Calvert, M. Alper, *Materials Synthesis Utilizing Biological Processes*, Vol. 174, Materials Research Society, Pittsburgh, PA, **1990**.
- [4] K. P. McGrath, D. Kaplan, *Protein-Based Materials*, Birkhauser, Boston, **1997**.
- [5] J. Aizenberg, J. M. McKittrick, C. A. Orme, *Biological and Biomimetic Materials—Properties to Function*, Vol. 724, Materials Research Society, Warrendale, PA, **2002**.
- [6] A. K. Dillow, A. M. Lowman, *Biomimetic Materials and Design: Biointerfacial Strategies, Tissue Engineering, and Targeted Drug Delivery*, Marcel Dekker, New York, **2002**.
- [7] J. L. Thomas, K. L. Kiick, L. A. Gower, *Materials Inspired by Biology*, Vol. 774, MRS, Warrendale, PA, **2003**.
- [8] V. Nanda, R. L. Koder, *Nat. Chem.* **2010**, *2*, 15.
- [9] J. Kofoed, J.-L. Reymond, *Curr. Opin. Chem. Biol.* **2005**, *9*, 656.
- [10] A. Mecke, C. Dittrich, W. Meier, *Soft Matter* **2006**, *2*, 751.
- [11] C. H. L. Nielsen in *Analytical & Bioanalytical Chemistry*, Vol. 395, Springer, Dordrecht, **2009**, p. 697.
- [12] K. Kalyanasundaram, M. Graetzel, *Curr. Opin. Biotechnol.* **2010**, *21*, 298.
- [13] D. G. Gibson, J. I. Glass, C. Lartigue, V. N. Noskov, R.-Y. Chuang, M. A. Algire, G. A. Benders, M. G. Montague, L. Ma, M. M. Moodie, et al., *Science* **2010**, *329*, 52.
- [14] I. Grunwald, K. Rischka, S. M. Kast, T. Scheibel, H. Bargel, *Philos. Trans. R. Soc. London Ser. A* **2009**, *367*, 1727.
- [15] H.-A. Klok, *J. Polym. Sci. Part A* **2005**, *43*, 1.
- [16] H. G. Börner, H. Schlaad, *Soft Matter* **2007**, *3*, 394.
- [17] J. C. M. van Hest, *Polym. Rev.* **2007**, *47*, 63.
- [18] M. Cusack, A. Freer, *Chem. Rev.* **2008**, *108*, 4433.
- [19] W. Kunz, M. Kellermeier, *Science* **2009**, *323*, 344.
- [20] C.-L. Chen, N. L. Rosi, *Angew. Chem.* **2010**, *122*, 1968; *Angew. Chem. Int. Ed.* **2010**, *49*, 1924.
- [21] J. Aizenberg, *MRS Bull.* **2010**, *35*, 323.
- [22] L. C. Palmer, C. J. Newcomb, S. R. Kaltz, E. D. Spörke, S. I. Stupp, *Chem. Rev.* **2008**, *108*, 4754.
- [23] L. B. Gower, *Chem. Rev.* **2008**, *108*, 4551.
- [24] W. J. Crookes-Goodson, J. M. Slocik, R. R. Naik, *Chem. Soc. Rev.* **2008**, *37*, 2403.
- [25] J. H. Waite, N. H. Andersen, S. Jewhurst, S. Chengjun, *J. Adhes.* **2005**, *81*, 297.
- [26] S. Hui, N. B. Kent, J. S. Russell, *Macromol. Biosci.* **2009**, *9*, 464.
- [27] B. Bhushan, *Philos. Trans. R. Soc. London Ser. A* **2009**, *367*, 1445.
- [28] Y. Liu, J. P. Li, E. B. Hunziker, K. de Groot, *Philos. Trans. R. Soc. London Ser. A* **2006**, *364*, 233.
- [29] M. P. Lutolf, J. A. Hubbell, *Nat. Biotechnol.* **2005**, *23*, 47.
- [30] J. Patterson, M. M. Martino, J. A. Hubbell, *Mater. Today* **2010**, *13*, 14.
- [31] H. Bader, K. Dorn, B. Hupfer, H. Ringsdorf in *Polymer Membranes*, Springer, Heidelberg, **1985**, p. 62.
- [32] H. Ringsdorf, B. Schlarb, J. Venzmer, *Angew. Chem.* **1988**, *100*, 117; *Angew. Chem. Int. Ed. Engl.* **1988**, *27*, 113.
- [33] Y. Bar-Cohen, *Biomimetics: Biologically Inspired Technologies*, Taylor & Francis, New York, **2006**.
- [34] T. Ackbarow, M. J. Buehler, *Nanotechnology* **2009**, *20*, 075103.
- [35] J. Gosline, M. Lillie, E. Carrington, P. Guerette, C. Ortlepp, K. Savage, *Philos. Trans. R. Soc. London Ser. B* **2002**, *357*, 121.
- [36] J. Aizenberg, P. Fratzl, *Adv. Mater.* **2009**, *21*, 387.
- [37] M. Antonietti, P. Fratzl, *Macromol. Chem. Phys.* **2010**, *211*, 166.
- [38] P. R. Shewry, A. S. Tatham, A. J. Bailey, *Elastomeric Proteins: Structures, Biomechanical Properties, and Biological Roles*, Cambridge University Press, Cambridge, **2003**.
- [39] M. E. Csete, J. C. Doyle, *Science* **2002**, *295*, 1664.
- [40] M. Baer, E. Schreiner, A. Kohlmeier, R. Rousseau, D. Marx, *J. Phys. Chem. B* **2006**, *110*, 3576.
- [41] S. Zhang, *Mater. Today* **2003**, *6*, 20.
- [42] J.-M. Lehn, *Science* **2002**, *295*, 2400.
- [43] J.-M. Lehn, *Supramolecular Chemistry: Concepts and Perspectives*, VCH, Weinheim, **1995**.
- [44] M. J. Buehler, Y. C. Yung, *Nat. Mater.* **2009**, *8*, 175.
- [45] D. W. Urry, T. Hugel, M. Seitz, H. E. Gaub, L. Sheiba, J. Dea, J. Xu, T. Parker, *Philos. Trans. R. Soc. London Ser. B* **2002**, *357*, 169.
- [46] W. R. Gray, L. B. Sandberg, J. A. Foster, *Nature* **1973**, *246*, 461.
- [47] P. Brown-Augsburger, C. Tisdale, T. Broekelmann, C. Sloan, R. P. Mecham, *J. Biol. Chem.* **1995**, *270*, 17778.
- [48] K. K. Kumashiro, J. P. Ho, W. P. Niemczura, F. W. Keeley, *J. Biol. Chem.* **2006**, *281*, 23757.
- [49] A. M. Tamburro, A. Pepe, B. Bochicchio, *Biochemistry* **2006**, *45*, 9518.
- [50] C. A. J. Hoeve, P. J. Flory, *Biopolymers* **1974**, *13*, 677.
- [51] D. A. Torchia, K. A. Piez, *J. Mol. Biol.* **1973**, *76*, 419.
- [52] J. M. Gosline, *Biopolymers* **1978**, *17*, 677.
- [53] J. M. Gosline, C. J. French, *Biopolymers* **1979**, *18*, 2091.
- [54] T. Weis-Fogh, S. O. Andersen, *Nature* **1970**, *227*, 718.
- [55] I. Pasquali-Ronchetti, M. Baccarani-Contri, C. Fornieri, G. Mori, D. Quaglino, Jr., *Micron* **1993**, *24*, 75.
- [56] D. W. Urry, *J. Protein Chem.* **1988**, *7*, 1.
- [57] D. W. Urry, *J. Protein Chem.* **1988**, *7*, 81.
- [58] D. W. Urry, *J. Protein Chem.* **1984**, *3*, 403.
- [59] S. Rimmer, S. Carter, R. Rutkaite, J. W. Haycock, L. Swanson, *Soft Matter* **2007**, *3*, 971.
- [60] D. W. Urry, T. L. Trapane, M. Iqbal, C. M. Venkatachalam, K. U. Prasad, *Biochemistry* **1985**, *24*, 5182.
- [61] H. Dong, S. E. Paramonov, L. Aulisa, E. L. Bakota, J. D. Hartgerink, *J. Am. Chem. Soc.* **2007**, *129*, 12468.
- [62] B. Li, D. O. V. Alonso, B. J. Bennion, V. Daggett, *J. Am. Chem. Soc.* **2001**, *123*, 11991.
- [63] B. Li, D. O. V. Alonso, V. Daggett, *J. Mol. Biol.* **2001**, *305*, 581.
- [64] J. Carlos Rodríguez-Cabello, J. Reguera, A. Girotti, M. Alonso, A. M. Testera, *Prog. Polym. Sci.* **2005**, *30*, 1119.
- [65] K. Okamoto, D. W. Urry, *Biopolymers* **1976**, *15*, 2337.
- [66] D. Chow, M. L. Nunelee, D. W. Lim, A. J. Simnick, A. Chilkoti, *Mater. Sci. Eng. R* **2008**, *62*, 125.
- [67] Y. Wu, J. A. MacKay, J. R. McDaniel, A. Chilkoti, R. L. Clark, *Biomacromolecules* **2009**, *10*, 19.
- [68] R. Dandu, H. Ghandehari, *Prog. Polym. Sci.* **2007**, *32*, 1008.
- [69] E. R. Wright, V. P. Conticello, *Adv. Drug Delivery Rev.* **2002**, *54*, 1057.
- [70] D. W. Lim, D. L. Nettles, L. A. Setton, A. Chilkoti, *Biomacromolecules* **2008**, *9*, 222.
- [71] W. F. Daamen, J. H. Veerkamp, J. C. M. van Hest, T. H. van Kuppevelt, *Biomaterials* **2007**, *28*, 4378.
- [72] L. Martín, M. Alonso, M. Moller, J. C. Rodríguez-Cabello, P. Mela, *Soft Matter* **2009**, *5*, 1591.
- [73] D. W. Urry, W. D. Cunningham, T. Ohnishi, *Biochemistry* **1974**, *13*, 609.

- [74] W. J. Cook, H. Einspahr, T. L. Trapane, D. W. Urry, C. E. Bugg, *J. Am. Chem. Soc.* **1980**, *102*, 5502.
- [75] D. W. Urry, T. L. Trapane, H. Sugano, K. U. Prasad, *J. Am. Chem. Soc.* **1981**, *103*, 2080.
- [76] C. M. Venkatachalam, D. W. Urry, *Macromolecules* **1981**, *14*, 1225.
- [77] X. L. Yao, M. Hong, *J. Am. Chem. Soc.* **2004**, *126*, 4199.
- [78] D. W. Urry, T. L. Trapane, K. U. Prasad, *Biopolymers* **1985**, *24*, 2345.
- [79] R. Henze, D. W. Urry, *J. Am. Chem. Soc.* **1985**, *107*, 2991.
- [80] F. Lelj, A. M. Tamburro, V. Villan, P. Grimaldi, V. Guantieri, *Biopolymers* **1992**, *32*, 161.
- [81] O. Arad, M. Goodman, *Biopolymers* **1990**, *29*, 1633.
- [82] O. Arad, M. Goodman, *Biopolymers* **1990**, *29*, 1651.
- [83] L. Y. Xiao, P. C. Vincent, H. Mei, *Magn. Reson. Chem.* **2004**, *42*, 267.
- [84] K. Ohgo, W. P. Niemczura, J. Ashida, M. Okonogi, T. Asakura, K. K. Kumashiro, *Biomacromolecules* **2006**, *7*, 3306.
- [85] T. Yamaoka, T. Tamura, Y. Seto, T. Tada, S. Kunugi, D. A. Tirrell, *Biomacromolecules* **2003**, *4*, 1680.
- [86] D. E. Meyer, A. Chilkoti, *Biomacromolecules* **2004**, *5*, 846.
- [87] C. Bouchiat, M. D. Wang, J. F. Allemand, T. Strick, S. M. Block, V. Croquette, *Biophys. J.* **1999**, *76*, 409.
- [88] A. Valiaev, D. W. Lim, S. Schmidler, R. L. Clark, A. Chilkoti, S. Zauscher, *J. Am. Chem. Soc.* **2008**, *130*, 10939.
- [89] J. B. Leach, J. B. Wolinsky, P. J. Stone, J. Y. Wong, *Acta Biomater.* **2005**, *1*, 155.
- [90] R. A. McMillan, V. P. Conticello, *Macromolecules* **2000**, *33*, 4809.
- [91] M. Martino, T. Perri, A. M. Tamburro, *Biomacromolecules* **2002**, *3*, 297.
- [92] E. R. Welsh, D. A. Tirrell, *Biomacromolecules* **2000**, *1*, 23.
- [93] L. Huang, R. A. McMillan, R. P. Apkarian, B. Pourdeyimi, V. P. Conticello, E. L. Chaikof, *Macromolecules* **2000**, *33*, 2989.
- [94] K. Nagapudi, W. T. Brinkman, J. E. Leisen, L. Huang, R. A. McMillan, R. P. Apkarian, V. P. Conticello, E. L. Chaikof, *Macromolecules* **2002**, *35*, 1730.
- [95] K. Nagapudi, W. T. Brinkman, B. S. Thomas, J. O. Park, M. Srinivasarao, E. Wright, V. P. Conticello, E. L. Chaikof, *Biomaterials* **2005**, *26*, 4695.
- [96] R. E. Sallach, W. Cui, J. Wen, A. Martinez, V. P. Conticello, E. L. Chaikof, *Biomaterials* **2009**, *30*, 409.
- [97] E. M. Srokowski, K. A. Woodhouse, *J. Biomater. Sci. Polym. Ed.* **2008**, *19*, 785.
- [98] F. W. Keeley, C. M. Bellingham, K. A. Woodhouse, *Philos. Trans. R. Soc. London Ser. B* **2002**, *357*, 185.
- [99] C. M. Bellingham, M. A. Lillie, J. M. Gosline, G. M. Wright, B. C. Starcher, A. J. Bailey, K. A. Woodhouse, F. W. Keeley, *Biopolymers* **2003**, *70*, 445.
- [100] H. C. Kolb, M. G. Finn, K. B. Sharpless, *Angew. Chem.* **2001**, *113*, 2056; *Angew. Chem. Int. Ed.* **2001**, *40*, 2004.
- [101] S. E. Grieshaber, A. J. E. Farran, S. Lin-Gibson, K. L. Kiick, X. Jia, *Macromolecules* **2009**, *42*, 2532.
- [102] Y. Chen, Z. Guan, *J. Am. Chem. Soc.* **2010**, *132*, 4577.
- [103] L. Ayres, M. R. J. Vos, P. J. H. M. Adams, I. O. Shklyarevskiy, J. C. M. van Hest, *Macromolecules* **2003**, *36*, 5967.
- [104] L. Ayres, K. Koch, J. C. M. van Hest, *Macromolecules* **2005**, *38*, 1699.
- [105] R. Koningsveld, A. J. Staverman, *J. Polym. Sci. Part A-2* **1968**, *6*, 325.
- [106] F. Fernández-Trillo, J. C. M. van Hest, J. C. Thies, T. Michon, R. Weberskirch, N. R. Cameron, *Chem. Commun.* **2008**, 2230.
- [107] S. K. Roberts, A. Chilkoti, L. A. Setton, *Biomacromolecules* **2007**, *8*, 2618.
- [108] H. D. Maynard, S. Y. Okada, R. H. Grubbs, *J. Am. Chem. Soc.* **2001**, *123*, 1275.
- [109] R. M. Conrad, R. H. Grubbs, *Angew. Chem.* **2009**, *121*, 8478; *Angew. Chem. Int. Ed.* **2009**, *48*, 8328.
- [110] D. W. Urry, *J. Phys. Chem. B* **1997**, *101*, 11007.
- [111] M. Alonso, V. Reboto, L. Guiscardo, A. San Martin, J. C. Rodriguez-Cabello, *Macromolecules* **2000**, *33*, 9480.
- [112] I. W. Hamley, *Angew. Chem.* **2007**, *119*, 8274; *Angew. Chem. Int. Ed.* **2007**, *46*, 8128.
- [113] O. Khakshoor, J. S. Nowick, *Curr. Opin. Chem. Biol.* **2008**, *12*, 722.
- [114] B. Caughey, P. T. Lansbury, *Annu. Rev. Neurosci.* **2003**, *26*, 267.
- [115] S. S. Ray, R. J. Nowak, K. Strokovich, R. H. Brown, T. Walz, P. T. Lansbury, *Biochemistry* **2004**, *43*, 4899.
- [116] D. E. Barlow, G. H. Dickinson, B. Orihuela, J. L. Kulp, D. Rittschof, K. J. Wahl, *Langmuir* **2010**, *26*, 6549.
- [117] A. J. Geddes, K. D. Parker, E. D. T. Atkins, E. Beighton, *J. Mol. Biol.* **1968**, *32*, 343.
- [118] S. J. Hamodrakas, A. Hoenger, V. A. Iconomidou, *J. Struct. Biol.* **2004**, *145*, 226.
- [119] H. Li, A. F. Oberhauser, S. B. Fowler, J. Clarke, J. M. Fernandez, *Proc. Natl. Acad. Sci. USA* **2000**, *97*, 6527.
- [120] A. M. Smith, T. Scheibel, *Macromol. Chem. Phys.* **2010**, *211*, 127.
- [121] J. E. Bear, M. Krause, F. B. Gertler, *Curr. Opin. Cell Biol.* **2001**, *13*, 158.
- [122] S. Inoué, *J. Struct. Biol.* **1997**, *118*, 87.
- [123] D. L. Cox, H. Lashuel, K. Y. C. Lee, R. R. P. Singh, *MRS Bull.* **2005**, *30*, 452.
- [124] A. Kishimoto, K. Hasegawa, H. Suzuki, H. Taguchi, K. Namba, M. Yoshida, *Biochem. Biophys. Res. Commun.* **2004**, *315*, 739.
- [125] M. F. Perutz, J. T. Finch, J. Beriman, A. Lesk, *Proc. Natl. Acad. Sci. USA* **2002**, *99*, 5591.
- [126] C. Sachse, N. Grigorieff, M. Fändrich, *Angew. Chem.* **2010**, *122*, 1343; *Angew. Chem. Int. Ed.* **2010**, *49*, 1321.
- [127] K. L. De Jong, B. Incledon, C. M. Yip, M. R. DeFelippis, *Biophys. J.* **2006**, *91*, 1905.
- [128] A. T. Petkova, Y. Ishii, J. J. Balbach, O. N. Antzutkin, R. D. Leapman, F. Delaglio, R. Tycko, *Proc. Natl. Acad. Sci. USA* **2002**, *99*, 16742.
- [129] C. Govaerts, H. Wille, S. B. Prusiner, F. E. Cohen, *Proc. Natl. Acad. Sci. USA* **2004**, *101*, 8342.
- [130] R. Paparccone, M. J. Buehler, *Appl. Phys. Lett.* **2009**, *94*, 243904.
- [131] J. L. Jimenez, E. J. Nettleton, M. Bouchard, C. V. Robinson, C. M. Dobson, H. R. Saibil, *Proc. Natl. Acad. Sci. USA* **2002**, *99*, 9196.
- [132] W. T. Astbury, S. Dickinson, *Biochem. J.* **1935**, *29*, 2351.
- [133] E. D. Eanes, G. G. Glenner, *J. Histochem. Cytochem.* **1968**, *16*, 673.
- [134] M. R. Sawaya, S. Sambashivan, R. Nelson, M. I. Ivanova, S. A. Sievers, M. I. Apostol, M. J. Thompson, M. Balbirnie, J. J. W. Wiltzius, H. T. McFarlane, et al., *Nature* **2007**, *447*, 453.
- [135] M. I. Ivanova, S. A. Sievers, M. R. Sawaya, J. S. Wall, D. Eisenberg, *Proc. Natl. Acad. Sci. USA* **2009**, *106*, 18990.
- [136] R. Nelson, M. R. Sawaya, M. Balbirnie, A. O. Madsen, C. Riek, R. Grothe, D. Eisenberg, *Nature* **2005**, *435*, 773.
- [137] L. Goldschmidt, P. K. Teng, R. Riek, D. Eisenberg, *Proc. Natl. Acad. Sci. USA* **2010**, *107*, 3487.
- [138] J. F. Smith, T. P. J. Knowles, C. M. Dobson, C. E. MacPhee, M. E. Welland, *Proc. Natl. Acad. Sci. USA* **2006**, *103*, 15806.
- [139] T. P. Knowles, A. W. Fitzpatrick, S. Meehan, H. R. Mott, M. Vendruscolo, C. M. Dobson, M. E. Welland, *Science* **2007**, *318*, 1900.
- [140] F. Chiti, C. M. Dobson, *Annu. Rev. Biochem.* **2006**, *75*, 333.
- [141] S. Ketten, M. J. Buehler, *Nano Lett.* **2008**, *8*, 743.
- [142] S. Ketten, M. J. Buehler, *Phys. Rev. E* **2008**, *78*, 061913.
- [143] A. Mostaert, M. Higgins, T. Fukuma, F. Rindi, S. Jarvis, *J. Biol. Phys.* **2006**, *32*, 393.
- [144] T. Fukuma, A. Mostaert, S. Jarvis, *Tribol. Lett.* **2006**, *22*, 233.

- [145] S. M. Anika, S. P. Jarvis, *Nanotechnology* **2007**, *18*, 044010.
- [146] S. Keten, M. J. Buehler, *Comput. Methods Appl. Mech. Eng.* **2008**, *197*, 3203.
- [147] M. Lopez de La Paz, K. Goldie, J. Zurdo, E. Lacroix, C. M. Dobson, A. Hoenger, L. Serrano, *Proc. Natl. Acad. Sci. USA* **2002**, *99*, 16052.
- [148] T. P. J. Knowles, T. W. Oppenheim, A. K. Buell, D. Y. Chirgadze, M. E. Welland, *Nat. Nanotechnol.* **2010**, *5*, 204.
- [149] T. Scheibel, R. Parthasarathy, G. Sawicki, X.-M. Lin, H. Jaeger, S. L. Lindquist, *Proc. Natl. Acad. Sci. USA* **2003**, *100*, 4527.
- [150] Y. Leng, H. P. Wei, Z. P. Zhang, Y. F. Zhou, J. Y. Deng, Z. Q. Cui, D. Men, X. Y. You, Z. N. Yu, M. Luo, et al., *Angew. Chem.* **2010**, *122*, 7401; *Angew. Chem. Int. Ed.* **2010**, *49*, 7243.
- [151] E. Gazit, *FASEB J.* **2002**, *16*, 77.
- [152] M. Reches, E. Gazit, *Science* **2003**, *300*, 625.
- [153] N. Kol, L. Adler-Abramovich, D. Barlam, R. Z. Shneck, E. Gazit, I. Roussio, *Nano Lett.* **2005**, *5*, 1343.
- [154] C. Valery, M. Paternostre, B. Robert, T. Gulik-Krzywicki, T. Narayanan, J.-C. Dedieu, G. Keller, M.-L. Torres, R. Cherif-Cheikh, P. Calvo, et al., *Proc. Natl. Acad. Sci. USA* **2003**, *100*, 10258.
- [155] E. Pouget, N. Fay, E. Dujardin, N. Jamin, P. Berthault, L. Perrin, A. Pandit, T. Rose, C. Valery, D. Thomas, et al., *J. Am. Chem. Soc.* **2010**, *132*, 4230.
- [156] A. Aggeli, M. Bell, L. M. Carrick, C. W. G. Fishwick, R. Harding, P. J. Mawer, S. E. Radford, A. E. Strong, N. Boden, *J. Am. Chem. Soc.* **2003**, *125*, 9619.
- [157] A. Aggeli, M. Bell, N. Boden, J. N. Keen, P. F. Knowles, T. C. B. McLeish, M. Pitkeathly, S. E. Radford, *Nature* **1997**, *386*, 259.
- [158] D. M. Marini, V. Hwang, D. A. Lauffenburger, S. Zhang, R. D. Kamm, *Nano Lett.* **2002**, *2*, 295.
- [159] S. Vauthey, S. Santos, H. Gong, N. Watson, S. Zhang, *Proc. Natl. Acad. Sci. USA* **2002**, *99*, 5355.
- [160] A. P. Nowak, V. Breedveld, L. Pakstis, B. Ozbas, D. J. Pine, D. Pochan, T. J. Deming, *Nature* **2002**, *417*, 424.
- [161] L. Aulisa, H. Dong, J. D. Hartgerink, *Biomacromolecules* **2009**, *10*, 2694.
- [162] J. P. Jung, J. L. Jones, S. A. Cronier, J. H. Collier, *Biomaterials* **2008**, *29*, 2143.
- [163] J. H. Collier, B. H. Hu, J. W. Ruberti, J. Zhang, P. Shum, D. H. Thompson, P. B. Messersmith, *J. Am. Chem. Soc.* **2001**, *123*, 9463.
- [164] P. Cao, D. P. Raleigh, *J. Am. Chem. Soc.* **2010**, *132*, 4052.
- [165] C. J. Bowerman, B. L. Nilsson, *J. Am. Chem. Soc.* **2010**, *132*, 9526.
- [166] H. A. Lashuel, S. R. LaBrenz, L. Woo, L. C. Serpell, J. W. Kelly, *J. Am. Chem. Soc.* **2000**, *122*, 5262.
- [167] J. P. Schneider, D. J. Pochan, B. Ozbas, K. Rajagopal, L. Pakstis, J. Kretsinger, *J. Am. Chem. Soc.* **2002**, *124*, 15030.
- [168] K. Oh, Z. Guan, *Chem. Commun.* **2006**, 3069.
- [169] T.-B. Yu, J. Z. Bai, Z. Guan, *Angew. Chem.* **2009**, *121*, 1117; *Angew. Chem. Int. Ed.* **2009**, *48*, 1097.
- [170] J. D. Hartgerink, E. Beniash, S. I. Stupp, *Proc. Natl. Acad. Sci. USA* **2002**, *99*, 5133.
- [171] J. D. Hartgerink, E. Beniash, S. I. Stupp, *Science* **2001**, *294*, 1684.
- [172] S. E. Paramonov, H.-W. Jun, J. D. Hartgerink, *J. Am. Chem. Soc.* **2006**, *128*, 7291.
- [173] E. T. Pashuck, H. Cui, S. I. Stupp, *J. Am. Chem. Soc.* **2010**, *132*, 6041.
- [174] T. Muraoka, H. Cui, S. I. Stupp, *J. Am. Chem. Soc.* **2008**, *130*, 2946.
- [175] J. M. Smeenk, M. B. J. Otten, J. Thies, D. A. Tirrell, J. C. M. van Hest, *Angew. Chem.* **2005**, *117*, 2004; *Angew. Chem. Int. Ed.* **2005**, *44*, 1968.
- [176] J. Hentschel, H. G. Börner, *J. Am. Chem. Soc.* **2006**, *128*, 14142.
- [177] J. Hentschel, E. Krause, H. G. Börner, *J. Am. Chem. Soc.* **2006**, *128*, 7722.
- [178] H. Kühnle, H. G. Börner, *Angew. Chem.* **2009**, *121*, 6552; *Angew. Chem. Int. Ed.* **2009**, *48*, 6431.
- [179] A. Verch, H. Hahn, E. Krause, H. Colfen, H. G. Börner, *Chem. Commun.* **2010**, *46*, 8938.
- [180] E.-K. Schillinger, E. Mena-Osteritz, J. Hentschel, H. G. Börner, P. Bäuerle, *Adv. Mater.* **2009**, *21*, 1562.
- [181] E. Jahnke, I. Lieberwirth, N. Severin, J. P. Rabe, H. Frauenrath, *Angew. Chem.* **2006**, *118*, 5510; *Angew. Chem. Int. Ed.* **2006**, *45*, 5383.
- [182] E. Jahnke, N. Severin, P. Kreutzkamp, J. P. Rabe, H. Frauenrath, *Adv. Mater.* **2008**, *20*, 409.
- [183] M. van den Heuvel, D. W. P. M. Lowik, J. C. M. van Hest, *Biomacromolecules* **2010**, *11*, 1676.
- [184] *Scientific American* **1943**, 78.
- [185] G. H. Altman, F. Diaz, C. Jakuba, T. Calabro, R. L. Horan, J. Chen, H. Lu, J. Richmond, D. L. Kaplan, *Biomaterials* **2003**, *24*, 401.
- [186] F. G. Omenetto, D. L. Kaplan, *Science* **2010**, *329*, 528.
- [187] R. V. Lewis, *Chem. Rev.* **2006**, *106*, 3762.
- [188] D. L. Kaplan, W. W. Adams, C. Viney, B. L. Farmer, *Silk Polymers: Materials Science and Biotechnology* (Ed.: D. Kaplan), American Chemical Society, Washington, DC, **1994**.
- [189] F. Vollrath, *Rev. Mol. Biotechnol.* **2000**, *74*, 67.
- [190] F. Vollrath, W. J. Fairbrother, R. J. P. Williams, E. K. Tillinghast, D. T. Bernstein, K. S. Gallagher, M. A. Townley, *Nature* **1990**, *345*, 526.
- [191] F. Vollrath, E. K. Tillinghast, *Naturwissenschaften* **1991**, *78*, 557.
- [192] N. Becker, E. Oroudjev, S. Mutz, J. P. Cleveland, P. K. Hansma, C. Y. Hayashi, D. E. Makarov, H. G. Hansma, *Nat. Mater.* **2003**, *2*, 278.
- [193] J. G. Hardy, T. R. Scheibel, *Biochem. Soc. Trans.* **2009**, *037*, 677.
- [194] J. C. M. van Hest, D. A. Tirrell, *Chem. Commun.* **2001**, 1897.
- [195] F. K. Ko, J. Jovicic, *Biomacromolecules* **2004**, *5*, 780.
- [196] O. Emile, A. L. Floch, F. Vollrath, *Nature* **2006**, *440*, 621.
- [197] F. Vollrath, D. Porter, *Soft Matter* **2006**, *2*, 377.
- [198] M. Heim, D. Keerl, T. Scheibel, *Angew. Chem.* **2009**, *121*, 3638; *Angew. Chem. Int. Ed.* **2009**, *48*, 3584.
- [199] F. Vollrath, D. P. Knight, *Nature* **2001**, *410*, 541.
- [200] J. O. Warwicker, *Trans. Farad. Soc.* **1956**, *52*, 554.
- [201] M. Xu, R. V. Lewis, *Proc. Natl. Acad. Sci. USA* **1990**, *87*, 7120.
- [202] R. V. Lewis, *Acc. Chem. Res.* **1992**, *25*, 392.
- [203] Y. Termonia, *Macromolecules* **1994**, *27*, 7378.
- [204] H. Heslot, *Biochimie* **1998**, *80*, 19.
- [205] J. M. Gosline, M. E. DeMont, M. W. Denny, *Endeavour* **1986**, *10*, 37.
- [206] A. H. Simmons, C. A. Michal, L. W. Jelinski, *Science* **1996**, *271*, 84.
- [207] S. Keten, Z. Xu, B. Ihle, M. J. Buehler, *Nat. Mater.* **2010**, *9*, 359.
- [208] L. W. Jelinski, A. Blye, O. Liivak, C. Michal, G. LaVerde, A. Seidel, N. Shah, Z. Yang, *Int. J. Biol. Macromol.* **1999**, *24*, 197.
- [209] J. D. van Beek, S. Hess, F. Vollrath, B. H. Meier, *Proc. Natl. Acad. Sci. USA* **2002**, *99*, 10266.
- [210] F. Vollrath, D. Porter, *Appl. Phys. A* **2006**, *82*, 205.
- [211] C. Y. Hayashi, R. V. Lewis, *J. Mol. Biol.* **1998**, *275*, 773.
- [212] D. R. Askeland, *The Science and Engineering of Materials*, PWS, Boston, **1994**.
- [213] D. Porter, F. Vollrath, *Adv. Mater.* **2009**, *21*, 487.
- [214] D. P. Knight, F. Vollrath, *Philos. Trans. R. Soc. London Ser. B* **2002**, *357*, 219.
- [215] H.-J. Jin, D. L. Kaplan, *Nature* **2003**, *424*, 1057.
- [216] R. Silvers, F. Buhr, H. Schwalbe, *Angew. Chem.* **2010**, *122*, 5538; *Angew. Chem. Int. Ed.* **2010**, *49*, 5410.
- [217] G. Askarieh, M. Hedhammar, K. Nordling, A. Saenz, C. Casals, A. Rising, J. Johansson, S. D. Knight, *Nature* **2010**, *465*, 236.



- [218] F. Hagn, L. Eisoldt, J. G. Hardy, C. Vendrely, M. Coles, T. Scheibel, H. Kessler, *Nature* **2010**, *465*, 239.
- [219] T. Scheibel, *Microb. Cell Fact.* **2004**, *3*, 14.
- [220] S. A. Fossey, G. Némethy, K. D. Gibson, H. A. Scheraga, *Biopolymers* **1991**, *31*, 1529.
- [221] M. T. Krejchi, E. D. T. Atkins, A. J. Waddon, M. J. Fournier, T. L. Mason, D. A. Tirrell, *Science* **1994**, *265*, 1427.
- [222] Y. Qu, S. C. Payne, R. P. Apkarian, V. P. Conticello, *J. Am. Chem. Soc.* **2000**, *122*, 5014.
- [223] S. Zhang, T. Holmes, C. Lockshin, A. Rich, *Proc. Natl. Acad. Sci. USA* **1993**, *90*, 3334.
- [224] R. Valluzzi, S. Szela, P. Avtges, D. Kirschner, D. Kaplan, *J. Phys. Chem. B* **1999**, *103*, 11382.
- [225] S. Szela, P. Avtges, R. Valluzzi, S. Winkler, D. Wilson, D. Kirschner, D. L. Kaplan, *Biomacromolecules* **2000**, *1*, 534.
- [226] S. Winkler, D. Wilson, D. L. Kaplan, *Biochemistry* **2000**, *39*, 12739.
- [227] K. Nagapudi, W. T. Brinkman, J. Leisen, B. S. Thomas, E. R. Wright, C. Haller, X. Wu, R. P. Apkarian, V. P. Conticello, E. L. Chaikof, *Macromolecules* **2005**, *38*, 345.
- [228] C. Vendrely, T. Scheibel, *Macromol. Biosci.* **2007**, *7*, 401.
- [229] J. P. O'Brien, S. R. Fahnestock, Y. Termonia, K. H. Gardner, *Adv. Mater.* **1998**, *10*, 1185.
- [230] A. Seidel, O. Liivak, L. W. Jelinski, *Macromolecules* **1998**, *31*, 6733.
- [231] A. Lazaris, S. Arcidiacono, Y. Huang, J.-F. Zhou, F. Duguay, N. Chretien, E. A. Welsh, J. W. Soares, C. N. Karatzas, *Science* **2002**, *295*, 472.
- [232] D. Huemmerich, C. Helsen, S. Quedzuweit, J. Oschmann, R. Rudolph, T. Scheibel, *Biochemistry* **2004**, *43*, 13604.
- [233] S. Rammensee, U. Slotta, T. Scheibel, A. R. Bausch, *Proc. Natl. Acad. Sci. USA* **2008**, *105*, 6590.
- [234] O. Rathore, D. Y. Sogah, *Macromolecules* **2001**, *34*, 1477.
- [235] Y. Liu, Z. Shao, F. Vollrath, *Nat. Mater.* **2005**, *4*, 901.
- [236] C. Zhou, B. Leng, J. Yao, J. Qian, X. Chen, P. Zhou, D. P. Knight, Z. Shao, *Biomacromolecules* **2006**, *7*, 2415.
- [237] L. T. J. Korley, B. D. Pate, E. L. Thomas, P. T. Hammond, *Polymer* **2006**, *47*, 3073.
- [238] Z.-R. Chen, J. A. Kornfield, S. D. Smith, J. T. Grothaus, M. M. Satkowski, *Science* **1997**, *277*, 1248.
- [239] W.-J. Zhou, J. A. Kornfield, V. M. Ugaz, W. R. Burghardt, D. R. Link, N. A. Clark, *Macromolecules* **1999**, *32*, 5581.
- [240] L. Pauling, R. B. Corey, H. R. Branson, *Proc. Natl. Acad. Sci. USA* **1951**, *37*, 205.
- [241] B. Alberts, A. Johnson, J. Lewis, M. Raff, K. Roberts, P. Walter, *Molecular Biology of the Cell*, 4th ed., Garland Science New York, **2002**.
- [242] H. G. M. Edwards, D. E. Hunt, M. G. Sibley, *Spectrochim. Acta Part A* **1998**, *54*, 745.
- [243] T. Ackbarow, D. Sen, C. Thaulow, M. J. Buehler, *PLoS ONE* **2009**, *4*, e6015.
- [244] T. Ackbarow, M. Buehler, *J. Mater. Sci.* **2007**, *42*, 8771.
- [245] M. J. Buehler, T. Ackbarow, *Mater. Today* **2007**, *10*, 46.
- [246] Z. Qin, L. Kreplak, M. J. Buehler, *Nanotechnology* **2009**, *20*, 425101.
- [247] L. Kreplak, J. Doucet, F. Briki, *Biopolymers* **2001**, *58*, 526.
- [248] L. Kreplak, J. Doucet, P. Dumas, F. Briki, *Biophys. J.* **2004**, *87*, 640.
- [249] A. Miserez, S. S. Wasko, C. F. Carpenter, J. H. Waite, *Nat. Mater.* **2009**, *8*, 910.
- [250] H. Herrmann, U. Aebi, *Curr. Opin. Struct. Biol.* **1998**, *8*, 177.
- [251] D. N. Woolfson, T. Alber, *Protein Sci.* **1995**, *4*, 1596.
- [252] C. Cohen, D. A. D. Parry, *Proteins Struct. Funct. Genet.* **1990**, *7*, 1.
- [253] N. L. Ogiyara, M. S. Weiss, D. Eisenberg, W. F. Degrad, *Protein Sci.* **1997**, *6*, 80.
- [254] G. G. Privé, D. H. Anderson, L. Wesson, D. Cascio, D. Eisenberg, *Protein Sci.* **1999**, *8*, 1400.
- [255] A. Lupas, *Trends Biochem. Sci.* **1996**, *21*, 375.
- [256] A. N. Lupas, M. Gruber, *Adv. Protein Chem.* **2005**, *70*, 37.
- [257] D. N. Woolfson, *Adv. Protein Chem.* **2005**, *70*, 79.
- [258] J. M. Mason, K. M. Arndt, *ChemBioChem* **2004**, *5*, 170.
- [259] F. H. C. Crick, *Nature* **1952**, *170*, 882.
- [260] R. S. Hodges, J. Sodak, L. B. Smillie, L. Jurasek, *Cold Spring Harbor Symp. Quant. Biol.* **1972**, *37*, 299.
- [261] A. D. McLachlan, M. Stewart, *J. Mol. Biol.* **1975**, *98*, 293.
- [262] E. K. O'Shea, R. Rutkowski, P. S. Kim, *Cell* **1992**, *68*, 699.
- [263] K. M. Arndt, J. N. Pelletier, K. M. Müller, T. Alber, S. W. Michnick, A. Plückthun, *J. Mol. Biol.* **2000**, *295*, 627.
- [264] E. K. O'Shea, K. J. Lumb, P. S. Kim, *Curr. Biol.* **1993**, *3*, 658.
- [265] M. L. Diss, A. J. Kennan, *J. Am. Chem. Soc.* **2008**, *130*, 1321.
- [266] S. Betz, R. Fairman, K. O'Neil, J. Lear, W. Degrad, *Philos. Trans. R. Soc. London Ser. B* **1995**, *348*, 81.
- [267] K. M. Campbell, A. J. Sholders, K. J. Lumb, *Biochemistry* **2002**, *41*, 4866.
- [268] J. R. S. Newman, A. E. Keating, *Science* **2003**, *300*, 2097.
- [269] G. Grigoryan, A. W. Reinke, A. E. Keating, *Nature* **2009**, *458*, 859.
- [270] A. E. Keating, V. N. Malashkevich, B. Tidor, P. S. Kim, *Proc. Natl. Acad. Sci. USA* **2001**, *98*, 14825.
- [271] G. Grigoryan, A. E. Keating, *Curr. Opin. Struct. Biol.* **2008**, *18*, 477.
- [272] J. M. Mason, M. A. Schmitz, K. M. Muller, K. M. Arndt, *Proc. Natl. Acad. Sci. USA* **2006**, *103*, 8989.
- [273] J. R. Lai, J. D. Fisk, B. Weisblum, S. H. Gellman, *J. Am. Chem. Soc.* **2004**, *126*, 10514.
- [274] A. W. Reinke, R. A. Grant, A. E. Keating, *J. Am. Chem. Soc.* **2010**, *132*, 6025.
- [275] E. H. C. Bromley, R. B. Sessions, A. R. Thomson, D. N. Woolfson, *J. Am. Chem. Soc.* **2009**, *131*, 928.
- [276] W. A. Petka, J. L. Harden, K. P. McGrath, D. Wirtz, D. A. Tirrell, *Science* **1998**, *281*, 389.
- [277] S. Kojima, Y. Kuriki, T. Yoshida, K. Yazaki, K.-i. Miura, *Proc. Jpn. Acad. Ser. B* **1997**, *73*, 7.
- [278] S. A. Potekhin, T. N. Melnik, V. Popov, N. F. Lanina, A. A. Vazina, P. Rigler, A. S. Verdini, G. Corradin, A. V. Kajava, *Chem. Biol.* **2001**, *8*, 1025.
- [279] A. V. Kajava, S. A. Potekhin, G. Corradin, R. D. Leapman, *J. Pept. Sci.* **2004**, *10*, 291.
- [280] T. N. Melnik, V. Villard, V. Vasiliev, G. Corradin, A. V. Kajava, S. A. Potekhin, *Protein Eng.* **2003**, *16*, 1125.
- [281] Y. Zimenkov, V. P. Conticello, L. Guo, P. Thiyagarajan, *Tetrahedron* **2004**, *60*, 7237.
- [282] Y. Zimenkov, S. N. Dublin, R. Ni, R. S. Tu, V. Breedveld, R. P. Apkarian, V. P. Conticello, *J. Am. Chem. Soc.* **2006**, *128*, 6770.
- [283] S. Dublin, Y. Zimenkov, V. P. Conticello, *Biochem. Soc. Trans.* **2009**, *037*, 653.
- [284] S. N. Dublin, V. P. Conticello, *J. Am. Chem. Soc.* **2008**, *130*, 49.
- [285] M. J. Pandya, G. M. Spooner, M. Sunde, J. R. Thorpe, A. Rodger, D. N. Woolfson, *Biochemistry* **2000**, *39*, 8728.
- [286] M. G. Ryadnov, D. N. Woolfson, *J. Am. Chem. Soc.* **2007**, *129*, 14074.
- [287] A. M. Smith, E. F. Banwell, W. R. Edwards, M. J. Pandya, D. N. Woolfson, *Adv. Funct. Mater.* **2006**, *16*, 1022.
- [288] D. Papapostolou, A. M. Smith, E. D. T. Atkins, S. J. Oliver, M. G. Ryadnov, L. C. Serpell, D. N. Woolfson, *Proc. Natl. Acad. Sci. USA* **2007**, *104*, 10853.
- [289] M. G. Ryadnov, D. N. Woolfson, *Nat. Mater.* **2003**, *2*, 329.
- [290] M. G. Ryadnov, D. N. Woolfson, *Angew. Chem.* **2003**, *115*, 3129; *Angew. Chem. Int. Ed.* **2003**, *42*, 3021.
- [291] M. G. Ryadnov, D. N. Woolfson, *J. Am. Chem. Soc.* **2005**, *127*, 12407.

- [292] D. E. Wagner, C. L. Phillips, W. M. Ali, G. E. Nybakken, E. D. Crawford, A. D. Schwab, W. F. Smith, R. Fairman, *Proc. Natl. Acad. Sci. USA* **2005**, *102*, 12656.
- [293] K. L. Lazar, H. Miller-Auer, G. S. Getz, J. P. R. O. Orgel, S. C. Meredith, *Biochemistry* **2005**, *44*, 12681.
- [294] H. Dong, J. D. Hartgerink, *Biomacromolecules* **2006**, *7*, 691.
- [295] H. Dong, S. E. Paramonov, J. D. Hartgerink, *J. Am. Chem. Soc.* **2008**, *130*, 13691.
- [296] K. Pagel, S. C. Wagner, K. Samedov, H. von Berlepsch, C. Bottcher, B. Kokscher, *J. Am. Chem. Soc.* **2006**, *128*, 2196.
- [297] M. R. Hicks, D. V. Holberton, C. Kowalczyk, D. N. Woolfson, *Folding Des.* **1997**, *2*, 149.
- [298] D. A. D. Parry, *J. Struct. Biol.* **2006**, *155*, 370.
- [299] F. Zhang, K. A. Timm, K. M. Arndt, G. A. Woolley, *Angew. Chem.* **2010**, *122*, 4035; *Angew. Chem. Int. Ed.* **2010**, *49*, 3943.
- [300] M. Suzuki, K. Saruwatari, T. Kogure, Y. Yamamoto, T. Nishimura, T. Kato, H. Nagasawa, *Science* **2009**, *325*, 1388.
- [301] P. T. Wilder, T. H. Charpentier, D. J. Weber, *ChemMedChem* **2007**, *2*, 1149.
- [302] R. N. Chapman, G. Dimartino, P. S. Arora, *J. Am. Chem. Soc.* **2004**, *126*, 12252.
- [303] J. T. Kellis, R. J. Todd, F. H. Arnold, *Nat. Biotechnol.* **1991**, *9*, 994.
- [304] F. H. Silver, J. W. Freeman, G. P. Seehra, *J. Biomech.* **2003**, *36*, 1529.
- [305] A. Rich, F. H. C. Crick, *Nature* **1955**, *176*, 915.
- [306] A. Rich, F. H. C. Crick, *J. Mol. Biol.* **1961**, *3*, 483.
- [307] G. N. Ramachandran, *Int. Rev. Connect. Tissue Res.* **1963**, *1*, 127.
- [308] G. N. Ramachandran, G. Kartha, *Nature* **1955**, *176*, 593.
- [309] G. N. Ramachandran, G. Kartha, *Nature* **1954**, *174*, 269.
- [310] G. N. Ramachandran, *Nature* **1956**, *177*, 710.
- [311] R. D. B. Fraser, T. P. MacRae, E. Suzuki, *J. Mol. Biol.* **1979**, *129*, 463.
- [312] T. V. Burjanadze, *Biopolymers* **1992**, *32*, 941.
- [313] D. A. Slatyer, C. A. Miles, A. J. Bailey, *J. Mol. Biol.* **2003**, *329*, 175.
- [314] E. Leikina, M. V. Merts, N. Kuznetsova, S. Leikin, *Proc. Natl. Acad. Sci. USA* **2002**, *99*, 1314.
- [315] N. Panasiak, Jr., E. S. Eberhardt, A. S. Edison, D. R. Powell, R. T. Raines, *Int. J. Pept. Protein Res.* **1994**, *44*, 262.
- [316] M. L. DeRider, S. J. Wilkens, M. J. Waddell, L. E. Bretscher, F. Weinhold, R. T. Raines, J. L. Markley, *J. Am. Chem. Soc.* **2002**, *124*, 2497.
- [317] S. K. Holmgren, K. M. Taylor, L. E. Bretscher, R. T. Raines, *Nature* **1998**, *392*, 666.
- [318] C. A. Miles, T. V. Burjanadze, A. J. Bailey, *J. Mol. Biol.* **1995**, *245*, 437.
- [319] J. Bella, B. Brodsky, H. M. Berman, *Connect. Tissue Res.* **1996**, *35*, 455.
- [320] B. L. Trus, K. A. Piez, *J. Mol. Biol.* **1976**, *108*, 705.
- [321] J. Khoshnoodi, J.-P. Cartailier, K. Alvares, A. Veis, B. G. Hudson, *J. Biol. Chem.* **2006**, *281*, 38117.
- [322] C. C. Banos, A. H. Thomas, C. K. Kuo, *Birth Defects Res. Part C* **2008**, *84*, 228.
- [323] K. A. Piez, B. L. Trus, *J. Mol. Biol.* **1977**, *110*, 701.
- [324] F. Jiang, H. Hörber, J. Howard, D. J. Müller, *J. Struct. Biol.* **2004**, *148*, 268.
- [325] W. Zhang, S. S. Liao, F. Z. Cui, *Chem. Mater.* **2003**, *15*, 3221.
- [326] D. A. Cisneros, C. Hung, C. M. Franz, D. J. Muller, *J. Struct. Biol.* **2006**, *154*, 232.
- [327] J. A. Spadaro, R. O. Becker, C. H. Bachman, *Nature* **1970**, *225*, 1134.
- [328] J. A. Spadaro, R. O. Becker, *Biochim. Biophys. Acta Protein Struct.* **1972**, *263*, 585.
- [329] N. Kuznetsova, S. Leikin, *J. Biol. Chem.* **1999**, *274*, 36083.
- [330] D. J. Prockop, A. Fertala, *J. Struct. Biol.* **1998**, *122*, 111.
- [331] R. Puxkandl, I. Zizak, O. Paris, J. Keckes, W. Tesch, S. Bernstorff, P. Purslow, P. Fratzl, *Philos. Trans. R. Soc. London Ser. B* **2002**, *357*, 191.
- [332] K. J. Coyne, X.-X. Qin, J. H. Waite, *Science* **1997**, *277*.
- [333] M. J. Buehler, *Proc. Natl. Acad. Sci. USA* **2006**, *103*, 12285.
- [334] W. Yang, M. L. Battineni, B. Brodsky, *Biochemistry* **1997**, *36*, 6930.
- [335] A. V. Persikov, R. J. Pillitteri, P. Amin, U. Schwarze, P. H. Byers, B. Brodsky, *Hum. Mutat.* **2004**, *24*, 330.
- [336] X. Y. Liu, S. Kim, Q. H. Dai, B. Brodsky, J. Baum, *Biochemistry* **1998**, *37*, 15528.
- [337] T. J. Hyde, M. A. Bryan, B. Brodsky, J. Baum, *J. Biol. Chem.* **2006**, *281*, 36937.
- [338] A. V. Buevich, T. Silva, B. Brodsky, J. Baum, *J. Biol. Chem.* **2004**, *279*, 46890.
- [339] M. Bhate, X. Wang, J. Baum, B. Brodsky, *Biochemistry* **2002**, *41*, 6539.
- [340] K. Beck, V. C. Chan, N. Shenoy, A. Kirkpatrick, J. A. M. Ramshaw, B. Brodsky, *Proc. Natl. Acad. Sci. USA* **2000**, *97*, 4273.
- [341] J. Baum, B. Brodsky, *Folding Des.* **1997**, *2*, R53.
- [342] M. L. Battineni, W. Yang, X. Y. Liu, J. Baum, B. Brodsky, *Matrix Biol.* **1996**, *15*, 175.
- [343] K. Okuyama, S. Arnott, *J. Mol. Biol.* **1981**, *152*, 427.
- [344] R. Berisio, L. Vitagliano, L. Mazzarella, A. Zagari, *Biopolymers* **2000**, *56*, 8.
- [345] L. Vitagliano, R. Berisio, L. Mazzarella, A. Zagari, *Biopolymers* **2001**, *58*, 459.
- [346] R. Z. Kramer, L. Vitagliano, J. Bella, R. Berisio, L. Mazzarella, B. Brodsky, A. Zagari, H. M. Berman, *J. Mol. Biol.* **1998**, *280*, 623.
- [347] R. Z. Kramer, J. Bella, P. Mayville, B. Brodsky, H. M. Berman, *Nat. Struct. Biol.* **1999**, *6*, 454.
- [348] J. Bella, M. Eaton, B. Brodsky, H. Berman, *Science* **1994**, *266*, 75.
- [349] J. Bella, B. Brodsky, H. M. Berman, *Structure* **1995**, *3*, 893.
- [350] M. Goodman, M. Bhumralkar, E. A. Jefferson, J. Kwak, E. Locardi, *Pept. Sci.* **1998**, *47*, 127.
- [351] C. G. Fields, B. Grab, J. L. Lauer, G. B. Fields, *Anal. Biochem.* **1995**, *231*, 57.
- [352] W. Roth, E. Heidemann, *Biopolymers* **1980**, *19*, 1909.
- [353] S. Thakur, D. Vadolas, H.-P. Germann, E. Heidemann, *Biopolymers* **1986**, *25*, 1081.
- [354] B. Grab, A. J. Miles, L. T. Furcht, G. B. Fields, *J. Biol. Chem.* **1996**, *271*, 12234.
- [355] Y. Greiche, E. Heidemann, *Biopolymers* **1979**, *18*, 2359.
- [356] Y. Feng, G. Melacini, J. P. Taulane, M. Goodman, *J. Am. Chem. Soc.* **1996**, *118*, 10351.
- [357] G. Melacini, Y. Feng, M. Goodman, *J. Am. Chem. Soc.* **1996**, *118*, 10359.
- [358] M. Goodman, Y. Feng, G. Melacini, J. P. Taulane, *J. Am. Chem. Soc.* **1996**, *118*, 5156.
- [359] J. Kwak, A. De Capua, E. Locardi, M. Goodman, *J. Am. Chem. Soc.* **2002**, *124*, 14085.
- [360] G. A. Kinberger, W. Cai, M. Goodman, *J. Am. Chem. Soc.* **2002**, *124*, 15162.
- [361] W. Cai, D. Wong, G. A. Kinberger, S. W. Kwok, J. P. Taulane, M. Goodman, *Bioorg. Chem.* **2007**, *35*, 327.
- [362] G. R. Newkome, X. Lin, *Macromolecules* **1991**, *24*, 1443.
- [363] G. Melacini, Y. Feng, M. Goodman, *J. Am. Chem. Soc.* **1996**, *118*, 10359.
- [364] G. Melacini, Y. Feng, M. Goodman, *J. Am. Chem. Soc.* **1996**, *118*, 10725.
- [365] G. Melacini, Y. Feng, M. Goodman, *Biochemistry* **1997**, *36*, 8725.
- [366] Y. Feng, G. Melacini, J. P. Taulane, M. Goodman, *Biopolymers* **1996**, *39*, 859.

- [367] W. Cai, S. W. Kwok, J. P. Taulane, M. Goodman, *J. Am. Chem. Soc.* **2004**, *126*, 15030.
- [368] T. Koide, M. Yuguchi, M. Kawakita, H. Konno, *J. Am. Chem. Soc.* **2002**, *124*, 9388.
- [369] V. Gauba, J. D. Hartgerink, *J. Am. Chem. Soc.* **2007**, *129*, 2683.
- [370] V. Gauba, J. D. Hartgerink, *J. Am. Chem. Soc.* **2007**, *129*, 15034.
- [371] J. A. Fallas, V. Gauba, J. D. Hartgerink, *J. Biol. Chem.* **2009**, *284*, 26851.
- [372] S. Fiori, B. Saccà, L. Moroder, *J. Mol. Biol.* **2002**, *319*, 1235.
- [373] D. A. Slatter, L. A. Foley, A. R. Peachey, D. Nietlispach, R. W. Farndale, *J. Mol. Biol.* **2006**, *359*, 289.
- [374] V. Gauba, J. D. Hartgerink, *J. Am. Chem. Soc.* **2008**, *130*, 7509.
- [375] L. E. Russell, J. A. Fallas, J. D. Hartgerink, *J. Am. Chem. Soc.* **2010**, *132*, 3242.
- [376] S. E. Paramonov, V. Gauba, J. D. Hartgerink, *Macromolecules* **2005**, *38*, 7555.
- [377] T. Kishimoto, Y. Morihara, M. Osanai, S.-i. Ogata, M. Kamitakahara, C. Ohtsuki, M. Tanihara, *Biopolymers* **2005**, *79*, 163.
- [378] F. W. Kotch, R. T. Raines, *Proc. Natl. Acad. Sci. USA* **2006**, *103*, 3028.
- [379] M. A. Cejas, W. A. Kinney, C. Chen, J. G. Vinter, H. R. Almond, K. M. Balss, C. A. Maryanoff, U. Schmidt, M. Breslav, A. Mahan, et al., *Proc. Natl. Acad. Sci. USA* **2008**, *105*, 8513.
- [380] D. E. Przybyla, J. Chmielewski, *J. Am. Chem. Soc.* **2008**, *130*, 12610.
- [381] M. M. Pires, J. Chmielewski, *J. Am. Chem. Soc.* **2009**, *131*, 2706.
- [382] M. M. Pires, D. E. Przybyla, J. Chmielewski, *Angew. Chem.* **2009**, *121*, 7953; *Angew. Chem. Int. Ed.* **2009**, *48*, 7813.
- [383] S. Rele, Y. Song, R. P. Apkarian, Z. Qu, V. P. Conticello, E. L. Chaikof, *J. Am. Chem. Soc.* **2007**, *129*, 14780.
- [384] L. Fischer, P. Claudon, N. Pendem, E. Miclet, C. Didierjean, E. Ennifar, G. Guichard, *Angew. Chem.* **2010**, *122*, 1085; *Angew. Chem. Int. Ed.* **2010**, *49*, 1067.
- [385] N. W. Owens, J. Stetefeld, E. Lattovai, F. Schweizer, *J. Am. Chem. Soc.* **2010**, *132*, 5036.
- [386] V. Vogel, *Annu. Rev. Biophys. Biomol. Struct.* **2006**, *35*, 459.
- [387] M. Ito, H. Ishikawa, S. Nonomura, M. Fujita, *Seitai no Kagaku* **2000**, *51*.
- [388] A. S. French, *Annu. Rev. Physiol.* **1992**, *54*, 135.
- [389] P. G. Gillespie, R. G. Walker, *Nature* **2001**, *413*, 194.
- [390] B. Martinac, *J. Cell Sci.* **2004**, *117*, 2449.
- [391] V. Vogel, G. Baneyx, *Annu. Rev. Biomed. Eng.* **2003**, *5*, 441.
- [392] K. Maruyama, *FASEB J.* **1997**, *11*, 341.
- [393] K. Wang, *Adv. Biophys.* **1996**, *33*, 123.
- [394] H. P. Erickson, *Proc. Natl. Acad. Sci. USA* **1994**, *91*, 10114.
- [395] S. Labeit, B. Kolmerer, *Science* **1995**, *270*, 293.
- [396] H. Granzier, M. Helmes, K. Trombitas, *Biophys. J.* **1996**, *70*, 430.
- [397] M. S. Z. Kellermayer, S. B. Smith, H. L. Granzier, C. Bustamante, *Science* **1997**, *276*, 1112.
- [398] P. E. Marszalek, H. Lu, H. Li, M. Carrion-Vazquez, A. F. Oberhauser, K. Schulten, J. M. Fernandez, *Nature* **1999**, *402*, 100.
- [399] H. Li, A. F. Oberhauser, S. D. Redick, M. Carrion-Vazquez, H. P. Erickson, J. M. Fernandez, *Proc. Natl. Acad. Sci. USA* **2001**, *98*, 10682.
- [400] M. Rief, M. Gautel, F. Oesterhelt, J. M. Fernandez, H. E. Gaub, *Science* **1997**, *276*, 1109.
- [401] L. Tskhovrebova, J. Trinick, J. A. Sleep, R. M. Simmons, *Nature* **1997**, *387*, 308.
- [402] F. Oesterhelt, D. Oesterhelt, M. Pfeiffer, A. Engel, H. E. Gaub, D. J. Müller, *Science* **2000**, *288*, 143.
- [403] P. E. Marszalek, H. Li, A. F. Oberhauser, J. M. Fernandez, *Proc. Natl. Acad. Sci. USA* **2002**, *99*, 4278.
- [404] H. Li, W. A. Linke, A. F. Oberhauser, M. Carrion-Vazquez, J. G. Kerkvliet, H. Lu, P. E. Marszalek, J. M. Fernandez, *Nature* **2002**, *418*, 998.
- [405] H. Clausen-Schaumann, M. Rief, C. Tolksdorf, H. E. Gaub, *Biophys. J.* **2000**, *78*, 1997.
- [406] B. L. Smith, T. E. Schaffer, M. Viani, J. B. Thompson, N. A. Frederick, J. Kindt, A. Belcher, G. D. Stucky, D. E. Morse, P. K. Hansma, *Nature* **1999**, *399*, 761.
- [407] H. Lu, K. Schulten, *Biophys. J.* **2000**, *79*, 51.
- [408] C. Chothia, E. Y. Jones, *Annu. Rev. Biochem.* **1997**, *66*, 823.
- [409] T. E. Fisher, M. Carrion-Vazquez, A. F. Oberhauser, H. Li, P. E. Marszalek, J. M. Fernandez, *Neuron* **2000**, *27*, 435.
- [410] A. F. Oberhauser, P. E. Marszalek, H. P. Erickson, J. M. Fernandez, *Nature* **1998**, *393*, 181.
- [411] D. Craig, A. Krammer, K. Schulten, V. Vogel, *Proc. Natl. Acad. Sci. USA* **2001**, *98*, 5590.
- [412] M. Gao, D. Craig, V. Vogel, K. Schulten, *J. Mol. Biol.* **2002**, *323*, 939.
- [413] S. P. Ng, R. W. S. Rounsevell, A. Steward, C. D. Geierhaas, P. M. Williams, E. Paci, J. Clarke, *J. Mol. Biol.* **2005**, *350*, 776.
- [414] E. Klotzsch, M. L. Smith, K. E. Kubow, S. Muntwyler, W. C. Little, F. Beyeler, D. Gourdon, B. J. Nelson, V. Vogel, *Proc. Natl. Acad. Sci. USA* **2009**, *106*, 18267.
- [415] K. A. Walther, F. Gräter, L. Dougan, C. L. Badilla, B. J. Berne, J. M. Fernandez, *Proc. Natl. Acad. Sci. USA* **2007**, *104*, 7916.
- [416] M. Gao, D. Craig, O. Lequin, I. D. Campbell, V. Vogel, K. Schulten, *Proc. Natl. Acad. Sci. USA* **2003**, *100*, 14784.
- [417] A. E. X. Brown, R. I. Litvinov, D. E. Discher, P. K. Purohit, J. W. Weisel, *Science* **2009**, *325*, 741.
- [418] W. Liu, L. M. Jawerth, E. A. Sparks, M. R. Falvo, R. R. Hantgan, R. Superfine, S. T. Lord, M. Guthold, *Science* **2006**, *313*, 634.
- [419] C. M. Kielty, C. Baldock, D. Lee, M. J. Rock, J. L. Ashworth, C. A. Shuttleworth, *Philos. Trans. R. Soc., London, Philos. Trans. R. Soc. London Ser. B* **2002**, *357*, 207.
- [420] M. Rief, J. Pascual, M. Saraste, H. E. Gaub, *J. Mol. Biol.* **1999**, *286*, 553.
- [421] H. Li, *Adv. Funct. Mater.* **2008**, *18*, 2643.
- [422] Y. Cao, H. Li, *Nat. Mater.* **2007**, *6*, 109.
- [423] Y. Cao, T. Yoo, H. Li, *Proc. Natl. Acad. Sci. USA* **2008**, *105*, 11152.
- [424] Y. Cao, H. Li, *Chem. Commun.* **2008**, 4144.
- [425] S. Lv, D. M. Dudek, Y. Cao, M. M. Balamurali, J. Gosline, H. Li, *Nature* **2010**, *465*, 69.
- [426] D. L. Guzman, A. Randall, P. Baldi, Z. Guan, *Proc. Natl. Acad. Sci. USA* **2010**, *107*, 1989.
- [427] *Comprehensive Polymer Science: The Synthesis Characterization, Reactions, and Applications of Polymers*, Vol. 2 (Eds.: C. Booth, C. Price), Pergamon, New York, **1989**.
- [428] Z. Guan, J. T. Roland, J. Z. Bai, S. X. Ma, T. M. McIntire, M. Nguyen, *J. Am. Chem. Soc.* **2004**, *126*, 2058.
- [429] Z. Guan, *Polym. Int.* **2007**, *56*, 467.
- [430] R. P. Sijbesma, F. H. Beijer, L. Brunsveld, B. J. B. Folmer, J. H. K. K. Hirschberg, R. F. M. Lange, J. K. L. Lowe, E. W. Meijer, *Science* **1997**, *278*, 1601.
- [431] H. Ohkawa, G. B. W. L. Ligthart, R. P. Sijbesma, E. W. Meijer, *Macromolecules* **2007**, *40*, 1453.
- [432] K. Yamauchi, J. R. Lizotte, T. E. Long, *Macromolecules* **2003**, *36*, 1083.
- [433] C. L. Elkins, T. Park, M. G. McKee, T. E. Long, *J. Polym. Sci. Part A* **2005**, *43*, 4618.
- [434] T. Park, S. C. Zimmerman, S. Nakashima, *J. Am. Chem. Soc.* **2005**, *127*, 6520.
- [435] J. T. Roland, Z. Guan, *J. Am. Chem. Soc.* **2004**, *126*, 14328.
- [436] Z. R. Guan, J. T. Roland, J. Z. Bai, X. S. Ma, T. M. McIntire, M. Nguyen, *J. Am. Chem. Soc.* **2004**, *126*, 2058.
- [437] D. Zhang, C. Ortiz, *Macromolecules* **2004**, *37*, 4271.

- [438] B. Y. Gong, Y. Yan, H. Q. Zeng, E. Skrzypczak-Jankunn, Y. W. Kim, J. Zhu, H. Ickes, *J. Am. Chem. Soc.* **1999**, *121*, 5607.
- [439] D. L. Guzmán, J. T. Roland, H. Keer, Y. P. Kong, T. Ritz, A. Yee, Z. Guan, *Polymer* **2008**, *49*, 3892.
- [440] A. M. Kushner, J. D. Vossler, G. A. Williams, Z. Guan, *J. Am. Chem. Soc.* **2009**, *131*, 8766.
- [441] S. L. Potisek, D. A. Davis, N. R. Sottos, S. R. White, J. S. Moore, *J. Am. Chem. Soc.* **2007**, *129*, 13808.
- [442] A. M. Kushner, V. Gabuchian, E. G. Johnson, Z. Guan, *J. Am. Chem. Soc.* **2007**, *129*, 14110.
- [443] D. W. P. M. Löwik, E. H. P. Leunissen, M. van den Heuvel, M. B. Hansen, J. C. M. van Hest, *Chem. Soc. Rev.* **2010**, *39*, 3394.
- [444] H. G. Börner, *Prog. Polym. Sci.* **2009**, *34*, 811.

# Handbook of Pharmaceutical Salts

Properties, Selection, and Use

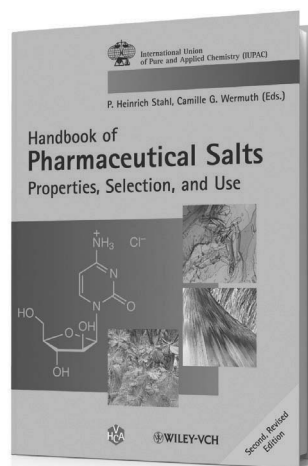
Second, Revised Edition

*'It should be in the library of every pharmaceutical company'*

Organic Process Research and Development Journal

*'A rare commodity, a body of knowledge on an important area, summarised in a single volume. This long overdue volume belongs on the personal shelf of every pharmaceutical scientist.'*

Pharmaceutical Development and Technology



P. Heinrich Stahl and  
Camille G. Wermuth (Eds.)  
Publication date: February 2011  
Hardcover  
ISBN: 978-3-90639-051-2

- A comprehensive resource addressing the preparation, selection, and use of pharmaceutically active salts
- Examines the opportunities for increased efficacy and improved drug delivery, provided by the selection of the optimal salt
- Updates the bestselling, first edition to cover new information in the area and provides the most up-to-date resource for medicinal chemists and research chemists, working in drug discovery and the pharmaceutical industry
- Contributions are presented by an international team of authors from both academia and the pharmaceutical industry
- The multidisciplinary contents reflect the nature of the science, presenting both the theoretical foundations as well as detailed practical advice
- Includes chapters on the practice of salt formation in an industrial R&D environment, as well as regulatory and patent issues
- Updated monographs on salt-forming acids and bases are also provided

For further information visit [www.wiley.com](http://www.wiley.com)

 **WILEY-VCH**

 **VERLAG HELVETICA CHIMICA ACTA**